# THERMODYNAMICS OF AQUEOUS ATMOSPHERIC AEROSOLS

Thesis by

Arthur Wesley Stelson

In Partial Fulfillment of the Requirements

for the Degree of

Doctor of Philosophy

California Institute of Technology

Pasadena, California

1982

(Submitted September 21, 1981)

ACKNOWLEDGEMENTS

I would like to thank the California Institute of Technology, the Environmental Protection Agency and the California Air Resources Board for funding this work and supporting me during my graduate years.

Citing everyone at Caltech who made a contribution to this thesis would be a very cumbersome task. Thanks for every smile, encouraging remark and caring action that always came at the most appropriate times.

To my closest coworkers, I wish the best. I will never forget three office mates; Fred Gelbard, Stan Sander and Dale Warren. You will all go far. Lenore Kerner, your magical ability to cope with my handwriting and Dr. Seinfeld's corrections is shown throughout this volume. Dan Duan, you were a good roommate and see you at the arranged meeting five years from now.

Special thanks goes to Dr. Glen R. Cass, Dr. Richard C. Flagan, Dr. Sheldon K. Friedlander, Dr. Gregory J. McRae and my advisor, Dr. John H. Seinfeld. Their guidance led me into an area of personal and intellectual satisfaction. It has been appreciated.

Final gracious words are due my family. Mom, Dad, Kim, Caren, Tom, Becky and John, let's get together and celebrate. Papa and Grandpa, I am glad you followed and supported me the whole way.

ABSTRACT

A novel application of classical thermodynamics is presented to understand the distribution of aerosol forming material between the gas and aerosol phases in the polluted troposphere. The particular system studied involves $NH_4NO_3$ and its interactions with the environmental variables, temperature, relative humidity, droplet pH and aqueous $(NH_4)_2SO_4$ concentration. In Chapter 1, the theoretical temperature dependence of the solid $NH_4NO_3$ dissociation constant is compared to ambient ammonia - nitric acid partial pressure products and general agreement is shown. Also, temperature is demonstrated to be a determining factor for ambient aerosol nitrate formation. Chapter 2 discusses how an urban aerosol can be chemically characterized and that the aqueous electrolytic aerosol solutions are very concentrated (> 8 molal). Thus, any attempt to model ion interactions in aerosol solutions must be able to represent the concentrated solution regime. The ammonia - nitric acid partial pressure product for concentrated $NH_4NO_3$ - $HNO_3$ - $H_2O$ solutions is shown to be sensitive to relative humidity but not to pH (1-7) in Chapter 3. Since the ammonia - nitric acid partial pressure product is insensitive to pH, the $NH_4NO_3$ dissociation constant over $NH_4NO_3$ - $H_2O$ solutions should typify the ammonia - nitric acid partial pressure product above slightly acidic solutions. The $NH_4NO_3$ dissociation constant temperature and relative humidity dependence is evaluated and compared to ambient data in Chapter 4. General agreement between the predictions and the data exists but the possible effect of additional solutes in aerosol droplets is evident. Since $NH_4NO_3$ and $(NH_4)_2SO_4$ are present in atmospheric particles of similar size, it is appropriate to calculate the effect of

$(NH_4)_2SO_4$ on the relative humidity dependence of the $NH_4NO_3$ dissociation constant. Chapter 5 shows the presence of $(NH_4)_2SO_4$ reduces the amount of ammonia and nitric acid in the gas phase and that the $NH_4NO_3$ dissociation constant is only 40% less for a 0.5 $(NH_4)_2SO_4$ ionic strength fraction in aqueous solution. Also, methods for predicting the particle growth, the solution density and the refractive index of $NH_4NO_3$ - $(NH_4)_2SO_4$ - $H_2O$ solutions are outlined in Chapter 5. Good accordance between experimental data and predictions is demonstrated indicating the possible applicability of these techniques to more complex multicomponent solutions.

In the Appendices, a density prediction technique for $(NH_4)_2SO_4$ - $H_2SO_4$ - $H_2O$ solutions is presented since this aspect of ambient aerosols is not contained in the major thrust of this work.

TABLE OF CONTENTS

# CHAPTER 1

## A NOTE ON THE EQUILIBRIUM RELATIONSHIP BETWEEN AMMONIA AND NITRIC ACID AND PARTICULATE AMMONIUM NITRATE

Published in Atmospheric Environment 13, 369 - 371, 1981.

*Atmospheric Environment* Vol. 13, pp. 369–371.




0004-6981/79/0301-0369 $02.00/0

# A NOTE ON THE EQUILIBRIUM RELATIONSHIP BETWEEN AMMONIA AND NITRIC ACID AND PARTICULATE AMMONIUM NITRATE

A. W. STELSON, S. K. FRIEDLANDER and J. H. SEINFELD

Department of Chemical Engineering, California Institute of Technology, Pasadena, California, U.S.A.

(*First received* 10 *July* 1978 *and in final form* 26 *September* 1978)

**Abstract** – Theoretical predictions of the atmospheric equilibrium involving gaseous ammonia and nitric acid and solid ammonium nitrate are compared with atmospheric measurements of ammonia and nitric acid concentrations reported by Spicer (1974) at West Covina, California. Qualitative agreement between the equilibrium constant and the product of the measured $NH_3$ and $HNO_3$ concentrations is found.

## INTRODUCTION

Elucidation of the paths of formation of and the factors governing the concentration of atmospheric particulate nitrates is of substantial current interest (Orel and Seinfeld, 1977). Particulate nitrate concentrations have been measured by several investigators (Gordon and Bryan, 1973; Kadowaki, 1976; Moskowitz, 1977; Appel *et al.*, 1978), frequently together with particulate ammonium levels. Figure 1 shows ammonium and nitrate concentrations reported in atmospheric particulate samples from a variety of locations. Most of the data lie above the 1 : 1 mole ratio line.

Recent studies have demonstrated that gaseous nitric acid is adsorbed onto the glass fiber filters used in many of the measurements shown in Fig. 1 (Schumacher and Spicer, 1976; Spicer and Schumacher, 1977; Witz and MacPhee, 1977). This process, which leads to artifact nitrate formation on the filter medium, if present, would lead to higher reported particulate nitrate levels than those actually existing. Correction for artifact nitrate formation would have the effect of shifting more points in Fig. 1 above the 1 : 1 mole ratio line.

Sulfate ions in substantial amounts are almost always present in the atmospheric aerosol with the ammonium and nitrate ions, and mixtures of ammonium sulfate and nitrate often represent a significant fraction of the atmospheric aerosol. However, the equilibrium vapor pressures of ammonia and sulfuric acid above solid ammonium sulfate are very low, compared with the vapor pressures of ammonia and nitric acid over ammonium nitrate.

The purpose of this note is to review the equilibrium relationship between ammonia and nitric acid in the gas phase and solid ammonium nitrate, and to compare theoretical predictions with atmospheric measurements. The equilibrium analysis should apply either to pure solid ammonium nitrate or to a mixture of immiscible solid phases one of which is ammonium nitrate. The analysis would have to be modified,

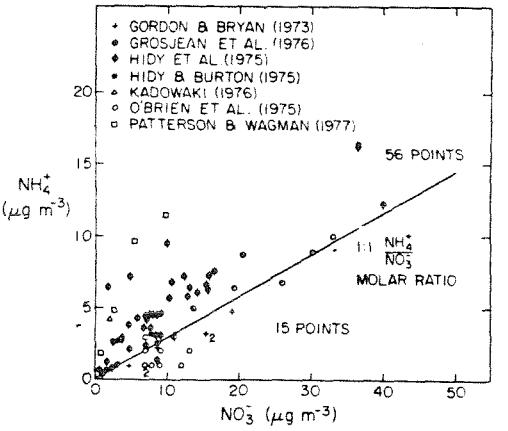


Fig. 1. Concentrations of $NH_4^+$ and $NO_3^-$ in ambient aerosols reported by various investigators.

however, if solid *solutions* are present (Denbigh, 1971, p. 160).

At temperatures below 170°C, solid ammonium nitrate exists in equilibrium with ammonia and nitric acid:

$$NH_4NO_3(s) \rightleftharpoons NH_3(g) + HNO_3(g). \quad (1)$$

In the notation of Denbigh (1971, p. 143), the equilibrium constant for this reaction, $K'_p$, is related to the partial pressures of $NH_3$ and $HNO_3$ by $K'_p = p_{NH_3}p_{HNO_3}$, and $K'_p$ is related to the standard Gibbs free energy change for reaction, $\Delta G^\circ_T$, by

$$\Delta G^\circ_T = -RT \ln K'_p. \quad (2)$$

Since the thermodynamic data for $NH_4NO_3$ are limited, an extrapolation formula for the equilibrium constant as a function of temperature can be derived by integrating the van't Hoff equation,

$$\ln K'_p = \alpha - \frac{\Delta H_0}{RT} + \int_{298}^{T} \frac{1}{RT^2} \int_{298}^{T''} (C_{P_{NH_3}} + C_{P_{HNO_3}} - C_{P_{NH_4NO_3}}) dT' dT''. \quad (3)$$

Table 1. Thermodynamic data at 298°K

| Species | Standard free energy of formation (kcal g mol$^{-1}$) | Heat of formation (kcal g mol$^{-1}$) | Heat capacity (cal g mol$^{-1}$) | |
|---|---|---|---|---|
| $NH_3(g)$ | −3.915 | −10.970 | 8.515 | JANAF (1971) |
| $HNO_3(g)$ | −17.690 | −32.100 | 12.748 | JANAF (1971) |
| $NH_4NO_3(s)$ | −43.98 | −87.37 | 33.3 | Wagman *et al.* (1968) |

Using the data in Table 1 and assuming the heat capacities are independent of temperature, we obtain from (3),

$$\ln K_c = 70.68 - \frac{24090}{T} - 6.04 \ln\left(\frac{T}{298}\right) \quad (4)$$

where $K_c$ is the equilibrium constant in terms of concentration, having units of ppm$^2$. Brandner *et al.* (1962) measured the dissociation pressure of solid $NH_4NO_3$ from 76 to 165°C. Based on their least squares expression representing their data, the following expression for $\ln K_c$ is obtained,

$$\ln K_c = 62.296 - \frac{21510}{T}. \quad (5)$$

Both formulas, (4) and (5) are shown in Fig. 2 and are seen to be in substantial agreement.

It is of interest to establish whether the equilibrium relation, Equation (1), holds in the atmosphere. For this purpose, it would be desirable to have simultaneous measurements of $P_{NH_3}$ and $P_{HNO_3}$ taken over a short time interval. We have not been able to find such data; however, Spicer (1974) has reported hourly data on the concentration of gaseous ammonia and nitric acid at West Covina, CA. From these data, we have calculated the product $\bar{c}_{NH_3}\bar{c}_{HNO_3}$, where $\bar{c}_{NH_3}$ and $\bar{c}_{HNO_3}$ denote the hourly average concentrations in ppm. The data points on Fig. 2 represent the $\bar{c}_{NH_3}\bar{c}_{HNO_3}$ products plotted vs $\bar{T}$, the hourly average temperature. Hourly measurements with the nitric acid or ammonia concentration less than 2 ppb were not included in Fig. 2 because of experimental error.

The relationship, Equation (1), should hold for solid ammonium nitrate in equilibrium with its dissociation products. At 25°C, solid ammonium nitrate deliquesces at a relative humidity of 62%. The corresponding relative humidities at 20 and 30°C are 64 and 58%, respectively (Dingemans, 1941). At these and higher relative humidities, solution droplets are present (at equilibrium) and the relationship shown in Fig. 2 would not be expected to apply. Clearly, the data at the highest relative humidity (>90%) are not in agreement with the equilibrium expression. The data corresponding to relative humidities less than 60% fall around the equilibrium lines but with considerable scatter in the lower concentration ranges where the percentage experimental error is greatest. The points which fall below the lines may correspond to concentrations too low for a solid phase to exist. The points which fall above would correspond to a non-equilibrium system or may result from experimental error.

## CONCLUSIONS

If ammonium nitrate is present in the aerosol phase, a substantial amount of $NH_3$ and $HNO_3$ must be present in the gas phase at equilibrium. For example, at 25°C the mass concentration of $NH_3$ plus $HNO_3$ (equimolar basis) in the gas in equilibrium with solid ammonium nitrate is about 22 $\mu g/m^{-3}$. This amount is of the same order or larger than the mass of aerosol ammonium nitrate usually reported in polluted atmospheres.

The $NH_3/HNO_3/NH_4NO_3$ equilibrium is very sensitive to the temperature. Over the range of 20–30°C, the equilibrium mass concentration in the gas phase of $NH_3$ and $HNO_3$ (equimolar) increases from 11.0 to

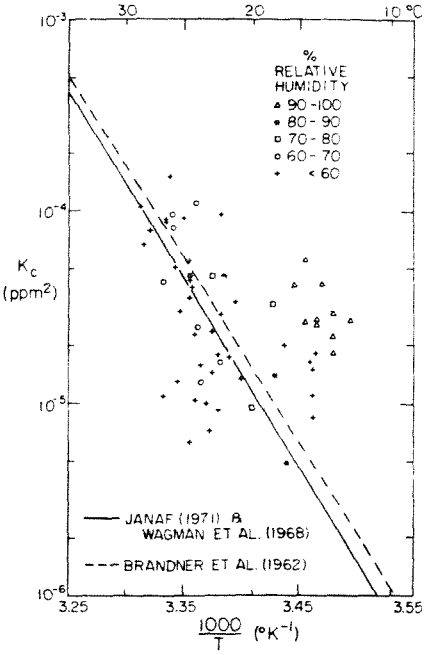


Fig. 2. The product $\bar{c}_{HNO_3}\bar{c}_{NH_3}$ calculated from the data of Spicer (1974) for West Covina (CA) compared with equilibrium theory, Equation (4) (——) and Equation (5) (– – –). Data for concentrations less than 2 ppb are not shown because of the large experimental error at the low concentrations.

38.4 $\mu g\ m^{-3}$. Thus, small changes in the temperature of the sampling train or in the analytical procedure can have a marked effect on the distribution between the gas and aerosol phases.

The effect of the presence of (immiscible) ammonium sulfate in the aerosol phase has also been evaluated. The available data show that the vapor pressure of the dissociation products of $(NH_4)_2SO_4(s)$ are too low to affect the concentrations of $NH_3$ and $HNO_3$ in the gas. The analysis would have to be modified if solid solutions of ammonium sulfate and nitrate are present (Denbigh, 1971, p. 160).

*Acknowledgement* – This work was supported in part by EPA Grant No. R805736. The contents do not necessarily reflect the view and policies of the Environmental Protection Agency.

## REFERENCES

Appel B. R., Kothny E. L., Hoffer E. M., Hidy G. M. and J. J. Weslowski (1978) Sulfate and nitrate data from the California Aerosol Characterization Experiment (ACHEX) *Environ. Sci. Technol.* **12**, 418–425.

Brandner J. D., Junk N. M., Lawrence J. W. and Robins J. (1962) Vapor pressure of ammonium nitrate. *J. Chem. Engng. Data* **7**, 227–228.

Denbigh K. (1971) *The Principles of Chemical Equilibrium*, 3rd Edn. Cambridge University Press, London.

Dingemans P. (1941) Die dampfspannung von gesättighten $NH_4NO_3$ – lösungen. *Rec. Trav. Chim.* **60**, 317–328.

Gordon R. J. and Bryan R. J. (1973) Ammonium nitrate in airborne particles in Los Angeles. *Environ. Sci. Technol.* **7**, 645–647.

Grosjean D., Doyle G. J., Mischke T. M., Poe M. P., Fitz D. R., Smith J. P. and Pitts J. M. (1976) The concentration, size distribution and modes of formation of particulate nitrate, sulfate, and ammonium compounds in the eastern part of the Los Angeles Basin. Presented at the 69th Annual Meeting of the Air Pollution Control Association, Portland.

Hidy G. M. *et al.* (1975) Characterization of aerosols in California. Rockwell Int. Rep. California Air Resour. Bd., ARB Contract No. 358.

Hidy G. M. and Burton C. S. (1975) Atmospheric aerosol formation by chemical reactions. *Int. J. Chem. Kinetics Symp.* **1**, 509–541.

JANAF Thermochemical Tables, 2nd Edn (1971). NSRDS-NBS 37.

Kadowaki S. (1976) Size distribution of atmospheric total aerosols, sulfate, ammonium and nitrate particulates in the Nagoya area. *Atmospheric Environment* **10**, 39–43.

Moskowitz A. H. (1977) Particle size distribution of nitrate aerosols in the Los Angeles Air Basin. EPA Report No. 600/3-77-053.

O'Brien R. J., Crabtree J. H., Holmes J. R., Hoggan M. C. and Bockian A. H. (1975) Formation of photochemical aerosol from hydrocarbons; atmospheric analysis. *Environ. Sci. Technol.* **9**, 577–582.

Orel A. E. and Seinfeld J. H. (1977) Nitrate formation in atmospheric aerosols. *Environ. Sci. Technol.* **11**, 1000–1007.

Patterson R. K. and Wagman J. (1977) Mass and composition of an urban aerosol as a function of particle size for several visibility levels. *J. Aerosol Sci.* **8**, 269–279.

Schumacher P. M. and Spicer C. W. (1976) Interferences in the sampling of particulate atmospheric nitrate. Presented at the 172nd ACS Meeting, San Francisco.

Spicer C. W. (1974) The fate of nitrogen oxides in the atmosphere. Batelle Columbus Rep. to Coordinating Res. Council and U.S. Environ. Protection Agency Rep. 600/3-76-030.

Spicer C. W. (1977) Photochemical atmospheric pollutants derived from nitrogen oxides. *Atmospheric Environment* **11**, 1089–1095.

Spicer C. W. and Schumacher P. M. (1977) Interferences in sampling atmospheric particulate nitrate. *Atmospheric Environment* **11**, 873–876.

Wagman D. D., Evans W. H., Parker V. B., Harlöw I., Baily S. M. and Schumm R. H. (1968) Selected values of chemical thermodynamic properties; tables for the first thirty-four elements in the standard order of arrangement, NBS technical note 270-3.

Witz S. and MacPhee R. D. (1977) Effect of different types of glass filters on total suspended particulates and their chemical composition. *J. Air Pollut. Control Ass.* **27**, 239–241.

# CHAPTER 2

## CHEMICAL MASS ACCOUNTING OF URBAN AEROSOL

Published in Environmental Science and Technology 15, 671 - 679, 1981.

Reprinted from ENVIRONMENTAL SCIENCE & TECHNOLOGY, Vol. 15, Page 671, June 1981


# Chemical Mass Accounting of Urban Aerosol

**Arthur W. Stelson and John H. Seinfeld***

Department of Chemical Engineering, California Institute of Technology, Pasadena, California 91125

■ A chemical mass accounting technique emphasizing the importance of chemical speciation is developed for analyzing atmospheric-aerosol data. The technique demonstrates that total aerosol mass can generally be characterized from measurements of $SO_4$, Cl, Br, $NO_3$, $NH_4$, Na, K, Ca, Fe, Mg, Al, Si, Pb, carbonaceous material, and aerosol water, the predominant species being $SO_4$, $NO_3$, $NH_4$, Si, carbonaceous material, and aerosol water. Since water is the major species distributed between the gas and aerosol phases, the interrelation between water and electrolytic mass is explored. It is shown that aerosol water is significantly correlated with electrolyte mass. Calculated aerosol ionic strengths lie in the region where the relative humidity/ionic strength relation is most sensitive, thereby suggesting the importance of relative-humidity monitoring during aerosol sampling.

## *Introduction*

The urban aerosol consists in general of a complex mixture of ionic salts, metal oxides, glasses, carbonaceous material, and water. Partitioning the aerosol into groups of materials with similar physical and thermodynamic properties can simplify the interpretation of experimental data and facilitate theoretical analysis. The main objective of this paper is to develop methods for obtaining an accurate overall aerosol mass balance from the least number of measured quantities.

The urban aerosol usually exhibits a bimodal volume distribution (see Figure 1). The fine-particle mode generally results from gas-to-particle conversion, whereas the coarse-particle mode arises from mechanically generated particles. The coarse mode is usually basic since the particles are formed from basic materials such as soil, cement, and fly ash. The fine mode can be neutral or acidic depending on the relative degree of neutralization of acidic material. In the eastern United States, the fine-particle mode in the urban aerosol generally dominates the total mass, so that the net aerosol pH is likely to be acidic, whereas Western aerosol has a greater tendency to be basic (*1*, *3*, *4*). Because the nature of the atmospheric aerosol depends strongly on its chemical speciation, it is important to be able to estimate its chemical composition based on measurements of elemental composition.

The atmospheric aerosol can be considered to consist of five major classes of constituents: ionic solids, electrolytes (dissolved ionic species), carbonaceous material, metal oxides and glasses, and water. An equation expressing this relation is

$$\mathrm{TSP} = \sum_i \sum_j [M_iO_j] + \sum_i [E_i] + \sum_i [CM_i] + \sum_i [I_i] + [H_2O] \quad (1)$$

where TSP = total suspended particulate matter ($\mu g\ m^{-3}$), $[M_iO_j]$ = mass concentration of metal oxide or glass ($\mu g\ m^{-3}$), $[E_i]$ = mass concentration of electrolyte i ($\mu g\ m^{-3}$), $[CM_i]$ = mass concentration of carbonaceous material i ($\mu g\ m^{-3}$), $[I_i]$ = mass concentration of ionic solid i ($\mu g\ m^{-3}$), and $[H_2O]$ = aerosol water concentration ($\mu g\ m^{-3}$). Electrolytes are dissociating ionic substances dissolved in water, whereas ionic solids are undissolved electrolytic material. Carbonaceous material refers to carbon-containing species, present as elemental carbon or organic or inorganic compounds. Metal oxides and glasses refer to oxidized elemental species, such as those present in soil and cement dust and fly ash. The water content refers to "free" water unassociated with hydrated salts.

The object of this paper is to show that, by making assumptions about each term on the right-hand side of eq 1, one can calculate the total suspended particulate mass concentration on the basis of conventional aerosol measurements.

From an accurate aerosol mass accounting, several important issues can be explored: (1) the possibility of biased total-mass measurements through alteration of the aerosol between sampling and analysis, (2) the relation between measured electrolyte mass-to-water ratios and solubilities of atmospherically significant electrolytes, (3) the aerosol ionic strength and possible dependence of aerosol water content on the prevailing relative humidity, (4) the net aerosol pH, and (5) the relative importance of different aerosol fractions—electrolytic, metal oxide and glass, carbonaceous, and aqueous—to the total aerosol mass and the possible interrelation between different fractions. Each of these issues will be evaluated and discussed with particular reference to the Los Angeles aerosol.

### *ACHEX*

One of the most detailed urban aerosol studies involving chemical analysis was the California Aerosol Characterization Experiment (ACHEX) (*5*). Ambient atmospheric aerosol was deposited on high-volume filters (Whatman 41) and analyzed for many chemical species. In addition, $\beta$-gauge, waterometer, and total-filter (47-mm Gelman GA-1 and Gelman A) measurements were performed. During some sampling periods, the aerosol carbonaceous material was analyzed (*6*). From the ACHEX data, 6 days are chosen for individual mass-balance analyses. More sampling periods would have been desirable, but these days were the only ones in which the aerosol was chemically analyzed for the major inorganic species, water, and carbonaceous material, in addition to continuous total-mass measurements. Even for these 6 days, the aerosol water content was not measured throughout the high-volume-filter sampling period. In Table I the sampling times and locations are summarized. Only at West Covina, CA (TC), did the aerosol water concentration and high-volume-filter sampling times totally overlap. Since the waterometer measurements overlapped the majority of the high-volume sampling period, it will be assumed that the time-averaged aerosol water concentration over its sampling time typifies the time-averaged aerosol water concentration over the total high-volume-filter sampling period.

The ACHEX ambient atmospheric aerosol high-volume-filter samples were analyzed for many chemical species. When only the major species, $SO_4$, Cl, Br, $NO_3$, $NH_4$, Na, K, Ca, Mg, Al, Si, and Pb, were considered, greater than 90% of the measured moles, excluding water and carbonaceous material, were accounted for. Therefore, the major species will only be considered in this study. Equation 1 will be modified as

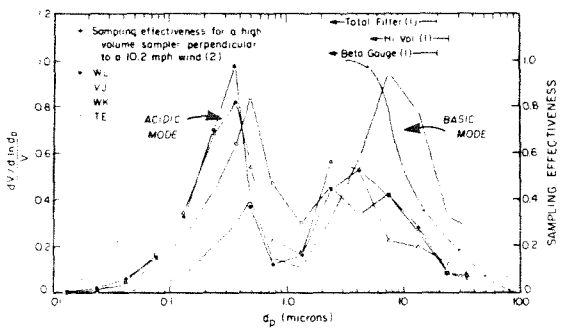


**Figure 1.** Time-averaged normalized aerosol volume distributions and sampler upper effective size limit (*1, 2, 5*). (See Table I for aerosol volume distribution sample code definition.)

$$\mathrm{TSP} = \sum_i \sum_j [\mathrm{M}_i\mathrm{O}_j] + \sum_i [\mathrm{E}_i] + \sum_i [\mathrm{CM}_i] + \sum_i [\mathrm{I}_i] + [\mathrm{H_2O}] + \sum_i [\mathrm{N}_i] \quad (2)$$

where $[N_i]$ is the concentration of minor specie i ($\mu g\ m^{-3}$). In Table II the sum of the minor species for the ACHEX data is listed. We see that this term is less than 1% of the total for the 6 days.

A basic object of this paper is to attempt to reconcile TSP measurements with eq 2 by studying the means of estimating the contributions of each of the terms on the right-hand side of eq 2. Although we focus on the ACHEX data, the techniques to be discussed will have general applicability. To evaluate the terms on the right-hand side of eq 2 other than $\Sigma[N_i]$, one must make assumptions about the chemical form of the different species. Each term and the assumptions needed in evaluating each will now be discussed. Then, the right-hand side of eq 2 will be evaluated theoretically and compared with the total suspended particulate measurements from ACHEX.

### *Aerosol Components*

**Ionic Solids.** Measurements of ionic-solid concentrations present difficult problems. In the measurement of the ion concentration in an aerosol, the filter is washed with a solvent and the ion concentration in the solvent is measured. Using this procedure, it is impossible to tell whether the ion was present in an ionic solid or an aqueous solution. Indirectly, the presence of ionic solids can be inferred. If the ambient relative humidity is less than the deliquescent humidity of the ionic solid, then it can be assumed that the salt is present as a solid. An additional check can be invoked if the solid is volatile, for example, $NH_4NO_3$ (*7*). The gas-phase concentrations of the precursors can be measured along with the temperature, and, if the calculated equilibrium coefficient matches the theoretical equilibrium coefficient for the ionic solid, it is assumed that the ionic solid is present. Both indirect methods fail if solid or supersaturated solutions are present.

For our analysis, it will be assumed that the ionic-solid concentration is zero. If the calculated ionic strength of the electrolytic aerosol solution is unreasonably high, then a correction must be made for the presence of ionic solids. For the mass accounting, it is immaterial whether the ionic-solid material is treated as an ionic solid or an electrolyte.

**Metal Oxides and Glasses.** The major elements possibly occurring in the form of oxides and glasses are Al, Ca, Fe, Si, Mg, Pb, K, and Na. When one follows the approach of Macias et al. (*8*), the chemical form of these elements can be assigned (see Table III). The majority of the oxides listed in Table III are known to be formed in combustion processes (*9, 10*). Additionally, Biggins et al. (*11*) have identified $Fe_2O_3$, $Al_2O_3$, and

**Table I. ACHEX Sampling Time and Location Summary (*5*)[a]**

| site | sample code | date | high-volume (HVM) sampling period | total-filter (TF, TV) sampling period | β-gauge ($\bar{\beta}$) sampling period | waterometer ($H_2O$) sampling period |
|---|---|---|---|---|---|---|
| Dominguez Hills, CA | WK | 10/4–10/5/73 | 2100–2105 | 2100–2100 | 2100–2100 | 2115–1515 |
| Dominguez Hills, CA | WL | 10/10–10/11/73 | 2100–2100 | 2100–2100 | 2100–2100 | 0000–1800 |
| Rubidoux, CA | VJ | 9/24–9/25/73 | 2300–1802 | 2300–1801 | 2300–1900 | 0400–1900 |
| West Covina, CA | TC | 7/24–7/25/73 | 2320–1605 | 2300–1600 | 2300–1600 | 2300–1600 |
| West Covina, CA | TD | 7/25–7/26/73 | 0500–1826 | 0500–1800 | 0500–1600 | 0445–1545 |
| West Covina, CA | TE | 8/8–8/9/73 | 2100–2100 | 2100–2100 | 2100–1800 | 2200–1400 |

[a] HVM = total mass from Whatman 41 8 × 10 in. high-volume filter ($\mu g\ m^{-3}$). $\overline{TF}$ = time-averaged total mass from Gelman GA-1, 47-mm filters ($\mu g\ m^{-3}$). $\overline{TV}$ = time-averaged total mass from Gelman A, 47-mm filters ($\mu g\ m^{-3}$). $\bar{\beta}$ = time-averaged total mass from $\beta$ gauge ($\mu g\ m^{-3}$). $\overline{H_2O}$ = time-averaged total water concentration from waterometer ($\mu g\ m^{-3}$).

**Table II. Summary of Measured and Calculated Los Angeles Aerosol Concentrations (*5*) [a]**

| | metal oxide and glass concn, $\mu g\ m^{-3}$ | | | | | | | |
|---|---|---|---|---|---|---|---|---|
| sample | $[Al_2O_3]$ | $[Fe_2O_3]$ | $[SiO_2]$ | [PbO] | [CaO] | [MgO] | $[K_2O]$ | $[Na_2O]$ |
| WK | 4.9 | 2.2 | 14.3 | 1.2 | 1.8 | 2.6 | 0.7 | 5.5 |
| WL | 3.8 | 2.8 | 13.4 | 4.0 | 2.4 | 1.8 | 0.7 | 3.0 |
| VJ | 8.6 | 5.9 | 28.5 | 0.8 | 4.1 | 1.9 | 1.7 | 1.5 |
| TC | 8.2 | 5.2 | 27.4 | 4.0 | 3.4 | 3.0 | 1.4 | 5.3 |
| TD | 6.4 | 3.7 | 19.8 | 3.2 | 2.8 | 1.8 | 1.0 | 3.9 |
| TE | 4.7 | 2.6 | 16.5 | 2.2 | 1.9 | 1.9 | 0.9 | 3.4 |

| | electrolyte concn, $\mu g\ m^{-3}$ | | | | | | | | | | | |
|---|---|---|---|---|---|---|---|---|---|---|---|---|
| sample | [Cl] | $[NO_3]$ | [Br] | $[NH_4]$ | [Na] | $[SO_4]$ | [Pb] | [Ca] | [K] | [Mg] | [H] | [H]′ | [OH]′ |
| WK | 0.3 | 0.9 | 0.2 | 6.7 | 4.1 | 31.4 | 1.1 | 1.3 | 0.6 | 1.6 | 0.3 | | 1.3 |
| WL | 1.2 | 7.3 | 1.2 | 3.1 | 2.2 | 4.2 | 3.8 | 1.7 | 0.6 | 1.1 | 0.1 | | 3.8 |
| VJ | 0.7 | 11.8 | 0.1 | 4.7 | 1.1 | 2.0 | 0.7 | 2.9 | 1.5 | 1.1 | 0.2 | | 2.3 |
| TC | 0.6 | 9.9 | 0.7 | 9.5 | 3.9 | 26.3 | 3.8 | 2.4 | 1.2 | 1.8 | 0.5 | 0.1 | |
| TD | 0.9 | 12.0 | 0.5 | 8.1 | 2.9 | 16.6 | 2.9 | 2.0 | 0.8 | 1.1 | 0.4 | 0.1 | |
| ]TE | 0.7 | 7.2 | 0.4 | 3.2 | 2.5 | 6.5 | 2.1 | 1.4 | 0.7 | 1.2 | 0.2 | | 1.5 |

| | summations, $\mu g\ m^{-3}$ | | | | | | | |
|---|---|---|---|---|---|---|---|---|
| sample | $\Sigma_i\Sigma_j[M_iO_j]$ | $\Sigma_i\Sigma_j[M_iO_j]'$ | $\Sigma_j[M_i]$ | $\Sigma_j[E_i]$ | $\Sigma_j[E_i]'$ | $\Sigma_j[N_i]$ | $\Sigma_j[CM_i]$ | $[H_2O]$ |
| WK | 33.2 | 21.4 | 11.4 | 39.8 | 49.5 | 0.7 | 18.7 | 54.2 |
| WL | 31.9 | 20.0 | 10.8 | 17.1 | 30.2 | 0.9 | 16.4 | 24.9 |
| VJ | 52.9 | 43.0 | 23.5 | 19.5 | 28.9 | 0.7 | 8.0 | 34.5 |
| TC | 55.9 | 40.8 | 22.0 | 47.5 | 60.2 | 1.4 | 29.8 | 75.2 |
| TD | 42.6 | 29.9 | 16.1 | 38.5 | 47.9 | 1.1 | 11.7 | 74.4 |
| TE | 34.1 | 23.8 | 12.7 | 18.2 | 27.4 | 0.8 | 10.8 | 29.7 |

[a] [A] = mass concentration of specie A. [H] = hydrogen concentration calculated from electroneutrality when $x_{Pb} = 0$, $x_{Ca} = 0$, $x_{Na} = 0$, $x_K = 0$, and $x_{Mg} = 0$. [H]′ or [OH]′ = hydrogen or hydroxyl ion concentration when $x_{Pb} = 1$, $x_{Ca} = 1$, $x_{Na} = 1$, $x_K = 1$, and $x_{Mg} = 1$. $\Sigma_i\Sigma_j[M_iO_j]$ = sum of metal oxide and glass concentrations when $x_{Pb} = 0$, $x_{Ca} = 0$, $x_{Na} = 0$, $x_K = 0$, and $x_{Mg} = 0$. $\Sigma_i\Sigma_j[M_iO_j]'$ = sum of metal oxide and glass concentrations when $x_{Pb} = 1$, $x_{Ca} = 1$, $x_{Na} = 1$, $x_K = 1$, and $x_{Mg} = 1$. $\Sigma_j[M_i]$ = sum of metal oxide and glass forming elements assuming no oxygen is present and $x_{Pb} = 1$, $x_{Ca} = 1$, $x_{Na} = 1$, $x_K = 1$, and $x_{Mg} = 1$. $\Sigma_j[E_i]$ = sum of electrolyte concentrations when $x_{Pb} = 0$, $x_{Ca} = 0$, $x_{Na} = 0$, $x_K = 0$, and $x_{Mg} = 0$. $\Sigma_j[E_i]'$ = sum of electrolyte concentrations when $x_{Pb} = 1$, $x_{Ca} = 1$, $x_{Na} = 1$, $x_K = 1$, and $x_{Mg} = 1$. $\Sigma_j[N_i]$ = sum of minor species concentrations. $\Sigma_j[CM_i]$ = sum of carbonaceous material.

**Table III. Aerosol Metal Oxides**

| element | oxide form | element | oxide form |
|---|---|---|---|
| Al | $Al_2O_3$ | Mg | MgO [a] |
| Ca | CaO [a] | Pb | PbO |
| Fe | $Fe_2O_3$ | Na | $Na_2O$ [a] |
| Si | $SiO_2$ | K | $K_2O$ [a] |

[a] Assumed

**Table IV. Equilibrium Analysis of Hydroxide Formation**

| free energy of formation data (*12*) | | | |
|---|---|---|---|
| species | $\Delta G°_{298}$, kcal/(g-mol) | species | $\Delta G°_{298}$, kcal/(g-mol) |
| CaO(s) | −144.4 | PbO(s) | −45.25,[a] −45.05[b] |
| $Ca(OH)_2$(s) | −214.33 | $Pb(OH)_2$(s) | −100.6 |
| MgO(s) | −136.13 | $H_2O$(g) | −54.64 |
| $Mg(OH)_2$(s) | −199.27 | | |

| oxide reactions with water | | |
|---|---|---|
| reaction | $\Delta G°_{298}$, kcal/(g-mol) | $P_{H_2O}$, atm |
| $CaO(s) + H_2O(g) \rightleftarrows Ca(OH)_2(s)$ | −15.29 | $6.0 \times 10^{-12}$ |
| $MgO(s) + H_2O(g) \rightleftarrows Mg(OH)_2(s)$ | −8.5 | $6.0 \times 10^{-7}$ |
| $PbO(s) + H_2O(g) \rightleftarrows Pb(OH)_2(s)$ | −0.71,[a] −0.91[b] | 0.3,[a] 0.2[b] |

[a] Red form. [b] Yellow form.

$SiO_2$ in roadside aerosol. The presence of CaO, MgO, and PbO can be examined from considerations of chemical equilibrium. Equilibrium constants for the reactions of CaO, MgO, and PbO with water are given in Table IV. The equilibrium analysis indicates that CaO and MgO should readily react to form $Ca(OH)_2$ and $Mg(OH)_2$, whereas the PbO should not. $Na_2O$ should readily react with water to form NaOH, and $K_2O$ should react similarly to CaO and MgO to form KOH. Biggins et al. (*11*) have measured $Pb_3O_4$ in roadside dust in addition to elemental lead, lead sulfates, lead carbonates, and lead hydroxides. The assumed form of lead, e.g., $Pb_3O_4$, PbO, or Pb, will not substantially affect the mass balance because of the high molecular weight of lead. We will assume lead to exist as PbO. Reiter et al. (*13*) have measured insoluble CaO, in disagreement with the pure thermochemical analysis. $Ca(OH)_2$ has a solubility similar to that of CaO, as shown in Table V. Thus, the insoluble CaO reported by Reiter et al. (*13*) could be $Ca(OH)_2$. MgO, $Na_2O$, and $K_2O$ have not apparently been identified in tropospheric aerosol.

MgO, $Na_2O$, $K_2O$, and CaO could exist in the atmospheric aerosol in solid solutions with $SiO_2$, $Al_2O_3$, and $Fe_2O_3$ in soil dust or rock flour. The ability to remove these elements by forming hydroxides depends on particle size, rock structure, and the acidic nature of the leaching agent. Goldich (*14*) measured the weathering loss in sedimentary rocks and obtained the following ordering: $Na_2O$, CaO, MgO, $K_2O$, $SiO_2$, $Al_2O_3$, and iron, where $Na_2O$ is the easiest to remove and iron is the hardest. This ordering supports the preceding thermodynamic and qualitative discussion. An additional calculation supporting the weathering ordering is obtained by using

**Table V. Solubility of Inorganic Salts**

| metal oxides and glasses | solubility,[a] g/100 g of $H_2O$ | ref | metal oxides and glasses | solubility,[a] g/100 g of $H_2O$ | ref |
|---|---|---|---|---|---|
| $SiO_2$ | insoluble in $H_2O$ | 12 | $Na_2O$ | decomposes | 12 |
| $Al_2O_3$ | insoluble in $H_2O$ | 12 | MgO | $0.0086^{30}$ | 12 |
| $Fe_2O_3$ | insoluble in $H_2O$ | 12 | PbO | $0.0023^{22}$ | 12 |
| CaO | $0.131^{10}$, decomposes | 12 | $K_2O$ | very soluble | 12 |
| **electrolytes** | **solubility,[a] g/100 g of $H_2O$** | **ref** | **electrolytes** | **solubility,[a] g/100 g of $H_2O$** | **ref** |
| NaOH | $113.2^{25}$ | 27 | NaCl | $35.91^{25}$ | 27 |
| KOH | $112^{20}$ | 28 | KCl | $34.7^{20}$ | 12 |
| $NH_4OH$ | soluble | 12 | $NH_4Cl$ | $39.5^{25}$ | 27 |
| $Mg(OH)_2$ | $0.0009^{18}$ | 12 | $MgCl_2$ | $54.25^{20}$ | 12 |
| $Ca(OH)_2$ | $0.162^{20}$ | 27 | $CaCl_2$ | $81.9^{25}$ | 27 |
| $Pb(OH)_2$ | $0.0155^{20}$ | 12 | $PbCl_2$ | $1.08^{25}$ | 27 |
| $NaNO_3$ | $91.79^{25}$ | 27 | $NH_4HSO_4$ | $288^{25}$ | 29 |
| $KNO_3$ | $31.6^{20}$ | 28 | $MgSO_4$ | $44.5^{20}$ | 12 |
| $NH_4NO_3$ | $192^{20}$ | 12 | $CaSO_4$ | $0.298^{20}$ | 28 |
| $Mg(NO_3)_2$ | $128.2^{20}$ | 27 | $PbSO_4$ | $0.00425^{25}$ | 12 |
| $Ca(NO_3)_2$ | $138^{25}$ | 27 | $H_2SO_4$ | $\infty$ | 12 |
| $Pb(NO_3)_2$ | $59.6^{25}$ | 27 | $HNO_3$ | $\infty$ | 12 |
| $Na_2SO_4$ | $27.8^{25}$ | 27 | HCl | $69.4^{25}$ | 18 |
| $NaHSO_4$ | $28.6^{25}$ | 12 | HBr | $198^{20}$ | 28 |
| $K_2SO_4$ | $12^{25}$ | 12 | NaBr | $90.5^{20}$ | 28 |
| $KHSO_4$ | $51.4^{20}$ | 28 | KBr | $65.2^{20}$ | 28 |
| $(NH_4)_2SO_4$ | $76.9^{25}$ | 27 | $NH_4Br$ | $97^{25}$ | 12 |
| $MgBr_2$ | $101.5^{20}$ | 12 | $PbBr_2$ | $0.85^{20}$ | 28 |
| $CaBr_2$ | $142^{20}$ | 12 | | | |

[a] For example, $0.131^{10}$ means a solubility of 0.131 g/100 g of $H_2O$ at 10 °C.

Clarke and Washington's (*15*) average composition of igneous rocks. Using the measured aerosol $SiO_2$ concentrations and the appropriate metal oxide-to-$SiO_2$ ratios calculated from Clarke and Washington's analysis, one can calculate the amounts of CaO, $Na_2O$, MgO, and $K_2O$. The calculated $K_2O$ concentrations agree within 6% of measured $K_2O$ concentrations, whereas the calculated and measured CaO, MgO, and $Na_2O$ concentrations differ by greater than 40%. Thus, it seems that $K_2O$ originates from soil dust and that the CaO, MgO, and the $Na_2O$ come from preferentially enriched sources, i.e., sea salt, cement dust, or fly ash. In light of the possibility that Pb, Ca, Na, K, and Mg are in either the glass and metal oxide or electrolytic phases, the metal oxide and glasses mass balance can be written as

$$\sum_i \sum_j [M_iO_j] = (1 - x_{Pb})\frac{M_{PbO}}{M_{Pb}}[Pb] + (1 - x_{Ca})\frac{M_{CaO}}{M_{Ca}}[Ca] + (1 - x_{Mg})\frac{M_{MgO}}{M_{Mg}}[Mg] + (1 - x_K)\frac{M_{K_2O}}{M_K}[K] + (1 - x_{Na})\frac{M_{Na_2O}}{M_{Na}}[Na] + \frac{M_{Fe_2O_3}}{2M_{Fe}}[Fe] + \frac{M_{Al_2O_3}}{2M_{Al}}[Al] + \frac{M_{SiO_2}}{M_{Si}}[Si] \quad (3)$$

where $M_A$ is the molecular weight of species A and $x_{Pb}$, $x_{Ca}$, $x_K$, $x_{Na}$, and $x_{Mg}$ are the fractions of Pb, Ca, K, Na, and Mg, respectively, in the ionic-solid or electrolytic form. Determination of $x_{Pb}$, $x_{Ca}$, $x_K$, $x_{Na}$, and $x_{Mg}$ could be based on a chemical-source balance. Even if the source signature is known, determination of the chemical form may be difficult. For example, Pb resulting from automobile exhaust may either be electrolytic or not depending on the fraction of Pb emitted as PbO or Pb vs. halogenated forms. In our analysis we will examine the two extremes: $x_{Pb} = x_{Ca} = x_K = x_{Na} = x_{Mg} = 1$, and $x_{Pb} = x_{Ca} = x_K = x_{Na} = x_{Mg} = 0$.

**Electrolytes.** An expression for the electrolyte mass of the atmospheric aerosol, i.e., ionic species dissolved in water, is

$$\sum_i [E_i] = [SO_4] + [Cl] + [NO_3] + [NH_4] + [Br] + x_{Pb}[Pb] + x_{Ca}[Ca] + x_K[K] + x_{Na}[Na] + x_{Mg}[Mg] + [H] + [OH] \quad (4)$$

The [H] or [OH] must be calculated on the basis of electroneutrality. If the aerosol is acidic, then [OH] may be neglected and

$$[H] = M_H\{2[SO_4]/M_{SO_4} + [Cl]/M_{Cl} + [NO_3]/M_{NO_3} - [NH_4]/M_{NH_4} + [Br]/M_{Br} - x_{Na}[Na]/M_{Na} - x_K[K]/M_k - 2x_{Pb}[Pb]/M_{Pb} - 2x_{Ca}[Ca]/M_{Ca} - 2x_{Mg}[Mg]/M_{Mg}\} \quad (5)$$

If $[H] < 0$ from eq 5, then $[OH] = -M_{OH}[H]/M_H$. Of course, eq 5 is an expression for the net acidity. Actually, the tropospheric aerosol would likely contain a mixture of acidic and basic particles (*16*).

**Water.** Ho et al. (*17*) have shown that the aerosol water content varies diurnally. Since the ACHEX chemical composition measurements were time-averaged, the aerosol water concentrations as measured by the waterometer were time-averaged. Since the average aerosol water concentrations were determined by integrating waterometer measurements, no assumptions were made concerning the amount of water on the filter material; i.e., the aerosol water is not assumed to be equal to the unaccounted mass on the filter as is typically done.

**Carbonaceous Material.** The carbonaceous fraction of the total aerosol mass must typically be estimated since carbo-

naceous aerosol concentration measurements are very limited. Interpretation of existing carbonaceous-material measurements is complicated by the different organic carbon extraction efficiencies of solvents and the mutual extraction of inorganic nitrates by polar solvents (*18*, *19*). Therefore, a calculation procedure must be devised that utilizes existing data to obtain values reflective of the actual carbonaceous-material loading.

Pierson and Russell (*20*) calculated for Denver a linear relation between the aerosol carbon, [C], and lead, [Pb], concentrations.

$$[C] = (5.84 \pm 0.34)[Pb] - 0.85 \pm 0.97\ \mu g\ m^{-3} \quad (6)$$

In Figure 2 this correlation is compared to data for aerosol lead and carbon measurements. The Los Angeles and Denver trends are similar except that, as [Pb] → 0, the Los Angeles data approach 10 $\mu$gC m$^{-3}$. The combined Los Angeles, San Jose, and Los Alamitos data indicate that eq 6 overpredicts the aerosol-carbon loading at high lead concentrations.

An additional correlation between total carbonaceous material and lead can be derived by utilizing data of Grosjean et al. (*23*), who reported an average noncarbon-to-carbon ratio of 0.37 in the organic aerosol fraction for 2 days in 1973 at Pasadena, CA. (The noncarbon material is nitrogen, oxygen, and hydrogen associated with carbon in organic molecules.) Thus, the total carbonaceous aerosol mass loading, $\Sigma_i[CM_i]$, can be approximated by multiplying the Pierson and Russell correlation by 1.37

$$\sum_i [CM_i] = (8.02 \pm 0.47)[Pb] - 1.17 \pm 1.33\ \mu g\ m^{-3} \quad (7)$$

In Figure 3 this correlation is compared with ACHEX aerosol lead and carbonaceous-material estimates using the data of Appel et al. (*6*). The $CH_3OH$–$CHCl_3$ extractables were corrected for the solubilization of ammonium nitrate by assuming that all of the nitrate measured was ammonium nitrate and subtracting the value obtained from the $CH_3OH$–$CHCl_3$ extractables. Subsequently, the $CH_3OH$–$CHCl_3$-extracted carbon value was subtracted from the total $CH_3OH$–$CHCl_3$-extractable mass. This procedure led to negative mass concentrations in 7 out of 11 cases. To check the extreme case, we subtracted the sum of the nitrate and $CH_3OH$–$CHCl_3$-extractable carbon loadings from the total $CH_3OH$–$CHCl_3$-extractable mass. This procedure led to negative values in 3 out of 11 cases. Therefore, either all of the nitrate must not have solubilized in the $CH_3OH$–$CHCl_3$ solution or some measurement error must have been present. Thus, the points plotted in Figure 3 represent the minimum aerosol carbonaceous material. As can be seen, the Los Angeles data are not well correlated with eq 7.

The correction for aerosol nitrate in the $CH_3OH$–$CHCl_3$-extractable mass is significant and can be shown by the following approximation:

$$[NO_3] = (M_{NO_3}/M_{NH_4NO_3}) \times [CH_3OH\text{–}CHCl_3\text{-extractable mass}] \times (1 - [\text{carbon fraction}][\text{carbon + noncarbon fraction}]/[\text{carbon fraction}])$$

$$[NO_3] = {}^{62}/_{80}\,[CH_3OH\text{–}CHCl_3\text{-extractable mass}] \times (1 - 1.37[\text{carbon fraction}]) \quad (8)$$

assuming nitrate is present as ammonium nitrate and that the $CH_3OH$–$CHCl_3$-extractable mass has the same noncarbon-to-carbon ratio as that measured by Grosjean et al. (*23*) for the organic aerosol fraction in Pasadena. The total noncarbon-to-carbon ratio of Grosjean is similar to those measured by Cukor et al. (*24*) and Ciacco et al. (*25*) in New York City. Based on their data for chloroform, 2-propanol, and methanol extractions, calculated noncarbon-to-carbon ratios varied between 1.36 and 1.49. Therefore, the total organic noncarbon-to-carbon ratio of Grosjean should approximate that in the $CH_3OH$–$CHCl_3$-extractable mass. In Figure 4 nitrate

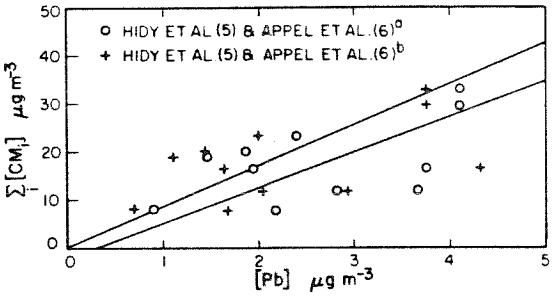


Figure 3. Relation between aerosol carbonaceous material and aerosol lead: (a) Pb from Whatman 41 high-volume filter; (b) time-averaged Pb from 47-mm Gelman GA-1 filters.

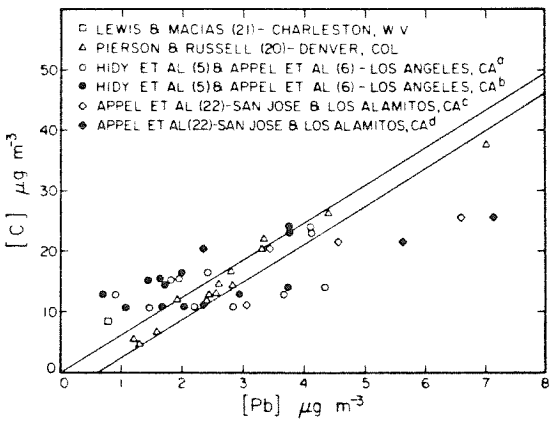


Figure 2. Relation between aerosol carbon and aerosol lead: (a) Pb from Whatman 41 high-volume filter; (b) time-averaged Pb from 47-mm Gelman GA-1 filters; (c) Pb from 47-mm Fluoropore filter; (d) Pb from Spectrograde high-volume filter. Solid lines: minimum and maximum of Pierson and Russell (*20*) correlation.

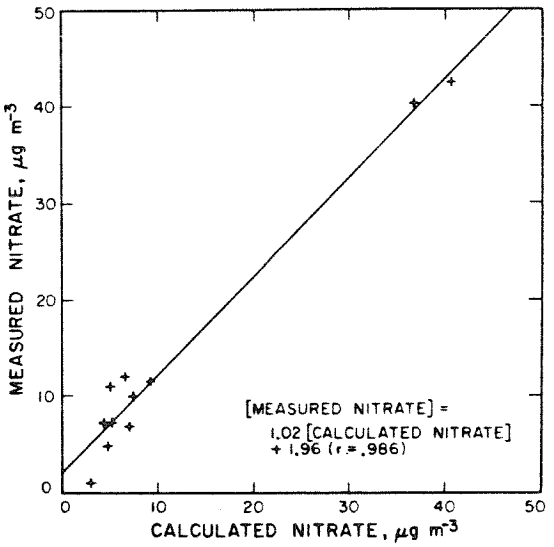


Figure 4. Measured nitrate vs. calculated nitrate. Solid line: linear least-squares fit to data.

values calculated from eq 8 are compared with the measured values of Hidy et al. (5).

Mueller et al. (26) measured aerosol carbonate carbon in Pasadena, CA, and determined it to be consistently less than 5% of the total carbon present. In light of the previously discussed inaccuracies, the carbonate fraction of the aerosol will be assumed to be negligible.

In summary, the total carbonaceous aerosol concentration can be estimated from the sum of the benzene- and $CH_3OH$–$CHCl_3$-extracted mass minus nitrate as ammonium nitrate plus the estimate for the maximum elemental carbon aerosol loading of Appel et al. (6). The carbonaceous aerosol concentration as calculated by the above procedure should generally reflect the atmospheric carbonaceous-material loading and is the best obtainable using the existing data.

*Aerosol Mass Accounting*

Table II presents a summary of the data used for the mass accounting calculation. The calculated and measured total-mass data are summarized in Table VI. In Table VI, $M_1$ is the total mass calculated by assuming $x_{Pb} = 0, x_{Ca} = 0, x_K = 0, x_{Na} = 0$, and $x_{Mg} = 0$, and $M_2$ is that when $x_{Pb} = 1, x_{Ca} = 1, x_K = 1, x_{Na} = 1$, and $x_{Mg} = 1$. $M_3$ is the calculated total mass assuming that the total mass is the sum of the measured species. Thus, no assumptions are made concerning chemical speciation in the calculation of $M_3$.

All three mass calculation procedures ($M_1$, $M_2$, $M_3$) yield similar values but disagree with the total-mass concentrations calculated from the $\beta$ gauge, total filters, and high-volume filters. To evaluate the trend among these seven variables, $M_1$, $M_2$, $M_3$, $\bar{\beta}$, $\overline{TF}$, $\overline{TV}$, and HVM, we performed a least-squares analysis between all pairs (see Table VII). (VJ was omitted from the least-squares analysis since a $\overline{TV}$ measurement was not performed.) All measured and calculated total suspended mass techniques correlated significantly. A notable feature seen in the results in Table VII is that the $\beta$-gauge measurements are consistently lower than the other calculated and measured total-mass concentrations. (Possibly the instrument gain was set too low.)

The mass ratio, $S$, of electrolytic material to water can be calculated by

$$S = \left(\sum_i [E_i]/\overline{H_2O}\right) \times 100 \text{ g}/100 \text{ g of } H_2O \qquad (9)$$

Calculated values of $S$ are listed in Table VIII for the two extreme cases of the distribution of Pb, Ca, K, Na, and Mg between the metal oxide–glass subset and the electrolyte subset. The values calculated for $S$ and $S'$ are within the typical range of solubilities of electrolyte materials listed in Table V. Since the calculated mass ratios vary between 50 and 125 g/100 g of $H_2O$, it can be inferred that the electrolyte portion of the atmospheric aerosol at these sampling locations is dominated by soluble sulfates, nitrates, and chlorides. The chemical analysis summary shows the dominance of nitrate and sulfate (Table II). Ochs and Gatz (30) recently measured the fraction of water-soluble material in particles of >4.6-$\mu$m radius as ~0.3. Using data from Tables II and VI, we compute the soluble fraction in the Los Angeles aerosol to lie between 0.15 and 0.35. Older Los Angeles aerosol data of Cadle (31) list water and volatile organics as 0.15 of the total aerosol mass, with a water-soluble fraction of 0.15.

The ionic strength of the aerosol solution can be calculated by

$$I = (1000/2\overline{H_2O})\left(\sum_i z_i^2[E_i]/M_i\right) \qquad (10)$$

where $M_i$ is the molecular weight and $z_i$ is the charge of species i. Calculated values of $I$ are listed in Table VIII for the two extreme cases of the distribution of Pb, Ca, K, Na, and Mg. The range of ionic strengths at each sampling location is compared with the ionic-strength dependence of water activity

**Table VI. Calculated and Measured Total Mass ($\mu$g m$^{-3}$) (5)**

| sample | $M_1$ | $M_2$ | $M_3$ | $\bar{\beta}$ | $\overline{TF}$ | $\overline{TV}$ | HVM |
|---|---|---|---|---|---|---|---|
| WK | 146.6 | 144.5 | 133.8 | 105.7 | 113.5 | 127.7 | 148 |
| WL | 91.2 | 92.4 | 82.4 | 77.7 | 101.5 | 107.5 | 114 |
| VJ | 115.6 | 115.1 | 96.0 | 85.8 | 160.9 | | 211 |
| TC | 209.8 | 207.4 | 192.0 | 173.1 | 210.9 | 215.4 | 241 |
| TD | 168.3 | 165.0 | 153.9 | 137.8 | 176.9 | 176.0 | 194 |
| TE | 93.6 | 92.5 | 82.3 | 87.1 | 101.0 | 113.4 | 123 |

**Table VII. Least-Squares Analysis of Measured and Calculated Total Mass**

| | $M_1$ | $M_2$ | $M_3$ | $\bar{\beta}$ | $\overline{TF}$ | $\overline{TV}$ | least squares parameters [a] |
|---|---|---|---|---|---|---|---|
| HVM | 0.974 | 0.975 | 0.972 | 0.999 | 0.986 | 0.997 | $r$ |
| | 0.929 | 0.905 | 0.867 | 0.738 | 0.933 | 0.870 | $m$ |
| | −10.4 | −8.1 | −13.3 | −4.8 | −12.3 | 5.4 | $b$ |
| $\bar{\beta}$ | 0.976 | 0.977 | 0.974 | 1.00 | 0.981 | 0.995 | $r$ |
| | 1.26 | 1.23 | 1.18 | 1.00 | 1.26 | 1.18 | $m$ |
| | −4.6 | −2.4 | −7.9 | 0.0 | −5.5 | −11.4 | $b$ |
| $\overline{TF}$ | 0.935 | 0.936 | 0.933 | 0.981 | 1.00 | 0.995 | $r$ |
| | 0.941 | 0.918 | 0.879 | 0.766 | 1.00 | 0.918 | $m$ |
| | 9.4 | 11.1 | 5.1 | 8.5 | 0.0 | 18.9 | $b$ |
| $\overline{TV}$ | 0.955 | 0.956 | 0.952 | 0.995 | 0.995 | 1.00 | $r$ |
| | 1.04 | 1.02 | 0.974 | 0.842 | 1.08 | 1.00 | $m$ |
| | −12.5 | −10.2 | −15.2 | −8.3 | −19.0 | 0.0 | $b$ |

[a] $r$ = correlation coefficient; $m$ = slope; $b$ = intercept.

**Table VIII. Calculated Electrolyte-to-Water Mass Ratios and Ionic Strengths for Los Angeles Aerosol [a]**

| sample | $S$ | $S'$ | $I$ | $I'$ |
|---|---|---|---|---|
| WK | 73.4 | 91.3 | 18.6 | 22.2 |
| WL | 68.7 | 121.3 | 14.2 | 25.9 |
| VJ | 56.5 | 83.8 | 8.0 | 16.5 |
| TC | 63.2 | 80.1 | 13.4 | 15.4 |
| TD | 51.7 | 64.4 | 10.0 | 11.5 |
| TE | 61.3 | 92.3 | 11.6 | 18.3 |

[a] $S$ = calculated mass ratio when $x_{Pb} = 0$, $x_{Ca} = 0$, $x_{Na} = 0$, $x_K = 0$, and $x_{Mg} = 0$, g/100 g of $H_2O$. $S'$ = calculated mass ratio when $x_{Pb} = 1$, $x_{Ca} = 1$, $x_{Na} = 1$, $x_K = 1$, and $x_{Mg} = 1$, g/100 g of $H_2O$. $I$ = ionic strength when $x_{Pb} = 0$, $x_{Ca} = 0$, $x_{Na} = 0$, $x_K = 0$, and $x_{Mg} = 0$, mol/1000 g of $H_2O$. $I'$ = ionic strength when $x_{Pb} = 1$, $x_{Ca} = 1$, $x_{Na} = 1$, $x_K = 1$, and $x_{Mg} = 1$, mol/1000 g of $H_2O$.

for several electrolytes at 25 °C in Figure 5. All of the calculated ionic strengths are in the region where the relative humidity–ionic strength variation is strongest, indicating the importance of the prevailing relative humidity and the aerosol chemical nature in determining the atmospheric aerosol water content.

The net aerosol pH was calculated for both extreme distributions of Pb, Ca, K, Na, and Mg (see Table II). Samples TC and TD were the only ones that were definitely acidic, whereas WK, WL, VJ, and TE could be basic or acidic. Although Liljestrand (*4*) measured net basic aerosol pHs in Los Angeles, his measurements and those reported in ACHEX (*5*) were taken by using quite different experimental techniques that might have different cutoff diameters. Since the coarse mode is generally basic and the fine mode acidic, a lower cutoff would lead to a lower net pH. Combining the coarse and fine modes can also lead to sampling errors (*35*).

The metal oxide–glass, electrolyte, carbonaceous, and water fractions are of equal importance in the total aerosol mass (see Table II). The dominance of different fractions at different locations and sampling periods is evident. In sample VJ the metal oxide–glass fraction was largest, and in WK, TC, and TD the water fraction predominated. In TE and WL the aerosol was fairly evenly distributed among the metal oxide–glass, electrolytic, and water fractions.

Finally, the electrolytic mass and the aerosol water concentrations are well correlated, indicating the presence of electrolytic solutions (see Figure 6).

*Implications for Measurement Techniques*

Several important experimental questions need to be considered when comparing the total suspended mass measurements obtained by using glass-fiber filters, cellulose filters, cellulose triacetate filters, and the $\beta$ gauge: (1) Does the $\beta$ gauge measure only suspended particles and not exhibit a relative-humidity interference? (2) Do filtration-efficiency differences have a significant influence on total-mass measurements? (3) Are the samplers' upper and lower aerosol size cutoffs similar? (4) What effect does equilibrating the filters to 55% relative humidity at 25 °C have on the water adsorbed or absorbed on the filter material and the water contained in the aerosol? (5) How important is filter artifact in prejudicing aerosol nitrate and sulfate measurements?

Landis (*36*) has reported a large positive interference in $\beta$-gauge measurements at high relative humidity (>75%). Data of Husar (*37*) and Yamamoto (*38*) do not show this interference but show the thermodynamically predicted absorption of water on filter-deposited NaCl and $(NH_4)_2SO_4$ aerosols as the relative humidity is increased above the deliquescence point. Additionally, ACHEX data using the $\beta$ gauge do not show instrument saturation during times of high relative humidity as would be predicted by Landis' measurements.

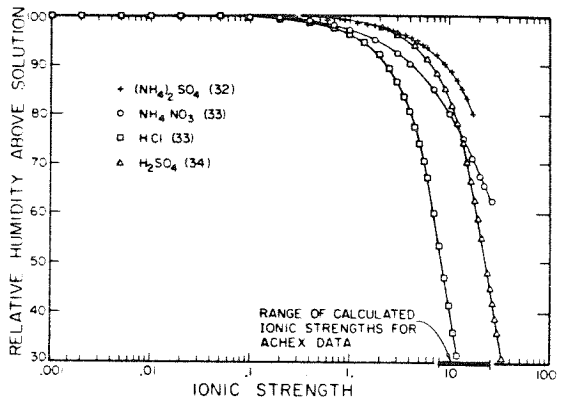


**Figure 5.** Water activities for typical electrolytes as a function of ionic strength ($T$ = 25 °C).

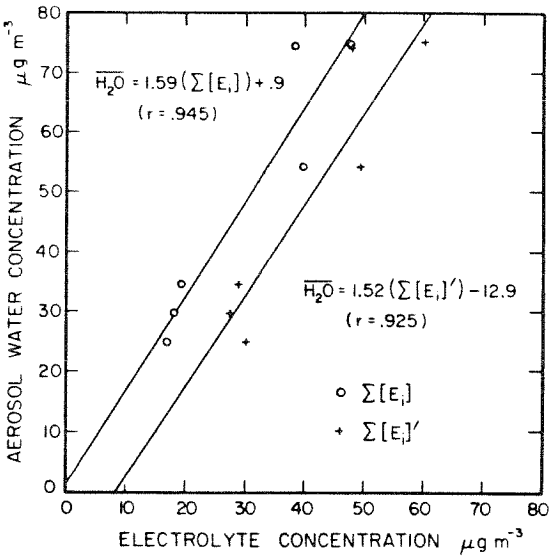


**Figure 6.** Aerosol water vs. electrolyte concentration. Solid lines: linear least-squares fits to data.

Landis' Figure 3 shows that $\beta$-gauge measurements are consistently lower than or equal to the total filter measurements. If the instrument responded to high relative humidity and had a response greater than the manufacturer's calibration for atmospheric aerosol, the filter-sample data should be less than the $\beta$-gauge measurements. Since the measured effect is the opposite of the calibration results, some inconsistency exists. Therefore, the $\beta$-gauge measurements were not considered in error and have been compared here to other mass measurement techniques.

Shown in Figure 7 is the initial filtration efficiencies of different filter materials vs. face velocity. The most recent data of John et al. (*39*) show that the efficiencies of Gelman GA-1 and Gelman A should be greater than 99% over the operating range of interest for a polydisperse room aerosol. Even though the data indicate higher efficiencies than those found by Appel et al. (*40*), the maximum discrepancy would account for an error of only 5%. The data for Whatman 41 filters do not agree as well with the other data in Figure 7. These differences can result from filter maturation, material construction variation, and different particle concentration measurement techniques. Since the filtration efficiency curves for Whatman

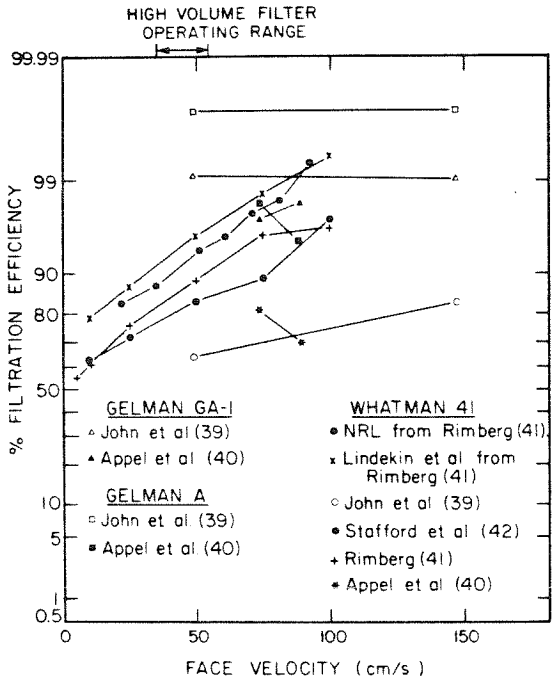


**Figure 7.** Filtration efficiencies for Whatman 41, Gelman A, and Gelman GA-1.

41 are lower than the curves for Gelman GA-1 and Gelman A, the effect of filtration loss must be evaluated. Lindeken et al. (*43*) and Stafford et al. (*42*) measured the increase in filter efficiency for Whatman 41 as a function of time. Using their data and making very conservative estimates, one can estimate the maximum error due to the initial filter inefficiencies as 1% for all samples. When one considers that the average standard deviation error of the three filter total suspended mass measurement techniques is 8%, initial filtration inefficiency differences cannot be the major source of error.

Shown in Figure 1 are the time-averaged normalized aerosol volume distributions for four sampling periods. Also, shown in Figure 1 are the sampler cutoffs for sampling in stagnant air (*1*). The value for the high-volume sampler is a more recent one than that reported in ACHEX (i.e., 60 $\mu$m). Wedding et al. (*2*) measured the sampling effectiveness of a high-volume sampler perpendicular to a 10.2 mi/h wind. Figure 1 shows that the presence of wind can significantly affect the fraction of the coarse mode sampled. Since the wind effect on the sampling efficiency of the total filter setup or the $\beta$ gauge has not been measured, it is assumed that wind affects all samplers similarly. Thus, the ambient aerosol should not be significantly preferentially measured by any sampler.

The filters used in ACHEX were equilibrated to 55% relative humidity and 25 °C as prescribed by NASN procedures. Tierney et al. (*44*) and Demuynck (*45*) showed that glass-fiber filters lose their adsorbed or absorbed water when equilibrated to NASN conditions. Demuynck demonstrated that Whatman 41 cellulose filters irreversibly absorb water. When Demuynck's data and the ratio of filter surface areas are used, this interference would amount to 107 $\mu g\ m^{-3}$ for a 24-h high-volume filter. In Table VI, $\overline{HVM}$ is consistently higher than $\overline{TV}$, verifying the irreversible absorption of water by Whatman 41. The cellulose triacetate filters did not irreversibly absorb water, as seen by comparing $\overline{TF}$ and $\overline{TV}$ values in Table VI. Whether the filter drying process removed water from the aerosol is very important. Table II and VI show that the aerosol contains between 20 and 45% water. If the water is removed, then 20–45% of the aerosol mass is unaccountable. This fraction is unreasonably high; therefore, only the loosely held absorbed water on the filter surface is removed by the initial drying. Whether the aerosol is a supersaturated solution or more dilute cannot be determinined from existing data.

Corrections for artifact nitrate and sulfate were not performed since assigning a correction would be somewhat arbitrary with current knowledge. Maximum artifact values can be calculated from the results of Appel et al. (*22*). The maximum artifact sulfate would be $\sim 2\ \mu g\ m^{-3}$ and nitrate would be $\sim 26\ \mu g\ m^{-3}$ (10 ppb 24-h average $HNO_3(g)$ concentration) for Whatman 41 high-volume filters. The measured sulfate values used in this study were consistently above 2 $\mu g\ m^{-3}$, whereas the nitrate values were below 26 $\mu g\ m^{-3}$ (see Table II). Thus, the sulfate data are presumed to be more accurate than the nitrate data, but no measured values were corrected since assignment of corrections could not be quantitatively performed. Recent work by Appel et al. (*46*) indicates that positive and negative nitrate artifacts exist, making corrections even more difficult to assign.

### *Conclusions*

The foregoing analysis demonstrates several important points concerning mass accounting, the presence of electrolytic solutions, and aerosol pH.

**Mass Acccounting.** A reasonably accurate mass balance for the Los Angeles aerosol has been obtained from measurements of $SO_4$, Cl, Br, $NO_3$, $NH_4$, Na, K, Ca, Fe, Mg, Al, Si, Pb, carbonaceous material, and aerosol water, the predominate species being $SO_4$, $NO_3$, $NH_4$, Si, carbonaceous material, and aerosol water. Chemical speciation was assigned, and the presence of oxygen in metal oxides and glasses was accounted for. The addition of metal oxide and glass oxygen to the mass balance did not have a significant effect on the total-mass correlations. The assignment of oxide forms to certain elements is, however, physically important, since metal oxides tend to be water insoluble. Thus, no "free" water would be associated with these oxides.

Since aerosol carbon measurements are limited, the aerosol carbon concentration typically must be estimated. The Pierson and Russell (*20*) correlation was examined and does not seem to apply to the Los Angeles aerosol data (Figure 2). In addition to quantification of the aerosol carbon concentration, determination of the associated oxygen, nitrogen, and hydrogen in the carbonaceous material is important. As indicated by Appel et al. (*6*), Grosjean (*18*), Gordon and Bryan (*19*), and this work, the $CH_3OH$–$CHCl_3$-extractable mass contains considerable nitrate. Thus, a correction to this measurement for dissolved inorganics would improve future mass accounting calculations.

Since certain chemical species are distributed between the gas and aerosol phases, the total aerosol mass, the aerosol water concentration, the relative humidity, and the temperature should be continuously monitored during sampling. Ideally, other volatile species that are distributed between the gas and aerosol phases should also be monitored, i.e., $NH_3$, $HNO_3$, HCl, and organics. By analyzing continuous data, one can determine the distribution of material between the gas and aerosol phases and the possibility of aerosol alteration between sampling and measurement due to volatilization, uptake of water, or displacement reactions. Since mass is reversibly distributed between the gas and aerosol phases, care must be taken when determining the total suspended particulate mass from filter samples such that the filters are equilibrated with a known relative humidity and temperature at the time of weight measurement. Ideally, filter weight measurements should be performed at several relative humidities.

**Presence of Electrolyte Solutions.** The calculated electrolyte-to-aerosol water mass ratios are typical of atmospherically significant electrolyte solutions near saturation (Tables V and VIII). By assigning valences to the electrolyte species, we have calculated the ionic strength. From the ionic strengths calculated and compared with typical ionic-strength dependence of water activities in binary electrolyte solutions, the electrolyte material appears to be present in highly concentrated solutions and/or ionic solids. The amount of water in the aerosol phase is very dependent on the chemical nature of the electrolytes and the prevailing relative humidity (Figure 5). Since the aerosol water and electrolyte concentrations are interdependent, a correlation between electrolyte mass and aerosol water was evaluated. The significant correlation between electrolyte mass and aerosol water highlights an important point, namely, that electrolyte material can cause greater visibility reduction per unit mass than organics or metal oxides because of hygroscopicity.

**Aerosol pH.** The fraction of electrolyte material for Ca, Pb, K, Na, and Mg must be determined to perform an accurate chemical mass and acidity balance. Biggins et al. (*11*) and Reiter et al. (13) recognized the importance of differentiating between water-soluble and -insoluble Pb and Ca. Depending on the assumptions of chemical speciation for Ca, Pb, K, Na, and Mg, metal oxide vs. electrolyte, the net aerosol pH may be basic or acidic (Table II). Knowing the net aerosol pH would improve the aerosol mass balance because an additional variable would exist to check chemical speciation assumptions or measurements. Recent aerosol data include aerosol pH measurements but do not have detailed chemical analyses and aerosol water measurements to perform a mass balance (*3*, *47*). An additional factor important to determining the net aerosol pH is the upper cutoff of the aerosol sampler. This point is graphically illustrated by Figure 1.

*Acknowledgment*

We extend appreciation to Bruce Appel for his helpful comments.

*Literature Cited*

(1) National Research Council, Subcommittee on Airborne Particles "Airborne Particles"; University Park Press: Baltimore, MD, 1979; Chapter 1.
(2) Wedding, J. B.; McFarland, A. R.; Cermack, J. E. *Environ. Sci. Technol.* **1977**, *11*, 387.
(3) Tanner, R. L.; Cederwall, R.; Garber, R.; Leahy, D.; Marlow, W.; Meyers, R.; Phillips, M.; Newman, L. *Atmos. Environ.* **1977**, *11*, 955.
(4) Liljestrand, H. M. Ph.D. Thesis, California Institute of Technology, Pasadena, CA, 1980.
(5) Hidy, G. M., et al. "Characterization of Aerosols in California", Rockwell International Report, California Air Resources Board, ARB Contract No. 358, 1975.
(6) Appel, B. R.; Colodny, P.; Wesolowski, J. J. *Environ. Sci. Technol.* **1976**, *10*, 359.
(7) Stelson, A. W.; Friedlander, S. K.; Seinfeld, J. H. *Atmos. Environ.* **1979**, *13*, 369.
(8) Macias, E. S.; Blumenthal, D. L.; Anderson, J. S.; Cantrell, B. K. "Size and Composition of Visibility-Reducing Aerosols in Southwestern Plumes", presented at the Conference on Aerosols: Anthropogenic and Natural-Sources and Transport, New York Academy of Sciences, New York, Jan 9–12, 1979.
(9) Bryers, R. W. "Influence of the Distribution of Mineral Matter in Coal on Fireside Ash Deposition", ASME Paper No. 78-WA/CD-4, 1978.
(10) Henry, W. M.; Knapp, K. T. *Environ. Sci. Technol.* **1980**, *14*, 450.
(11) Biggins, P. D. E.; Harrison, R. M. *Environ. Sci. Technol.* **1980**, *14*, 336.
(12) Weast, R. C., Ed. "Handbook of Chemistry and Physics", 54th ed.; CRC Press: Cleveland, OH, 1973.
(13) Reiter, R.; Sladkovic, R.; Pötzl, K. *Atmos. Environ.* **1976**, *10*, 841.
(14) Pettijohn, F. J. "Sedimentary Rocks"; Harper and Brothers: New York, 1957; Chapter 11.
(15) Mason, B. "Principles of Geochemistry"; Wiley: New York, 1966; Chapter 3.
(16) Brosset, C. *Atmos. Environ.* **1978**, *12*, 25.
(17) Ho, W.; Hidy, G. M.; Govan, R. M. *J. Appl. Meteorol.* **1974**, *13*, 871.
(18) Grosjean, D. *Anal. Chem.* **1975**, *47*, 797.
(19) Gordon, R. J.; Bryan, R. J. *Environ. Sci. Technol.* **1973**, *7*, 645.
(20) Pierson, W. R.; Russell, P. A. *Atmos. Environ.* **1979**, *13*, 1623.
(21) Lewis, C. W.; Macias, E. S. *Atmos. Environ.* **1980**, *14*, 185.
(22) Appel, B. R.; Tokiwa, Y.; Wall, S. M.; Hoffer, E. M.; Haik, M.; Wesolowski, J. J. "Effect of Environmental Variables and Sampling Media on the Collection of Atmospheric Sulfate and Nitrate"; Final Report, California Air Resources Board, ARB Contract No. 5-1032, 1978.
(23) Grosjean, D.; Friedlander, S. K. *J. Air Pollut. Control Assoc.* **1975**, *25*, 1038.
(24) Cukor, P.; Ciaccio, L. L.; Lanning, E. W.; Rubino, R. L. *Environ. Sci. Technol.* **1972**, *6*, 633.
(25) Ciaccio, L. L.; Rubino, R. L.; Flores, J. *Environ. Sci. Technol.* **1974**, *8*, 935.
(26) Mueller, P. K.; Mosley, R. W.; Pierce, L. B. In "Aerosols and Atmospheric Chemistry"; Hidy, G. M., Ed.; Academic Press: New York, 1972.
(27) West, C. J., Ed. "International Critical Tables of Numerical Data, Physics, Chemistry and Technology"; McGraw-Hill: New York, 1933; Vol. IV.
(28) Lange, N. A., Ed. "Handbook of Chemistry", 5th ed.; Handbook Publishers: Sandusky, OH, 1944.
(29) Tang, I. N.; Munkelwitz, H. R. *J. Aerosol Sci.* **1977**, *8*, 321.
(30) Ochs, H. T., III; Gatz, D. F. *Atmos. Environ.* **1980**, *14*, 615.
(31) Cadle, R. D. "Particles in the Atmosphere and Space"; Reinhold: New York, 1966; Chapter 2.
(32) Wishaw, B. F.; Stokes, R. H. *Trans. Faraday Soc.* **1954**, *50*, 952.
(33) Hamer, W. J.; Wu, Y. C. *J. Phys. Chem. Ref. Data* **1972**, *1*, 1047.
(34) Robinson, R. A.; Stokes, R. H. "Electrolyte Solutions; The Measurement and Interpretation of Conductance, Chemical Potential and Diffusion in Solutions of Simple Electrolytes", 2nd ed. (revised); Butterworths: London, 1959.
(35) Brosset, C. "Possible Changes in Aerosol Composition Due to Departure from Equilibrium Conditions during Sampling"; Swedish Water and Air Pollution Research Laboratory; Goteborg, 1978; PB-298 947.
(36) Landis, D. A. *Atmos. Environ.* **1975**, *9*, 1079.
(37) Husar, R. B. *Atmos. Environ.* **1974**, *8*, 183.
(38) Macias, E. S.; Husar, R. B. In "Fine Particles. Aerosol Generation, Measurement, Sampling, and Analysis"; Liu, B. Y. H., Ed.; Academic Press: New York, 1976.
(39) John, W.; Reischl, G. *Atmos. Environ.* **1978**, *12*, 2015.
(40) Appel, B. R.; Wesolowski, J. J. In "The Character and Origins of Smog Aerosols; A Digest of Results from the California Aerosol Characterization Experiment (ACHEX)"; Hidy, G. M., Mueller, P. K., Grosjean, D., Appel, B. R., Wesolowski, J. J., Eds.; Wiley: New York, 1980.
(41) Rimberg, D. *Am. Ind. Hyg. Assoc. J.* **1969**, *30*, 394.
(42) Stafford, R. G.; Ettinger, H. J. *Am. Ind. Hyg. Assoc. J.* **1971**, *32*, 319.
(43) Lindeken, C. L.; Morgin, R. L.; Petrock, K. F. *Health Phys.* **1963**, *9*, 305.
(44) Tierney, G. P.; Conner, W. D. *Am. Ind. Hyg. Assoc. J.* **1967**, *28*, 363.
(45) Demuynck, M. *Atmos. Environ.* **1975**, *9*, 523.
(46) Appel, B. R.; Tokiwa, Y.; Haik, M. *Atmos. Environ.*, **1981**, *15*, 283.
(47) Stevens, R. K.; Dzubay, T. G.; Russwurm, G.; Rickel, D. *Atmos. Environ.* **1978**, *12*, 55.

*Received for review May 16, 1980. Accepted February 17, 1981. This work was supported by U.S. Environmental Protection Agency grant R806844 and by State of California Air Resources Board contract A7-169-30.*

# CHAPTER 3

## RELATIVE HUMIDITY AND pH DEPENDENCE OF THE VAPOR PRESSURE OF AMMONIUM NITRATE - NITRIC ACID SOLUTIONS AT 25°C

Accepted for publication in Atmospheric Environment.

# RELATIVE HUMIDITY AND pH DEPENDENCE OF THE VAPOR PRESSURE OF AMMONIUM NITRATE - NITRIC ACID SOLUTIONS AT 25°C

Arthur W. Stelson and John H. Seinfeld
Department of Chemical Engineering
California Institute of Technology
Pasadena, California 91125

## ABSTRACT

Quantitative expressions for the ammonia-nitric acid equilibrium product and the partial pressures of ammonia and nitric acid over non-ideal nitric acid-ammonium nitrate solutions are developed. The relative humidity and pH dependence of the equilibrium product and the partial pressures are obtained from free energy thermodynamic data. The thermodynamic predictions show the ammonia-nitric acid equilibrium product is inversely related to relative humidity. The importance of correcting for non-ideality is demonstrated. The assumption of ideality for ammonium nitrate in solution incurs an error of an order of magnitude in the ammonia-nitric acid equilibrium product prediction at the point of deliquescence and of 20 percent in the relative humidity of deliquescence. The trends indicated by the analysis are consistent with the filter study results of Forrest et al. (1980) and Appel et al. (1980).

INTRODUCTION

The presence of ammonium nitrate in atmospheric aerosols has been confirmed by a number of investigators (Lundgren, 1970; Stephens and Price, 1972; Gordon and Bryan, 1973; Mamane and Pueschel, 1980). The studies of Doyle et al. (1979) and Stelson et al. (1979) have inferred the existence of an equilibrium between ammonium nitrate precursors, ammonia and nitric acid, and solid particulate ammonium nitrate. Using the ambient ammonia and nitric acid data of Spicer (1974) at West Covina, CA, Stelson et al. (1979) showed that the measured and predicted concentration products, $K = P_{NH_3} P_{HNO_3}$, were in essential agreement. Doyle et al. (1979) demonstrated the same phenomenon at Riverside, CA based on FT-IR ammonia and nitric acid measurements.

Significant problems in the measurement of aerosol nitrate have been experienced. Smith et al. (1978) found substantial losses of particulate nitrate and ammonium from high volume glass fiber filter samples taken at Riverside, CA when stored at room temperature. The data of Smith et al. (1978) are re-interpreted in Figure 1, where a least squares fit of the molar ammonium and nitrate losses produces a line with slope 1.094, strongly indicative of $NH_4NO_3$ volatilization. Forrest et al. (1980) spiked filters with $NH_4NO_3$ and drew ambient air through the filters for three to five hours. The greatest $NH_4NO_3$ losses occurred at relative humidities below 60 percent, whereas at 100 percent relative humidity, no $NH_4NO_3$ was lost. Appel et al. (1980) measured $NH_3$ and $HNO_3$ concentration products, $P_{NH_3} P_{HNO_3}$, at Pittsburg, CA using filter techniques and obtained values generally below those needed for saturation even though aerosol nitrate was present.

Stelson and Seinfeld (1981) have shown that Los Angeles aerosols contain ionic solids or concentrated solutions, 8 to 26 molal. The ionic strengths

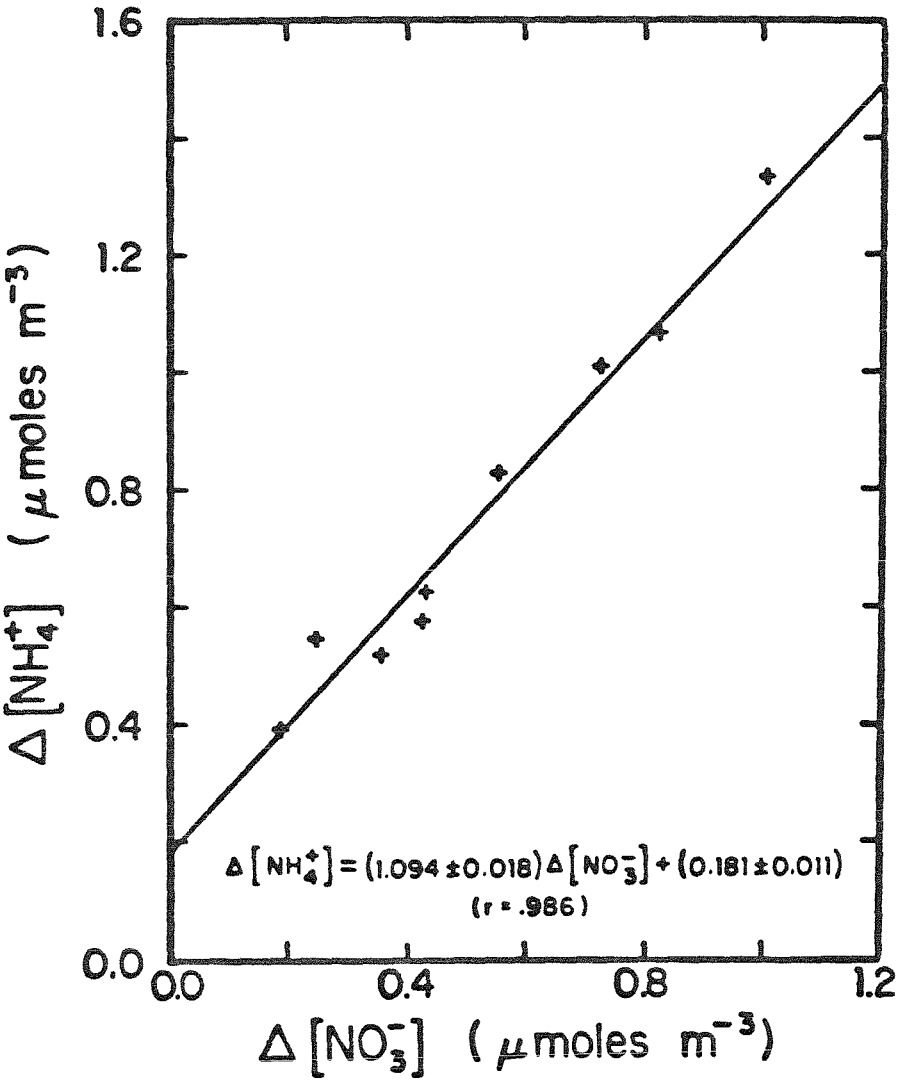


Figure 1. Molar ammonium and nitrate losses from high volume glass fiber filters stored at room temperature.

_____ Linear least square fit

\+ Data of Smith et al. (1978)

corresponding to these concentrations lie in the range where ionic strength is most sensitive to relative humidity, suggesting that relative humidity is an important determinant of aerosol water content.

The object of this work is to further our understanding of the $NH_3$-$HNO_3$-$H_2O$ system by studying the role of relative humidity and pH on the system's equilibrium. One issue that can be addressed with such a study, for example, is explanation of the filter results of Appel et al. (1980) and Forrest et al. (1980). Specifically, we wish to carry out a thermodynamic analysis of the $NH_3$-$HNO_3$-$H_2O$ system at $25^oC$ for pH varying from 1 to 7 and relative humidity varying between 0 and 100 percent. In our analysis no assumptions concerning the ideality of solutions will be made. The results can be compared to those of ideal solution theory as well as to the semi-quantitative ones of Tang (1980a). No corrections will be made for the Kelvin effect, since the aerosols of interest have been shown generally to exceed 0.5 μm diameter (Lundgren, 1970; Mamane and Pueschel, 1980).

A calculation procedure for the ammonia-nitric acid equilibrium product relative humidity dependence over solid and aqueous ammonium nitrate is developed. Then, expressions for the individual ammonia and nitric acid partial pressures over non-ideal ammonium nitrate-nitric acid solutions are derived. Finally, the influence of pH on the partial pressures of ammonia and nitric acid is explored.

AMMONIA-NITRIC ACID EQUILIBRIUM PRODUCT OVER SOLID AND AQUEOUS AMMONIUM NITRATE

Below 62 percent relative humidity at 25°C, ammonium nitrate should be present as a solid, and above this value it should be in solution (Stelson et al., 1979). Although recent work of Tang (1980b) indicates ammonium nitrate does not exhibit traditional deliquescence but is hygroscopic at relative humidities greater than about 30 percent, we will assume ammonium nitrate deliquesces at 62 percent relative humidity for the purpose of this work.

Recent available free energy data for the $NH_3$-$HNO_3$-$H_2O$ system are given in Table 1, from which the equilibrium constants for the $NH_3$-$HNO_3$- $H_2O$ system in Table 2 can be calculated. The equilibrium constants in Table 2 and throughout this paper are thermodynamic equilibrium constants where pressure is referenced to one atmosphere and aqueous solute concentration to unit molality. The differences between the values for reactions 4 to 6 and those of Tang (1980a) are less than 6 percent. A 21 percent difference exists between the equilibrium constant used for reaction 3 by Tang (1980a) and the value in Table 2.

The equilibrium constants listed in Table 2 can be tested for internal consistency in two ways. First, $K_2$ should equal $K_5K_4K_3/K_6$. Based on the values given, $K_5K_4K_3/K_6 = 2.46\times10^{-18}$ versus $K_2 = 2.71\times10^{-18}$, an error of 9.2 percent. Second, $K_1$ should equal $K_2\ a_{NH_4NO_3}$ where $a_{NH_4NO_3}$ = saturated ammonium nitrate solution activity. Using the value of $a_{NH_4NO_3}$ of Hamer and Wu (1972), $K_1 = 3.14\times10^{-17}$, which agrees well with $K_1 = 3.03\times10^{-17}$ as calculated and given in Table 2.

For ammonium nitrate at 25°C below 62 percent relative humidity, the equilibrium product is $K_1$. Above 62 percent the equilibrium product is given by

Table 1. Free Energy Data for the $NH_3$-$HNO_3$-$H_2O$ System at 298°K

| Species | $\Delta G/R$, °K$^{-1}$ | Reference |
|---|---|---|
| $NH_3(g)$ | - 1,977 | Parker et al. (1976) |
| $HNO_3(g)$ | - 8,903 | JANAF (1971) |
| $NH_4NO_3(c,IV)$ | -22,220 | Parker et al. (1976) |
| $NH_4NO_3(aq, m=1)$ | -22,940 | Wagman et al. (1968) |
| $NO_3^-(aq, m=1)$ | -13,410 | Parker et al. (1976) |
| $H^+(aq, m=1)$ | 0 | Parker et al. (1976) |
| $NH_4^+(aq, m=1)$ | - 9,558 | Parker et al. (1976) |
| $H_2O(\ell)$ | -28,530 | Parker et al. (1976) |
| $NH_3 \cdot H_2O(aq)$ | -31,730 | Wagman et al. (1968) |
| $OH^-(aq, m=1)$ | -18,925 | Parker et al. (1976) |

Table 2. Equilibrium Constants for the $NH_3$-$HNO_3$-$H_2O$ System at 298°K

| | Reaction | Equilibrium Constant[a] |
|---|---|---|
| 1 | $NH_4NO_3(c,IV) \rightleftharpoons NH_3(g) + HNO_3(g)$ | $3.03 \times 10^{-17}$ |
| 2 | $NH_4NO_3(aq) \rightleftharpoons NH_3(g) + HNO_3(g)$ | $2.71 \times 10^{-18}$ |
| 3 | $NO_3^-(aq) + H^+(aq) \rightleftharpoons HNO_3(g)$ | $2.72 \times 10^{-7}$ |
| 4 | $NH_3 \cdot H_2O(aq) \rightleftharpoons H_2O(\ell) + NH_3(g)$ | $1.65 \times 10^{-2}$ |
| 5 | $NH_4^+(aq) + OH^-(aq) \rightleftharpoons NH_3 \cdot H_2O(aq)$ | $5.37 \times 10^{4}$ |
| 6 | $H^+(aq) + OH^-(aq) \rightleftharpoons H_2O(\ell)$ | $9.79 \times 10^{13}$ |

[a]Values calculated from the free energy data of Table 1.

$$P_{NH_3}P_{HNO_3} = K_2\gamma_{NH_4}\gamma_{NO_3}m_{NH_4}m_{NO_3} = K_2(\gamma_{\pm})^2_{NH_4NO_3}m^2_{NH_4NO_3} \qquad (1)$$

where $P_{NH_3}$, $P_{HNO_3}$ = the partial pressures of ammonia and nitric acid; $\gamma_{NH_4}$, $\gamma_{NO_3}$ = the molal activity coefficients of the $NH_4^+$ and $NO_3^-$ ions; $m_{NH_4}$, $m_{NO_3}$, $m_{NH_4NO_3}$ = the molalities of $NH_4^+$, $NO_3^-$ and $NH_4NO_3$ and $(\gamma_{\pm})_{NH_4NO_3}$ = the mean molal activity coefficient for $NH_4NO_3$. Using the $NH_4NO_3$ solution activity coefficient data from Hamer and Wu (1972), the equilibrium product can be calculated as a function of $NH_4NO_3$ molality. The relative humidity, R.H., over the solution can be calculated as a function of $NH_4NO_3$ molality from the molal osmotic coefficients in Hamer and Wu (1972),

$$\text{R.H.} = 100.0\ a_w = 100.0 \exp\left(-3.6027\times10^{-2} m_{NH_4NO_3}\ \phi_m\right) \qquad (2)$$

where $a_w$ = the water activity, and $\phi_m$ = the molal osmotic coefficient at $m_{NH_4NO_3}$. Since the equilibrium product and the relative humidity over solution are both solely dependent on $m_{NH_4NO_3}$, the equilibrium product - $m_{NH_4NO_3}$ functionality can be replaced by a function relating the equilibrium product directly to the relative humidity, as in Figure 2. Note that the product, $P_{NH_3}P_{HNO_3}$, is expressed in units of $ppb^2$ in Figure 2 for convenience in atmospheric applications. The effect of non-ideality can be examined by assuming $\phi_m$ and $(\gamma\pm)_{NH_4NO_3}$ are unity. (See the curve labelled ideal solution in Figure 2.) The ideal solution curve ends at $m_{NH_4NO_3}$ = 25.954, saturated $NH_4NO_3$ solution at 25°C, which shows the ideal solution approach grossly mispredicts the deliquiescence relative humidity.

The approach of Tang (1980a) can also be used to evaluate the product, $P_{NH_3}P_{HNO_3}$ for pH, 1 to 7, and ammonium nitrate concentrations, 1.0 to 10.5

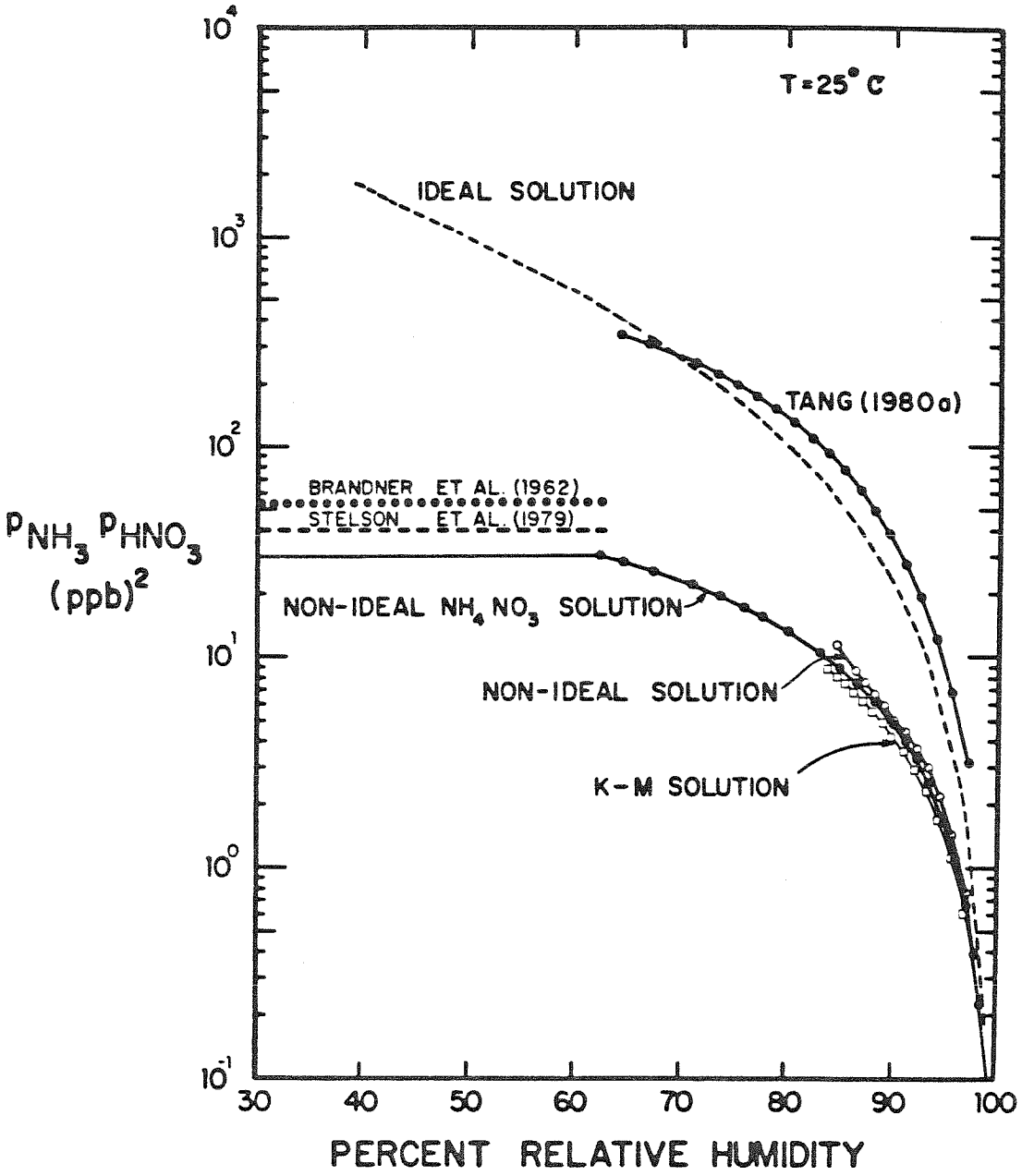


Figure 2. Effect of relative humidity on ammonia-nitric acid partial pressure product.

molar. Over this range of hydrogen, ammonium and nitrate concentrations, the amount of undissociated nitric acid predicted by the approach of Tang (1980a) was less than 0.3 percent. Thus, it is appropriate within this regime to consider the amount of undissociated nitric acid to be zero, i.e. purely an ionic solution. For very acidic solutions, pH < 1, the presence of undissociated nitric acid must be taken into account. The $p_{NH_3}p_{HNO_3}$ values shown in Figure 2 on the curve labelled Tang (1980a) represent the limit as pH → 7, although the variation between pH = 1 and 7 is not large. The water activity was determined assuming the solution was purely ammonium nitrate. The molal osmotic coefficient data from Hamer and Wu (1972) were used to calculate the water activity, and the molar to molal concentration conversion was carried out using $NH_4NO_3$ solution density data of Adams and Gibson (1932). The calculated result is shown in Figure 2.

The solid $NH_4NO_3$ vapor pressure product calculated using a least squares fit of the data of Brandner et al. (1962) and the thermodynamic prediction of Stelson et al. (1979) are also shown in Figure 2. The new solid vapor pressure product prediction and the non-ideal $NH_4NO_3$ solution curve at saturation join closely, indicating the improved quality of this prediction for the $NH_4NO_3$ solid vapor pressure product at 25°C over that of Stelson et al. (1979).

Finally, curves labelled non-ideal and K-M solution are shown in Figure 2. The K-M solution curve was calculated by multiplying ammonia and nitric acid partial pressures determined from equilibria 3-6 in Table 2. The non-ideal solution curve serves as a check of the assumptions used in deriving quantitative expressions for the ammonia and nitric acid partial pressures. The procedure used in calculating the individual nitric acid and ammonia partial pressures will now be developed.

NITRIC ACID PARTIAL PRESSURE

The nitric acid partial pressure is determined from the equilibrium of reaction 3 in Table 2,

$$P_{HNO_3} = K_3 \gamma_H \gamma_{NO_3} m_H m_{NO_3} \quad (3)$$

where $\gamma_H$ = the molal activity coefficient for $H^+$ ion and $m_H$ = $H^+$ ion molality. Kusik and Meissner (1978) developed an expression for predicting the activity coefficient of a salt in a multicomponent electrolytic mixture from which the $\gamma_H \gamma_{NO_3}$ product can be evaluated,

$$\gamma_H \gamma_{NO_3} = (\gamma_\pm)^{1+x}_{H,NO_3} (\gamma_\pm)^{1-x}_{NH_4NO_3} \quad (4)$$

where $x = m_H/m_{NO_3}$ and $(\gamma_\pm)_{H,NO_3}$ = mean molal activity coefficient for dissociated nitric acid. Using the value for $K_3$ determined from thermodynamic data in Table 1,

$$P_{HNO_3} = 272(\gamma_\pm)^{1+x}_{H,NO_3} (\gamma_\pm)^{1-x}_{NH_4NO_3} \times m^2_{NO_3} (ppb) \quad (5)$$

By specifying $m_H$, $m_{NO_3}$ and $m_{NH_4}$, the ionic strength, I, is determined by $I = m_{NO_3} + m_{NH_4}$, and only $(\gamma_\pm)_{H,NO_3}$ needs to be evaluated to calculate the nitric acid partial pressure. The ionic strength functional dependence of $(\gamma_\pm)_{H,NO_3}$ must be calculated by an indirect method which is different from the usual experimental activity coefficient determination methods, vapor pressure, freezing point depression or electrochemical, since nitric acid does not totally dissociate in water.

The degree of dissociation of nitric acid in water as a function of acid concentration can be determined using the approach of Högfeldt (1963), in which the dissociation of nitric acid is represented by three equilbria;

$$HNO_3(H_2O)_3(aq) \rightleftarrows H^+(aq) + NO_3^-(aq) + 3H_2O(\ell) \quad K_a = \frac{[HNO_3(H_2O)_3]}{\{H^+\}\{NO_3^-\}\{H_2O\}^3}$$

$$HNO_3(H_2O)(aq) \rightleftarrows H^+(aq) + NO_3^-(aq) + H_2O(\ell) \quad K_b = \frac{[HNO_3(H_2O)]}{\{H^+\}\{NO_3^-\}\{H_2O\}}$$

$$HNO_3(aq) \rightleftarrows H^+(aq) + NO_3^-(aq) \quad K_c = \frac{[HNO_3]}{\{H^+\}\{NO_3^-\}}$$

where [] represents molar concentration and {} refers to the activity. $K_a$, $K_b$ and $K_c$ are $3.63 \times 10^{-2}$, $8.13 \times 10^{-3}$ and $1.66 \times 10^{-4}$, respectively (Högfeldt, 1963). Högfeldt (1963) assumes the molar activity coefficients of the undissociated aqueous nitrate species to be unity. When converting to a molal basis, the undissociated nitric acid species molal activity coefficient, $\gamma_u$, is not unity, but rather is given by

$$\gamma_u = \frac{1000d}{d_o(1000 + M_{HNO_3} m_s)} \tag{6}$$

where d and $d_o$ are the nitric acid solution and pure water densities in gm $ml^{-1}$, respectively, $M_{HNO_3}$ = the molecular weight of nitric acid, and $m_s$ = the stoichiometric nitric acid molality. Using Högfeldt's equilibria and Equation (6), the fraction of nitric acid that is dissociated, $\alpha$, can be calculated from

$$\alpha = 1 - \frac{d_o \gamma_s^2 m_s}{\gamma_u} (K_a a_w^3 + K_b a_w + K_c) \tag{7}$$

where $\gamma_s$ = the stoichiometric molal nitric acid activity coefficient. The dissociation of nitric acid can be calculated using the stoichiometric molal nitric acid activity and water activity data fit of Hamer and Wu (1972), pure water density and nitric acid molecular weight of Weast (1973), and the nitric acid solution density interpolation formula of Granzhan and Laktionova

(1975). The dissociation calculated from Equation (7) is compared to the dissociation data of Krawetz (1955) and Redlich, et al. (1968) in Figure 3. The agreement, especially with the data of Redlich et al. (1968), is good.

The total nitric acid dissociation constant can be expressed in terms of $K_a$, $K_b$ and $K_c$ by

$$K_N = \frac{1}{K_a a_w^3 + K_b a_w + K_c} \tag{8}$$

Using Högfeldt's equilibrium constants and noting that $a_w = 1.0$ at infinite dilution, $K_N = 22.4$, which compares favorably with values of 15.4, 20.0 and 26.8 from Davis and De Bruin (1964), Redlich et al. (1968) and Young et al. (1959), respectively.

The mean molal ionic activity coefficients for the $H^+$ and $NO_3^-$ ions, $(\gamma_{\pm})_{H,NO_3}$, can be found from

$$(\gamma_{\pm})_{H,NO_3} = \gamma_s/\alpha \tag{9}$$

Using Equations (6), (7) and (9), $(\gamma_{\pm})_{H,NO_3}$ can be calculated as a function of ionic strength. The maximum ionic strength is about 8.3 molal and occurs between 17 to 21 stoichiometric nitric acid molality. The mean molal ionic activity coefficient polynomial regression up to 7.5 molal is

$$\ln(\gamma_{\pm})_{H,NO_3} = \frac{-1.17625\sqrt{I}}{1+1.44\sqrt{I}} + 2.260\times10^{-1} I - 4.722\times10^{-2} I^2$$

$$+ 1.656\times10^{-2} I^3 - 2.396\times10^{-3} I^4 + 1.384\times10^{-4} I^5 \tag{10}$$

where the standard deviation is $\pm$ 0.0022. Although $(\gamma_{\pm})_{H,NO_3}$ should also be a function of the undissociated nitric acid concentration, the effect of undissociated nitric acid will be shown to be negligible up to 7.0 ionic strength.

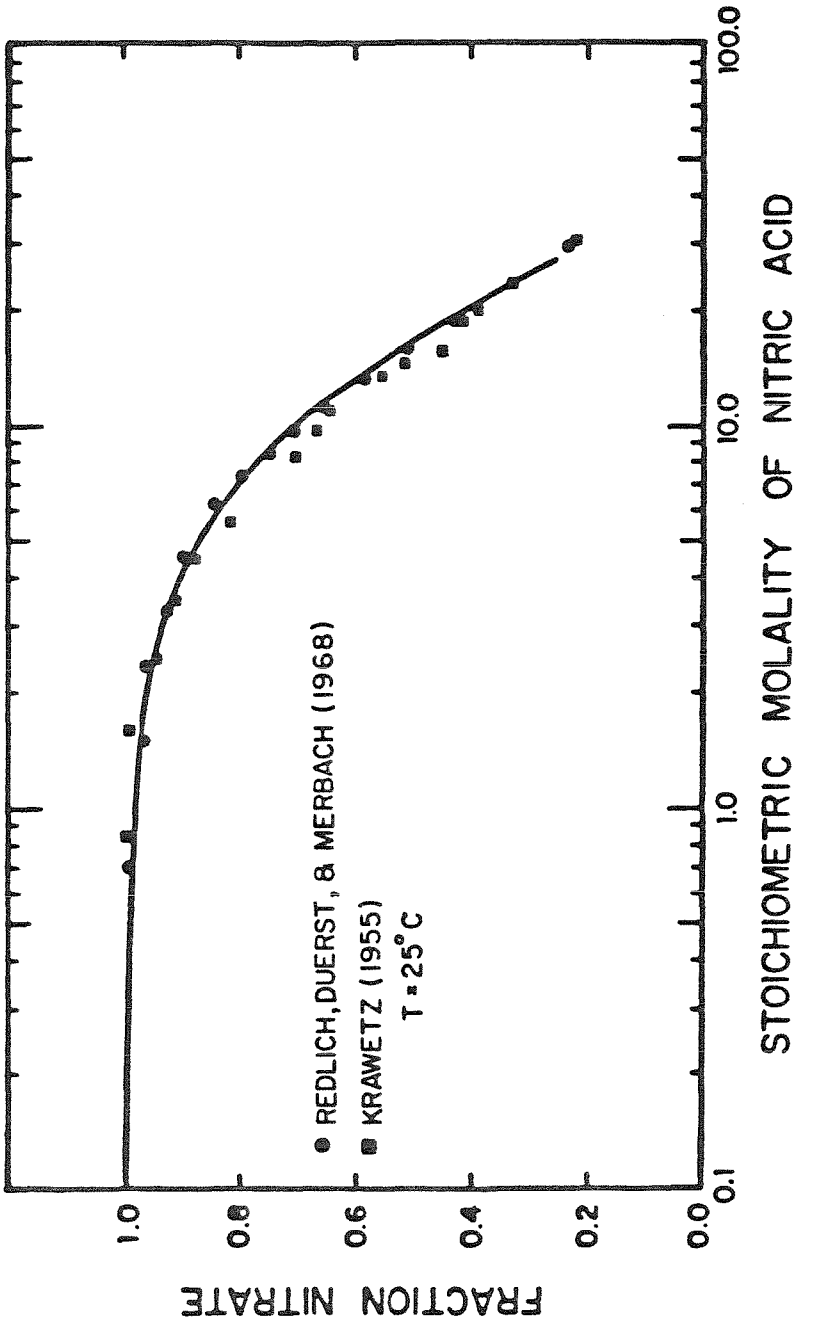


Figure 3. Ionization of nitric acid.

AMMONIA PARTIAL PRESSURE

The partial pressure of ammonia over the solution is (Tang, 1980a)

$$p_{NH_3} = \frac{K_4 K_5}{K_6} \frac{\gamma_{NH_4}}{\gamma_H} \frac{m_{NH_4}}{m_H} \tag{11}$$

By specifying $m_{NH_4}$, $m_H$ and $m_{NO_3}$, the ionic strength is determined, and $\gamma_{NH_4}/\gamma_H$ depends on the ionic strength. From the approach of Kusik and Meissner (1978)

$$\frac{\gamma_{NH_4}}{\gamma_H} = \frac{(\gamma_\pm)_{NH_4NO_3}}{(\gamma_\pm)_{H,NO_3}} \tag{12}$$

and Equation (11) simplifies to

$$p_{NH_3} = 9.05 \times 10^{-3} \frac{(\gamma_\pm)_{NH_4NO_3}}{(\gamma_\pm)_{H,NO_3}} \left( \frac{1-x}{x} \right) \text{(ppb)} \tag{13}$$

with the values for the equilibrium constants from Table 2.

VARIATION OF AMMONIA AND NITRIC ACID PARTIAL PRESSURES AS A FUNCTION OF pH

The variation of the ammonia and nitric acid partial pressures as a function of pH can be evaluated using the expression for $(\gamma_\pm)_{NH_4NO_3}$ from Hamer and Wu (1972) and Equations (5), (10) and (13). The water activity of the $NH_4NO_3$-$HNO_3$ solution, $(a_w)_{MIX}$, is given by

$$(a_w)_{MIX} = (a_w)^x_{H,NO_3} (a_w)^{1-x}_{NH_4NO_3} \tag{14}$$

where $(a_w)_{H,NO_3}$ is obtained from Equation (10) and the Gibbs-Duhem relationship (Kusik and Meissner, 1978). The variation of $p_{NH_3}$ and $p_{HNO_3}$ with pH is shown in Figure 4 for a relative humidity of 94.5 percent. Also, shown are the

results of Tang (1980a) and those calculated assuming an ideal solution. The solid lines labelled Tang (1980a) were taken directly from Tang (1980a), and the points labelled Tang (1980a) were calculated using his procedure to insure an accurate duplication of that work. Figure 4 shows the approach of this work and that of Tang (1980a) differ in both the individual ammonia and nitric acid partial pressures, differences that become larger so the relative humidity decreases or ionic strength increases.

The product of the ammonia and nitric acid partial pressures calculated from Equations (5) and (13) as a function of relative humidity is compared to the equilibrium product calculated using ammonium nitrate activities in Figure 2. By comparing the curves labelled K-M solution and non-ideal $NH_4NO_3$ solution, the agreement is shown to be good. The major source of disagreement between the K-M solution and the non-ideal $NH_4NO_3$ solution curves is the 9.2% difference between $K_5K_4K_3/K_6$ and $K_2$. The insensitivity of $p_{NH_3}p_{HNO_3}$ to pH can be seen in the range of relative humidity variation by multiplying Equations (5) and (13),

$$p_{NH_3}p_{HNO_3} = 2.46(\gamma_{\pm})^{x}_{H,NO_3}(\gamma_{\pm})^{2-x}_{NH_4NO_3}(1-x)m^{2}_{NO_3}(ppb^2). \qquad (15)$$

As the relative humidity decreases, the maximum x, which occurs at pH = 1, becomes smaller. Thus, the difference between an acidic ammonium nitrate solution (pH > 1) and a pure ammonium nitrate solution partial pressure product decreases with relative humidity.

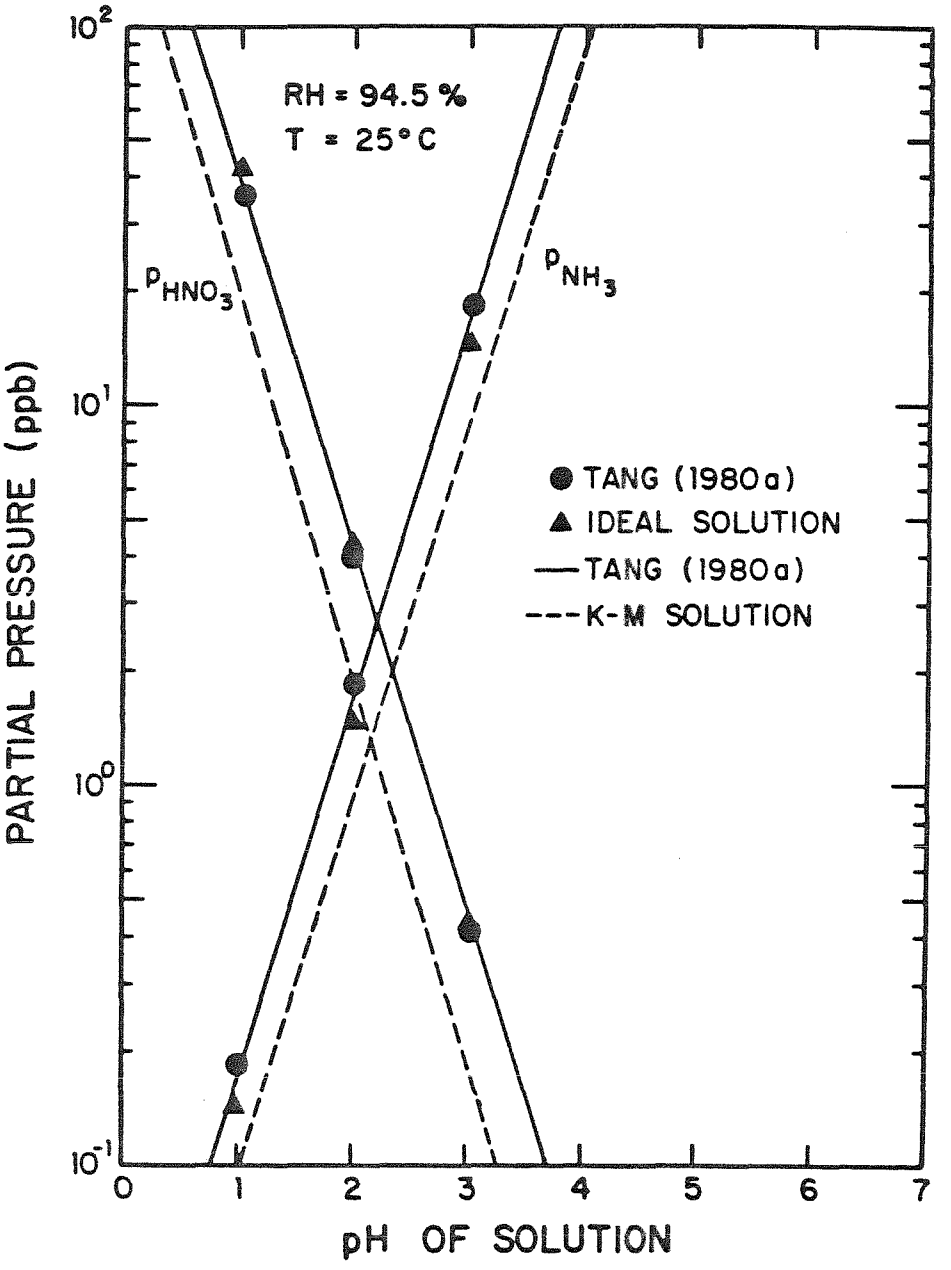


Figure 4. Effect of pH on the ammonia and nitric acid partial pressures.

EFFECT OF NEGLECTING UNDISSOCIATED NITRIC ACID AND ION-PAIRING

In developing quantitative expressions for the ammonia and nitric acid partial pressures, two assumptions were invoked. First, the effect of undissociated nitric acid on the $(\gamma_{\pm})_{H,NO_3}$ ionic strength functionality is small below 7.0 molal. Second, ion-pairing of $NH_4^+$ and $NO_3^-$ ions has a minimal effect on the ammonia partial pressures predicted. Equation (15) requires as $x \to 0$, the solute activity approaches $(\gamma_{\pm})^2_{NH_4NO_3} m^2_{HN_4NO_3}$. Similarly, Equation (4) requires $\gamma_H \gamma_{NO_3}$ to approach $(\gamma_{\pm})^2_{H,NO_3}$ as $x \to 1$. Inherent in Equations (4) and (15) are the correct limits but neither equation gives insight into the effect of these two assumptions. By an alternative expression for $(\gamma_{\pm})^2_{NH_4NO_3}$,

$$(\gamma_{\pm})^2_{NH_4NO_3} = \gamma_{NH_4}\gamma_{NO_3} = \frac{\gamma_{NH_4}}{\gamma_H} (\gamma_H \gamma_{NO_3}) \qquad (16)$$

where $\gamma_{NH_4}/\gamma_H$ and $\gamma_H\gamma_{NO_3}$ are evaluated independently from $NH_4NO_3$, the relative error can be ascertained.

The $\gamma_H\gamma_{NO_3}$ product will be given by $(\gamma_{\pm})^2_{H,NO_3}$ which assumes the undissociated nitric acid contribution is small.

The ammonium to hydrogen ion activity coefficient ratio, $\gamma_{NH_4}/\gamma_H$, can be evaluated from mean molal activity coefficients of an ammoniated salt, $NH_4X$, and the acid with the same anion, HX, provided the acid completely dissociates. The ammonium to hydrogen ion activity coefficient ratio can be calculated noting that

$$\frac{\gamma_{NH_4}}{\gamma_H} = \left( \frac{(\gamma_{\pm})_{NH_4X}}{(\gamma_{\pm})_{HX}} \right)^2 \qquad (17)$$

where $(\gamma_{\pm})_{NH_4X}$ = the mean molal activity coefficient of salt $NH_4X$ and $(\gamma_{\pm})_{HX}$ = the mean molal activity coefficient of acid HX. This approach was tested with five different anions, $C\ell^-$, $NO_3^-$, $I^-$, $Br^-$ and $C\ell O_4^-$. (See Figure 5.) The assumption that $HC\ell$, HBr, HI and $HC\ell O_4$ totally dissociate in solutions below 7 molal

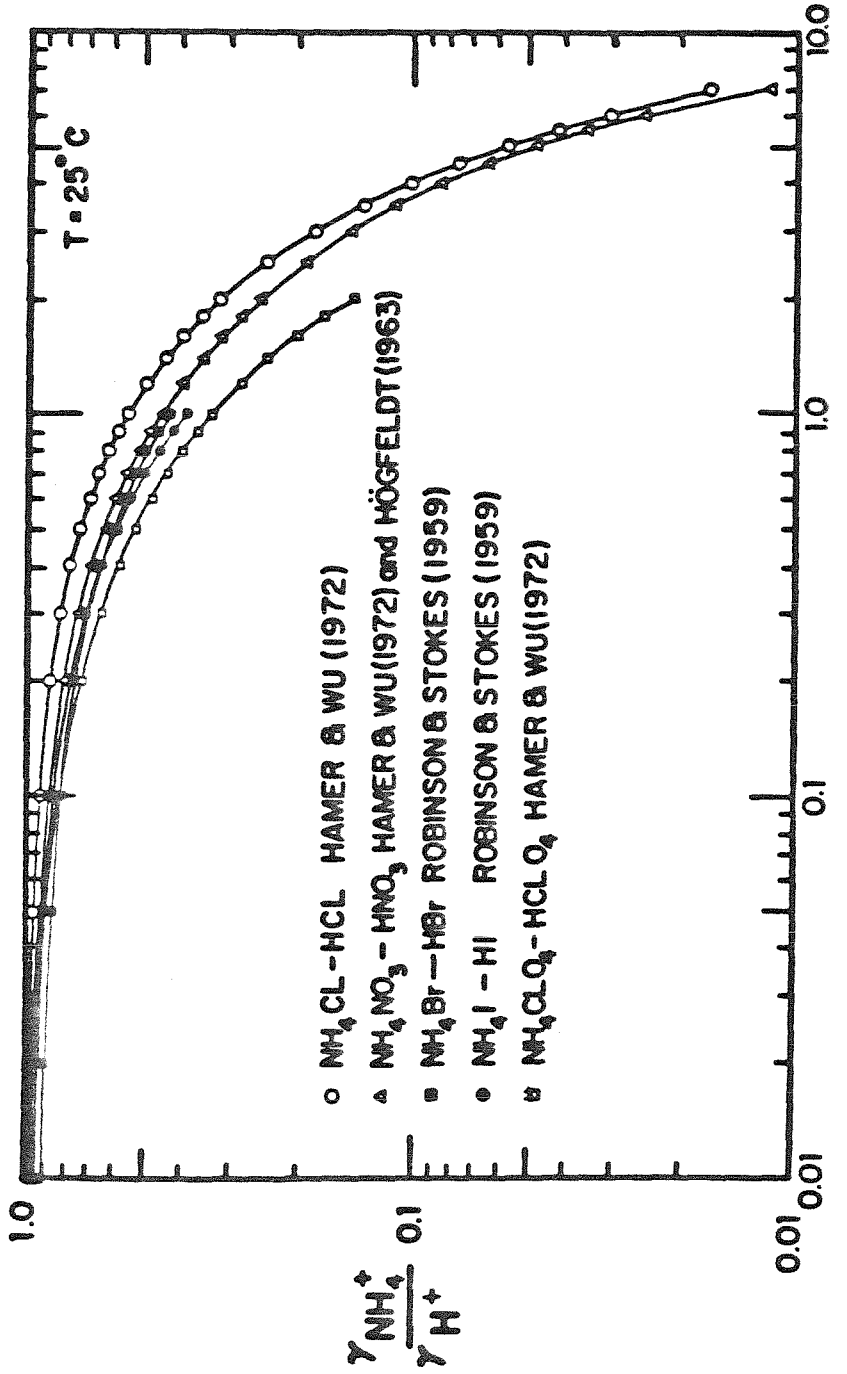


Figure 5. Effect of ionic strength on calculated ammonium/hydrogen ion mean molal activity coefficient ratio.

or saturation is appropriate since the dissociation constants are very large, $> 10^7$ (McCoubrey, 1955; Bockris and Reddy, 1970). It is incorrect to assume that $HNO_3$ completely dissociates, so the $NO_3^-$ curve was calculated using $(\gamma_{\pm})_{H,NO_3}$ as previously derived.

Lee and Wilmshurst (1964) have shown that a 5 molar $NH_4C\ell$ solution forms ion-pairs. The observed mean molal activity coefficient, $(\gamma_{\pm})_{NH_4X}$, must be corrected as follows (Bockris and Reddy, 1970),

$$(\gamma_{\pm})'_{NH_4X} = \frac{(\gamma_{\pm})_{NH_4X}}{1-\theta} \qquad (18)$$

where $(\gamma_{\pm})'_{NH_4X}$ = the corrected mean molal activity coefficient for salt $NH_4X$ and $\theta$ = the fraction of $NH_4$ and X ions forming ion-pairs. Equation (18) assumes the ion-pairs are symmetric (Robinson and Stokes, 1959). Also, the ionic strength would be corrected to $(1-\theta)m_{NH_4X}$. The net effect of ion-pairing on the curves in Figure 5 is not obvious since the $NH_4X$ mean molal activity coefficient would increase and the ionic strength would decrease. Using density data of Pearce and Pumplin (1937), a 5-molar $NH_4C\ell$ solution is approximately 6.25-molal. The $NH_4C\ell$-$HC\ell$ ammonium to hydrogen ion activity coefficient ratio is used to represent $\gamma_{NH_4}/\gamma_H$ to 7.0 molal. Thus, some $NH_4C\ell$ ion-pairing must be present above 6.25 molal.

With Equations (1), (10), (16), and (17) and replacing $K_2$ by $K_5K_4K_3/K_6$, the effect of ion-pairing and the undissociated nitric acid can be ascertained. We refer the reader to the curve labelled non-ideal solution in Figure 2. The water activity was calculated from Equation (2). The agreement between the non-ideal, non-ideal $NH_4NO_3$, and K-M solution curves supports the assumptions

of neglecting both the influence of undissociated nitric acid on the mean molal activity coefficient of dissociated nitric acid, $(\gamma_{\pm})_{H,NO_3}$, and the presence of ion-pairing in calculating $\gamma_{NH_4}/\gamma_H$. By comparing the K-M and non-ideal solution curves, the maximum possible error in the individual partial pressures can be ascertained as about 30%.

Assuming $\gamma_H\gamma_{NO_3} \equiv (\gamma_{\pm})^2_{H,NO_3}$ and Equation (17) holds, the $\gamma_H\gamma_{NO_3}$ product and the $\gamma_{NH_4}/\gamma_H$ ratio calculated cannot be used for calculating the individual partial pressures of ammonia and nitric acid because $\gamma_H\gamma_{NO_3}$ goes to the wrong limit as $x \to 0$ and $\gamma_{NH_4}/\gamma_H$ goes to the wrong limit as $x \to 1$. Even though these expressions cannot be used for the individual partial pressures, they can be multiplied together to check the ammonia-nitric acid partial pressure product calculated from Equations (1) and (15) and the possible significance of ion-pairing and the undissociated nitric acid in calculating $(\gamma_{\pm})_{H,NO_3}$.

DISCUSSION

This approach gives theoretical justification for the results of Forrest et al. (1980) and Appel et al. (1980). As the relative humidity approaches 100 percent, the equilibrium vapor pressure product sharply decreases by several orders of magnitude. At 98 percent relative humidity and 25°C, the mass concentration of $NH_3$ plus $HNO_3$ (equimolar basis) in the gas in equilibrium with an aqueous ammonium nitrate solution is about 1.9 $\mu g\ m^{-3}$ versus 17.9 $\mu g\ m^{-3}$ needed if ammonium nitrate is present as a solid. Thus, the observation of Forrest et al. (1980) that greatest ammonium nitrate filter losses occurred at relative humidities below 60 percent, and no losses occurred at 100 percent relative humidity, and the observations of Appel et al. (1980) that nitrate aerosol is present even though the equilibrium product of ammonia and nitric acid is much less than the solid equilibrium product are consistent with this work.

The ammonia-nitric acid equilibrium product relative humidity functionality does not significantly change when the pH is varied between 1 and 7. The insensitivity of the ammonia-nitric acid equilibrium product with pH variation results from the ammonia-nitric acid equilibrium product being dominantly dependent on ionic strength. As the pH decreases below 1, the approach used in this work is not applicable since the role of undissociated nitric acid becomes significant and similarly for high pH undissociated dissolved ammonia would appear. From the electroneutrality balance and the average aerosol water data in Stelson and Seinfeld (1981), a range of possible mass distribution averaged pHs between 2 and 12 is calculable for several locations in the Los Angeles Basin. Since the atmospheric aerosol is often a mixture of acidic and basic particles,

a distribution of aerosol pH would exist, the basic particles existing predominantly in the coarse mode (> 1 μm) and the acidic particles in the fine mode (< 1 μm). Thus, these results have limited applicability to the possible range of existing ambient aerosol acidity.

Qualitatively, the result of adding an unreactive solute on the vapor pressure product-relative humidity curve can be discussed. The unreactive solute would lower the water vapor pressure but would not affect the ammonia-nitric acid vapor pressure product. Thus, the resulting situation would be a measured vapor pressure product and relative humidity location lying below the $NH_4NO_3$ non-ideal vapor pressure product-relative humidity curve in Figure 2.

The presence of a saturated ammonium nitrate solution around a solid ammonium nitrate aerosol core can be examined. Since the saturated solution must be in equilibrium with solid ammonium nitrate, the vapor pressure product must be the same over the saturated solution as for the solid ammonium nitrate. Thus, the presence of a saturated aqueous layer around a solid ammonium nitrate core at relative humidities below 62 percent would not affect the equilibrium vapor pressure product prediction.

An additional important thermodynamic concept is the Gibbs-Duhem relationship which shows the solute activities determine the water activity. Thus, the equilibrium product and the relative humidity cannot be varied independently and to be theoretically consistent the solute or water activity must be determined by the other activities. Equation (14) shows the water activity can be taken as the water activity of a pure ammonium nitrate solution since the solutions are greater than 90 percent ammonium nitrate and the correction to make this theoretically rigorous is small.

Finally, this work illustrates an important concept in devising methods for performing equilibrium analysis. The equilibrium approach must be consistent, and certain limits must be satisfied. Internal consistency was demonstrated by the agreement between $K_2$ and $K_5K_4K_3/K_6$ and by the ammonia-nitric acid vapor pressure products of solid ammonium nitrate and a saturated ammonium nitrate solution being equal.

## CONCLUSIONS

Some important conclusions are evident from this work:

(1) The ammonia-nitric acid equilibrium product is strongly and inversely dependent on the relative humidity.

(2) A consistent set of free energy data exists such that the ammonia-nitric acid equilibrium products for solid ammonium nitrate and for a saturated ammonium nitrate aqueous solution are equal; i.e. no discontinuity exists in the ammonia-nitric acid equilibrium product prediction at the relative humidity of deliquescence at $25^{o}C$.

(3) The ammonium to hydrogen ion molal activity coefficient ratio is not unity for concentrated ionic solutions. By assuming it is unity, significant error in the calculated ammonia partial pressure results.

(4) The predicted relative humidity dependence of the ammonia-nitric acid equilibrium product is consistent with filter study results of Forrest et al. (1980) and Appel et al. (1980).

## ACKNOWLEDGMENT

This work was supported by Environmental Protection Agency grant R806844 and State of California Air Resources Board contract A7-169-30.

REFERENCES

Adams L.H. and Gibson R.E. (1932) Equilibrium in binary systems under pressure. III. The influence of pressure on the solubility of ammonium nitrate in water at 25°C. J. Amer. Chem. Soc. 54, 4520-4537.

Appel B.R., Wall S.M., Tokiwa Y. and Haik M.(1980) Simultaneous nitric acid, particulate nitrate and acidity measurements in ambient air. Atmospheric Environment 14, 549-554.

Bockris J. O'M. and Reddy A.K.N. (1970) Modern Electrochemistry; An Introduction to an Interdisciplinary Area, Volume 1, Plenum Press, New York.

Brandner J.D., Junk N.M., Lawrence J.W. and Robins J. (1962) Vapor pressure of ammonium nitrate. J. Chem. Engng. Data 7, 227-228.

Davis W. Jr. and De Bruin H.J. (1964) New activity coefficients of 0-100 per cent aqueous nitric acid. J. Inorg. Nucl. Chem. 26, 1069-1083.

Doyle G.J., Tuazon E.C., Graham R.S., Mischke T.M., Winer A.M. and Pitts J.N. Jr. (1979) Simultaneous concentrations of ammonia and nitric acid in a polluted atmosphere and their equilibrium relationship to particulate ammonium nitrate. Environ. Sci. Technol. 13, 1416-1419.

Forrest J., Tanner R.L., Spandau D., D'Ottavio T. and Newman L. (1980) Determination of total inorganic nitrate utilizing collection of nitric acid on NaCℓ-impregnated filters. Atmospheric Environment 14, 137-144.

Gordon R.J. and Bryan R.J. (1973) Ammonium nitrate in airborne particles in Los Angeles. Environ. Sci. Technol. 7, 645-647.

Granzhan V.A. and Laktionova S.K. (1975) The densities, viscosities, and surface tensions of aqueous nitric acid solutions. Russ. J. Phys. Chem. 49, 1448.

Hamer W.J. and Wu Y.C. (1972) Osmotic coefficients and mean activity coefficients of uni-univalent electrolytes in water at 25°C. J. Phys. Chem. Ref. Data 1, 1047-1099.

Högfeldt E. (1963) The complex formation between water and strong acids. Acta Chemica Scandinavica 17, 785-796.

JANAF Thermochemical Tables, 2nd Edn (1971), NSRDS-NBS 37.

Krawetz A.A. (1955) A Raman Spectral Study of Equilibria in Aqueous Solutions of Nitric Acid, Thesis, University of Chicago.

Kusik C.L. and Meissner H.P. (1978) Electrolyte activity coefficients in inorganic processing. A.I.Ch.E. Symp. Ser. 173, 14-20.

Lee H. and Wilmhurst J.K. (1964) Observation of ion-pairs in aqueous solutions by vibrational spectroscopy. Aust. J. Chem. 17, 943-945.

Lundgren D.A. (1970) Atmospheric aerosol composition and concentration as a function of particle size and of time. J. Air Pollut. Control Ass. 20, 603-608.

Mamane Y. and Pueschel R.F. (1980) A method for the detection of individual nitrate particles. Atmospheric Environment 14, 629-639.

McCoubrey J.C. (1955) The acid strength of the hydrogen halides. Faraday Soc. Trans. 51, 743-747.

Parker V.B., Wagman D.D. and Garvin D. (1976) Selected thermochemical data compatible with the CODATA recommendations. NBSIR 75-968.

Pearce J.N. and Pumplin G.G. (1937) The apparent and partial molal volumes of ammonium chloride and of cupric sulfate in aqueous solution at 25°C. J. Amer. Chem. Soc. 59, 1221-1222.

Redlich O., Duerst R.W. and Merbach A. (1968) Ionization of strong electrolytes. XI. The molecular states of nitric acid and perchloric acid. J. Chem. Phys. 49, 2986-2994.

Robinson R.A. and Stokes R.H. (1959) Electrolyte Solutions; The Measurement and Interpretation of Conductance, Chemical Potential and Diffusion in Solutions of Simple Electrolytes, 2nd. Edn. Butterworths, London.

Smith J.P., Grosjean D. and Pitts J.N. Jr. (1978) Observation of significant losses of particulate nitrate and ammonium from high volume glass fiber filter samples stored at room temperature. J. Air Pollut. Control Ass. 28, 930-933.

Spicer C.W. (1974) The fate of nitrogen oxides in the atmosphere. Batelle Columbus Rep. to Coordinating Res. Council and U.S. Environ. Protection Agency Rep. 600/3-76-030.

Stelson A.W., Friedlander S.K. and J.H. Seinfeld (1979) A note on the equilibrium relationship between ammonia and nitric acid and particulate ammonium nitrate. Atmospheric Environment 13, 369-371.

Stelson A.W. and Seinfeld J.H. (1981) Chemical mass accounting of urban aerosol, submitted to Environ. Sci. Technol.

Stephens E.R. and Price M.A. (1972) Comparison of synthetic and smog aerosols. J. Coll. Int. Sci. 39, 272-286.

Tang I.N. (1980a) On the equilibrium partial pressures of nitric acid and ammonia in the atmosphere. Atmospheric Environment 14, 819-828.

Tang I.N. (1980b) Deliquescence properties and particle size change of hygroscopic aerosols. In Generation of Aerosols, Ch. 7, ed. by K. Willeke, Ann Arbor Science Publisher, Ann Arbor, Michigan.

Wagman D.D., Evans W.H., Parker V.B., Harlöw I., Baily S.M. and Schumm R.H. (1968) Selected values of chemical thermodynamic properties; tables for the first thirty-four elements in the standard order of arrangement, NBS technical note 270-3.

Weast R.C. (1973) Handbook of Chemistry and Physics, 54th. Edn. CRC Press, Cleveland.

Young T.F., Maranville L.F. and Smith H.M. (1959) Raman spectral investigation of ionic equilibria in solutions of strong electrolytes. In The Structure of Electrolytic Solutions, Ch. 4, ed. by W.J. Hamer, John Wiley & Sons, New York.

# CHAPTER 4

## RELATIVE HUMIDITY AND TEMPERATURE DEPENDENCE OF THE AMMONIUM NITRATE DISSOCIATION CONSTANT

Accepted for publication in Atmospheric Environment.

# RELATIVE HUMIDITY AND TEMPERATURE DEPENDENCE OF THE AMMONIUM NITRATE DISSOCIATION CONSTANT

A. W. Stelson and J. H. Seinfeld
Department of Chemical Engineering
California Institute of Technology
Pasadena, California 91125

## ABSTRACT

Expressions for predicting the temperature and relative humidity dependence of the $NH_4NO_3$ dissociation constant are derived from fundamental thermodynamic principles. The general trends predicted by the theory agree with the atmospheric data of Appel et al. (1979, 1980), Pitts (1978, 1979) and Tuazon et al. (1980).

## INTRODUCTION

Ammonium nitrate has been identified in atmospheric aerosol (Lundgren, 1970; Stephens and Price, 1972; Gordon and Bryan, 1973; Mamane and Pueschel, 1980). An understanding of the temperature and relative humidity dependence of the relationship between $NH_4NO_3$ and its precursors, $NH_3$ and $HNO_3$, is desirable.

Stelson et al. (1979) and Doyle et al. (1979) showed that measured atmospheric ammonia-nitric acid partial pressure products scattered about the thermodynamically predicted solid $NH_4NO_3$ dissociation constant, indicating the likelihood of chemical equilibrium existing in this system. Stelson and Seinfeld (1981a) demonstrated that Los Angeles aerosols contain ionic solids or concentrated solutions, 8 to 26 molal, indicating that any thermodynamic analysis must account for non-idealities present in concentrated solutions. Stelson and Seinfeld (1981b) calculated the ammonia and nitric acid partial pressures over ammonium nitrate-nitric acid solutions accounting for nitrate, hydrogen and ammonium ion non-idealities. Their analysis showed the ammonia-nitric acid partial pressure product is sensitive to relative humidity but insensitive to pH(1-7). Thus, the aqueous $NH_4NO_3$ dissociation constant at a specific temperature and relative humidity should typify the ammonia-nitric acid partial pressure product of a slightly acidic ammonium nitrate solution.

Atmospheric gas phase ammonia and nitric acid and particulate nitrate measurements demonstrate important trends. Significant amounts of ammonium nitrate precursors, ammonia and nitric acid, have been found in urban air

accompanied by strong diurnal trends (Spicer, 1974; Pitts, 1978, 1979; Appel et al., 1979; Tuazon et al., 1980). Stelson et al. (1979) and Doyle et al. (1979) explained these observations through temperature dependence of the solid $NH_4NO_3$ dissociation constant. Appel et al. (1979) observed that measured ammonia-nitric acid partial pressure products were less than the predicted dissociation constant even though aerosol nitrate was present. Forrest et al. (1980) spiked filters with $NH_4NO_3$ and drew ambient air through the filters for three to five hours. The greatest $NH_4NO_3$ losses occurred at relative humidities below 60 percent, whereas at 100 percent relative humidity, no $NH_4NO_3$ was lost. Stelson and Seinfeld (1981b) were able to explain the results of Appel et al. (1979) and Forrest et al. (1980) by the relative humidity dependence of the $NH_4NO_3$ dissociation constant at 25°C. Appel et al. (1980) observed a temperature and relative humidity dependence of measured ammonia-nitric acid partial pressure products.

The object of this work is to derive expressions for the temperature and relative humidity dependence of the $NH_4NO_3$ dissociation constant based on fundamental thermodynamic principles. The temperature dependence of the solid $NH_4NO_3$ dissociation constant will be calculated using the method developed by Stelson et al. (1979). The regions where ammonium nitrate is in the solid form or in aqueous solution will be determined from expressions for the $NH_4NO_3$ relative humidity of deliquescence and solubility. For aqueous ammonium nitrate, the $NH_4NO_3$ dissociation constant and solution relative humidity will be calculated by non-ideal aqueous solution thermodynamics. Using appropriate expressions for the $NH_4NO_3$ dissociation constant, a diagram can be constructed for the temperature and relative humidity dependence of the $NH_4NO_3$ dissociation constant. Finally, the thermodynamic predictions are compared with ambient measurements of Appel et al. (1979, 1980), Pitts (1978, 1979) and Tuazon et al. (1980).

## THEORY AND THERMODYNAMIC DATA FOR THE AMMONIUM NITRATE SYSTEM

### Solid $NH_4NO_3$ Dissociation Constant

At temperatures below 170°C, solid ammonium nitrate exists in equilibrium with ammonia and nitric acid:

$$NH_4NO_3(s) \rightleftharpoons NH_3(g) + HNO_3(g). \tag{1}$$

The equilibrium constant for this reaction, $K_p'$, is related to the partial pressures of $NH_3$ and $HNO_3$ by $K_p' = p_{NH_3} p_{HNO_3}$, and $K_p'$ is related to the standard Gibbs free energy change for reaction, $\Delta G_T^o$, by

$$\Delta G_T^o = - RT \ln K_p'. \tag{2}$$

Since the thermodynamic data for $NH_4NO_3$ are limited, an extrapolation formula for the equilibrium constant as a function of temperature can be derived by integrating the van't Hoff equation,

$$\ln K_p' = \alpha - \frac{\Delta H_o}{RT} + \int_{298}^{T} \frac{1}{RT''^2} \int_{298}^{T''} \left( C_{p_{NH_3}} + C_{p_{HNO_3}} - C_{p_{NH_4NO_3}} \right) dT' dT''. \tag{3}$$

where $\alpha$ = integration constant, $\Delta H_0$ = change in enthalpy at 298°K, and $C_{p_{NH_3}}$, $C_{p_{HNO_3}}$, $C_{p_{NH_4NO_3}}$ = the heat capacities of $NH_3$, $HNO_3$ and $NH_4NO_3$, respectively. Using the data in Table 1 and assuming the heat capacities are independent of temperature, we obtain from (3),

$$\ln K = 84.6 - \frac{24220}{T} - 6.1 \ln \left( \frac{T}{298} \right) \tag{4}$$

where K is the equilibrium constant in units of $ppb^2$.

Table 1. Thermodynamic Data for the Ammonium Nitrate System at 298°K

| Species | $\frac{\Delta G}{R}$, °K$^{-1}$ | $\frac{\Delta H}{R}$, °K$^{-1}$ | $\frac{C_p}{R}$ | Reference |
|---|---|---|---|---|
| $NH_3(g)$ | - 1,977* | - 5,526* | 4.285 | Parker et al. (1976)* and JANAF (1971) |
| $HNO_3(g)$ | - 8,903 | -16,155 | 6.416 | JANAF (1971) |
| $NH_4NO_3(c,IV)$ | -22,220* | -44,080* | 16.8 | Parker et al. (1976)* and Wagman et al. (1968) |
| $NH_4NO_3(aq,m=1)$ | -22,940$^+$ | -40,880$^+$ | -0.505 | Wagman et al. (1968)$^+$ and Roux et al. (1978) |

$\Delta G$ = Standard free energy of formation

$\Delta H$ = Heat of formation

$C_p$ = Heat capacity

Relative Humidity of Deliquescence and Solubility

Up to the relative humidity of deliquescence, ammonium nitrate should be present as a solid. The results of Tang (1980 ) indicate $NH_4NO_3$ aerosol is quite hygroscopic at ~30% relative humidity versus ~62% observed for bulk $NH_4NO_3$ at 25°C (Dingemans, 1941; Adams and Merz, 1929; Edgar and Swan, 1922; Prideaux, 1920). Whether the observation of Tang (1980 ) is the result of a property unique to the size of the $NH_4NO_3$ aerosol or the presence of an impurity is difficult to ascertain. Prideaux (1920) observed that the presence of a small amount of sodium nitrate in ammonium nitrate significantly reduced the relative humidity of deliquescence. Since we cannot adequately evaluate the observations of Tang (1980 ), we will assume $NH_4NO_3$ exhibits traditional deliquescence as implied by the majority of the literature.

An expression can be derived for the saturated solution relative humidity

$$\text{ln}(RHD) = -\frac{L}{R}\left(\frac{1}{T} - \frac{1}{298}\right) + \text{ln}\,(RHD)_{298} \qquad (5)$$

where RHD = percent relative humidity of deliquescence and L = water heat of fusion (Denbigh, 1971). Using the water heat of fusion from Weast (1973) and the relative humidity of a saturated $NH_4NO_3$ solution at 298.15°K from Hamer and Wu (1972),

$$\text{ln}\,(RHD) = \frac{723.7}{T} + 1.7037. \qquad (6)$$

Equation (6) agrees well with the least square expression derived from the data of Dingemans (1941),

$$\text{ln}\,(RHD) = \frac{856.23 \pm 13.25}{T} + 1.2306 \pm 0.0439 \qquad (7)$$

Equations (6) and (7) are shown with experimental data in Figure 1.

For an ideal solution, the solubility temperature dependence is

$$\left(\frac{\partial \ln(m^2)}{\partial T}\right)_p = \frac{\bar{H}^o - h^s}{RT^2} \tag{8}$$

where m = $NH_4NO_3$ molality, $\bar{H}^o$ = the $NH_4NO_3$ partial molal enthalpy at infinite dilution and $h^s$ = enthalpy of crystalline $NH_4NO_3$. By integrating Equation (8),

$$\ln m = -\frac{(\bar{H}^o - h^s)}{2R}\left(\frac{1}{T} - \frac{1}{298}\right) + \ln(m)_{298} \tag{9}$$

is obtained. Using the thermodynamic data in Table 1 and noting that $(m)_{298}$ = 25.954 from Hamer and Wu (1972),

$$\ln m = -\frac{1600}{T} + 8.6228 \ . \tag{10}$$

Equation (10) agrees well with the least squares expression for the data of Stephen and Stephen (1963),

$$\ln m = -\frac{1837.3 \pm 18.0}{T} + 9.4235 \pm 0.0602. \tag{11}$$

Equations (10) and (11) are shown with the data of Stephen and Stephen (1963) in Figure 2.

Figures 1 and 2 show the strong temperature dependence of the relative humidity of deliquescence and the solubility of ammonium nitrate. This temperature dependence is an unfortunate complication when attempting to extrapolate aqueous ammonium nitrate thermodynamic data to temperatures above 25°C.

Aqueous $NH_4NO_3$ Dissociation Constant

Analogous to the solid $NH_4NO_3$ dissociation constant derivation, an expression for the equilibrium constant over aqueous $NH_4NO_3$ can be derived,

$$\ln K_p^* = \alpha - \frac{\Delta H_o}{RT} + \int_{298}^{T} \frac{1}{RT''^2} \int_{298}^{T''} \left( C_{p_{NH_3}} - C_{p_{HNO_3}} - \bar{C}^o_{p_{NH_4NO_3}} \right) dT' dT'' \tag{12}$$

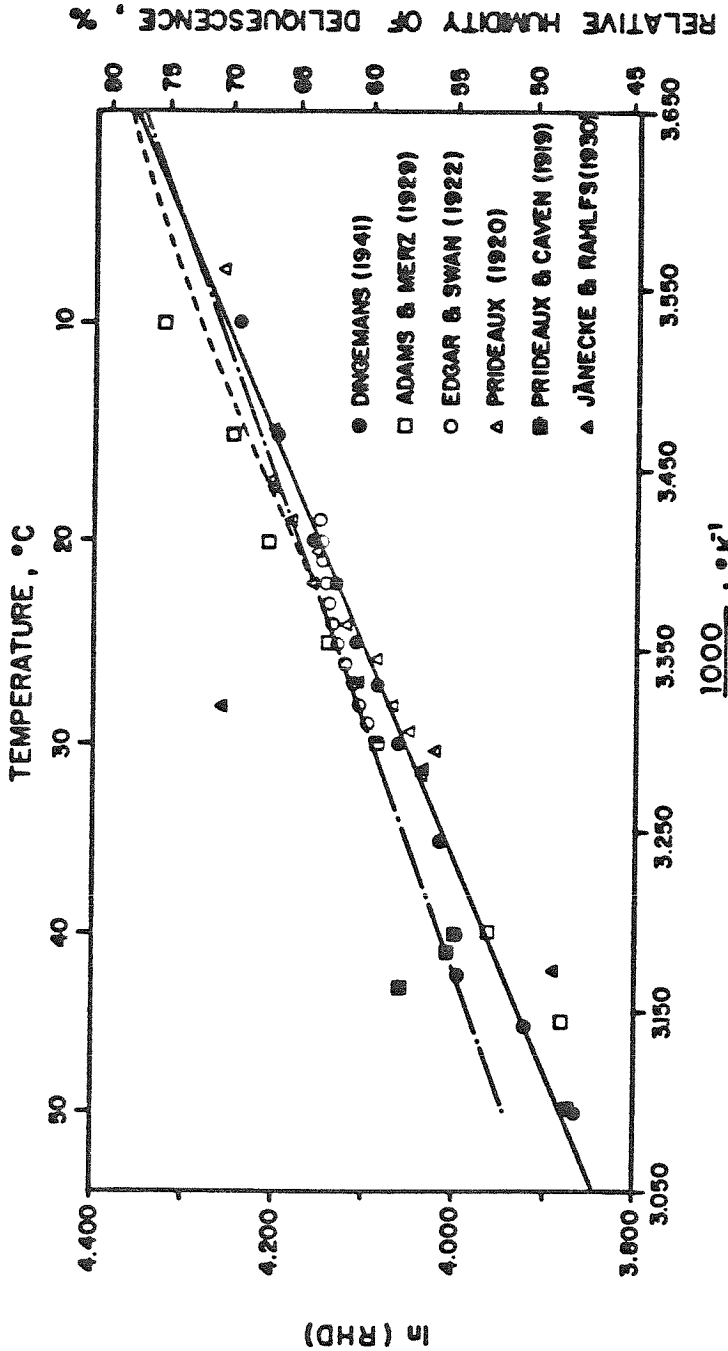


Figure 1. $NH_4NO_3$ relative humidity of deliquescence temperature dependence: (•-•-•) Equation (6); (——) Equation (7); (- - -) Equations (11), (15), (21) and (22).

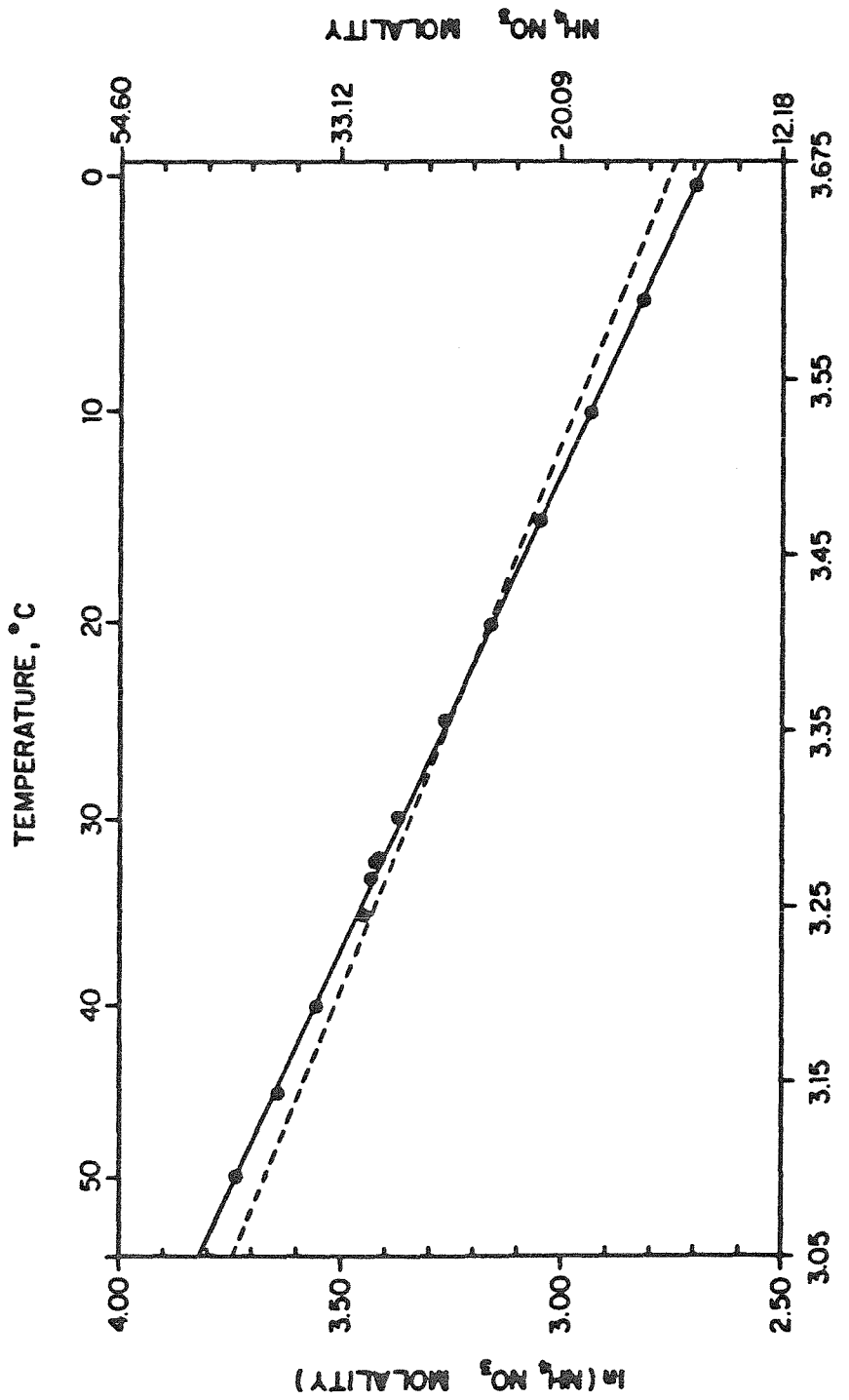


Figure 2. $NH_4NO_3$ solubility temperature dependence: (——) Equation (11); (- - ) Equation (10); Data from Stephen and Stephen (1963).

where $K_p^* = p_{NH_3} p_{HNO_3} / a_{NH_4NO_3} = K_p' / a_{NH_4NO_3}$, $a_{NH_4NO_3} = \gamma^{\pm 2}_{NH_4NO_3} m^2$, $\bar{C}^o_{p_{NH_4NO_3}}$ = $NH_4NO_3$ partial heat capacity at infinite dilution, and $\gamma^{\pm}_{NH_4NO_3}$ = mean molal ionic activity coefficient of dissolved $NH_4NO_3$. Using the data in Table 1 and assuming the heat capacities are independent of temperature, we obtain from (12),

$$\ln K^* = \ln \frac{K}{a_{NH_4NO_3}} = 54.18 - \frac{15860}{T} + 11.206 \ln\left(\frac{T}{298}\right) \qquad (13)$$

where $K^*$ has units of $ppb^2$ $molal^{-2}$. The temperature variation of $\gamma^{\pm}_{NH_4NO_3}$ can be calculated from

$$\left(\frac{\partial \ln \gamma^{\pm}_{NH_4NO_3}}{\partial T}\right)_p = \frac{\bar{H}^o - \bar{H}}{RT^2} \qquad (14)$$

where $\bar{H}$ = the $NH_4NO_3$ partial molal enthalpy at m (Denbigh, 1971, p. 279). By integrating (14),

$$\left(\ln \gamma^{\pm}_{NH_4NO_3}\right)_T = \left(\ln \gamma^{\pm}_{NH_4NO_3}\right)_{298} + \left(\frac{\bar{H}-\bar{H}^o}{R}\right)_{298}\left(\frac{1}{T} - \frac{1}{298}\right) - \left(\frac{\bar{C}_p - \bar{C}^o_p}{R}\right)\left(\ln \frac{T}{298} + \frac{298}{T} - 1\right) \qquad (15)$$

is obtained, where $\bar{C}^o_p$, $\bar{C}_p$ = $NH_4NO_3$ partial molal heat capacities at infinite dilution and m, respectively, and $\left(\frac{\bar{H}-\bar{H}^o}{R}\right)_{298}$ = the normalized $NH_4NO_3$ relative partial molal enthalpy difference between infinite dilution and m at 298.15°K. To evaluate $(\ln \gamma^{\pm}_{NH_4NO_3})_T$, the concentration dependence of $(\ln \gamma^{\pm}_{NH_4NO_3})_{298}$, $(\frac{\bar{H}-\bar{H}^o}{R})_{298}$ and $\left(\frac{\bar{C}_p - \bar{C}^o_p}{R}\right)$ must be known. The expression of Hamer and Wu (1972) can be used to represent the concentration dependence of $(\ln \gamma^{\pm}_{NH_4NO_3})_{298}$ to 25.954 molal. Obtaining expressions for $(\frac{\bar{H}-\bar{H}^o}{R})_{298}$ and $\left(\frac{\bar{C}_p - \bar{C}^o_p}{R}\right)$ is more complicated.

Relative apparent molal heat content data can be obtained from Wagman et al. (1968) and Vanderzee et al. (1980). Since the data of Vanderzee et al. (1980) are more recent and span a larger concentration range, they will be used to represent the variation in enthalpy with concentration. A polynomial regression can be calculated using ideal gas constant normalized relative apparent molal heat content data of Vanderzee et al. (1980) between 0.1 and 25 molal. The partial molal enthalpy was derived using Equation (8-2-7) from Harned and Owen (1958), as

$$(\bar{H}-\bar{H}^{o}) = \phi_L + m\frac{\partial(\phi_L)}{\partial m} \tag{16}$$

where $\phi_L$ = relative apparent molal heat content at m. The resulting polynomial regression is

$$\left(\frac{\bar{H}-\bar{H}^{o}}{R}\right)_{298} = 297.85\ m^{1/2} - 983.98m + 508.08m^{3/2} - 133.86m^{2}$$

$$+ 19.328m^{5/2} - 1.2071m^{3} \tag{17}$$

where the standard deviation for the normalized relative apparent molal heat content polynomial regression is $\pm$ 3.54 $^{o}K^{-1}$. The error in the relative partial molal enthalpy polynomial regression is unknown since it was obtained using the normalized relative apparent molal heat content polynomial regression and (16).

Roux et al. (1978) measured the apparent molal heat capcity, $\phi_{C_p}$, of aqueous ammonium nitrate at 25$^{o}$C to 22.4 molal. Their expression for their data,

$$\frac{\Phi_{C_p}}{R} = -0.505 + 3.482\, m^{1/2} + 3.159\, m - 1.605\, m^{3/2} + 0.274\, m^2 - 0.0161\, m^{5/2} \quad (18)$$

agrees well with the measurements of Gucker et al. (1936) and Sorina et al. (1977). Using Equation (8-4-7) from Harned and Owen (1958),

$$\bar{C}_p = \Phi_{C_p} + m \frac{\partial \Phi_{C_p}}{\partial m} \quad (19)$$

the partial molal heat capacity can be calculated from (18) as,

$$\frac{\bar{C}_p}{R} = -0.505 + 5.223\, m^{1/2} + 6.318\, m - 4.013\, m^{3/2} + 0.822\, m^2 - 0.0564\, m^{5/2}. \quad (20)$$

The data of Sorina et al. (1977) extend to 50 molal, supersaturation at 25°C. With relative apparent molal heat content and solute activity data to 50 molal, the temperature extrapolation of $\gamma^{\pm}_{NH_4NO_3}$ could be performed to saturation at 50°C. Unfortunately, the relative apparent molal heat content data are limited to 25 molal (Vanderzee et al., 1980). Even though (20) is based on data to 22.4 molal, it will be used to 25 molal. Within the region 22.4-25 molal, (20) is a smoothly continuous extrapolation of the data below 22.4 molal and represents the data of Gucker et al. (1936) and Sorina et al. (1977) fairly well.

Once $(\ell n\, \gamma^{\pm}_{NH_4NO_3})_T$ has been calculated, the osmotic coefficient of the solution, $\phi_T$, can be derived from the Gibbs-Duhem equation,

$$\phi_T = 1 + \frac{1}{m}\int_0^m m\, d(\ln \gamma^{\pm}_{NH_4NO_3})_T \qquad (21)$$

The percent relative humidity at temperature T, $RH_T$, can be calculated from

$$RH_T = 100 \exp\left(-\frac{\nu\, m\, M\phi_T}{1000}\right) \qquad (22)$$

where $\nu$ = the number of moles of ions formed by the ionization of one mole of solute and M = molecular weight of water.

RESULTS

By using appropriate expressions for the temperature dependence of solid or aqueous phase $NH_4NO_3$ thermodynamic properties, the dissociation constant can be calculated at a specific temperature and relative humidity. With (7), the form of ammonium nitrate, solid or aqueous, can be determined. At a specific temperature the $NH_4NO_3$ dissociation constant is invariant below the relative humidity of deliquescence and can be obtained from (4). Above the relative humidity of deliquescence, the $NH_4NO_3$ dissociation constant relative humidity dependence can be calculated from (13), (15), (21) and (22) to 25 molal. Equation (11) is used to calculate the solubility temperature dependence. Figure 3 has been constructed using the previously mentioned techniques. Notice discontinuities exist between the solid $NH_4NO_3$ dissociation constant and the dissociation constant for a saturated solution at $25^oC$ and below.

The possible sources of these discontinuities at temperatures below $25^oC$ are manifold and the relative error from each source is difficult to evaluate. First, the temperature extrapolations for the solid $NH_4NO_3$ and the aqueous $NH_4NO_3$ dissociation constants are based on different thermodynamic data sets so an inconsistent value in one data set can cause discontinuity. Second, the relative humidity of deliquescence is obtained by different methods for solid $NH_4NO_3$ and aqueous $NH_4NO_3$. The relative humidity of deliquescence for solid $NH_4NO_3$ was calculated from (7) and aqueous $NH_4NO_3$ from (11), (15), (21) and (22). The relative error can be seen by comparing the solid and dashed curves in Figure 1. Third, error is introduced by differentiating the polynomial regressions obtained for the relative apparent molal heat content and the apparent molal heat capacity to get expressions for the partial molal enthalpy and heat capacity. The amount of error is known for the original

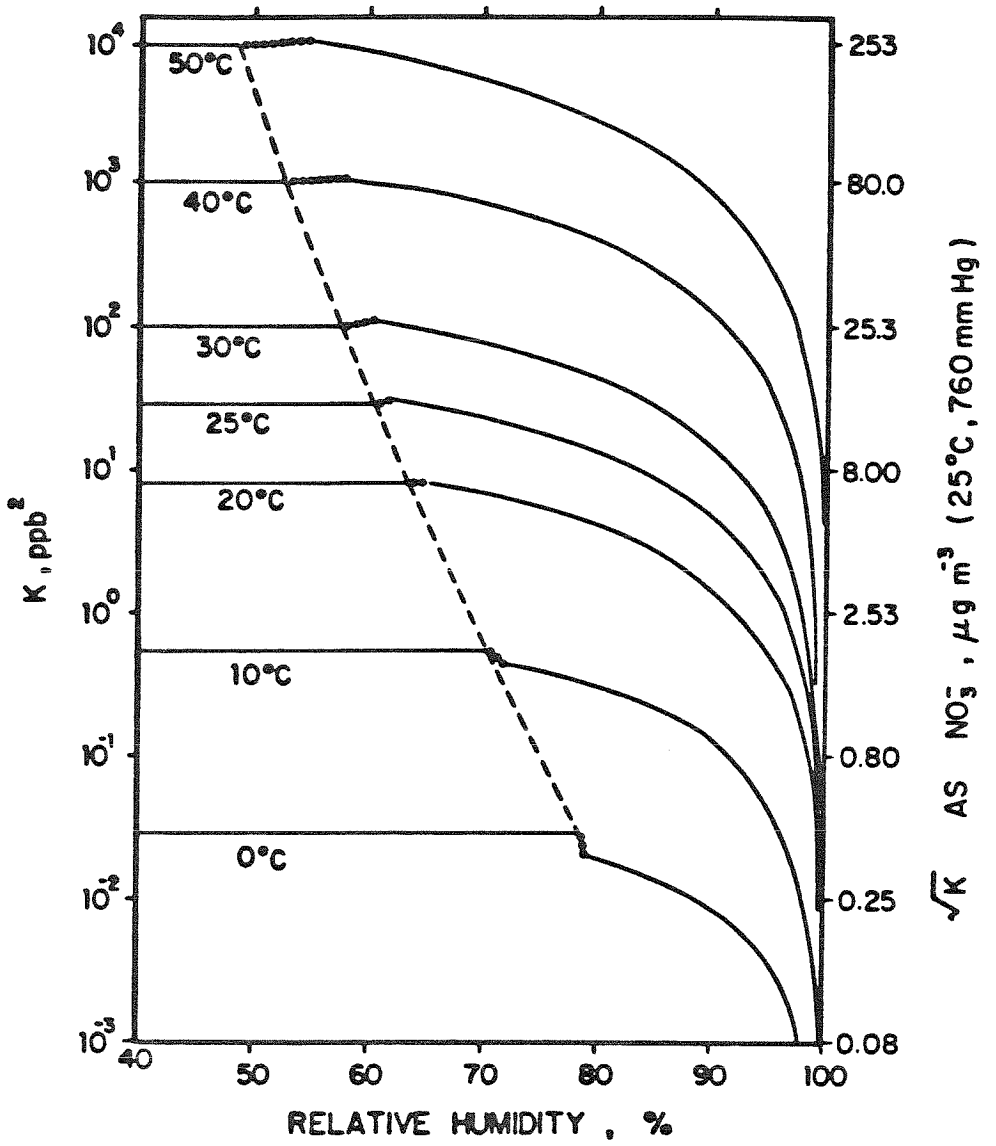


Figure 3. $NH_4NO_3$ dissociation constant temperature and relative humidity dependence: (- - -) solid $NH_4NO_3$ to aqueous $NH_4NO_3$ solution transition predicted from Equation (7); (——) Isothermal prediction of $NH_4NO_3$ dissociation constant for solid $NH_4NO_3$ and non-ideal $NH_4NO_3$ solutions at indicated temperatures; (••••) Extrapolation between predicted solid and maximum calculable aqueous $NH_4NO_3$ dissociation constant.

polynomial regressions but not for the derived regressions. Finally, the error must be introduced by the enthalpy, heat capacity, relative humidity of deliquescence or solubility data or the temperature extrapolation technique, since the free energy data are consistent at 298°K (Stelson and Seinfeld, 1981b).

Above 25°C, an interpolation must be performed between the relative humidity corresponding to 25 molal and saturation. Since the curves are fairly flat in the region between 25 molal and saturation, a linear interpolation between the dissociation constant at 25 molal and at saturation should approximate the dissociation constant in this region.

The temperature dependence of the saturated solution relative humidity can be calculated using (11), (15), (21) and (22) for temperatures below 25°C. A curve calculated using this method is shown in Figure 1.

Data for the molal variation of the solution relative humidity at various temperatures are shown in Figure 4. The data scatter is considerable and shows no definite temperature variation trend. Curves for the relative humidity concentration dependence were calculated at 0, 25 and 50°C using (15), (21) and (22) and are shown in Figure 4. The predictions coincide with the general area of the data but do not show agreement with any particular data set. Also shown in Figure 4 is the relative humidity concentration dependence for an ideal $NH_4NO_3$ solution which poorly predicts the non-ideal $NH_4NO_3$ behavior.

Figure 4 illustrates the infeasibility of attempting to use water activities at higher temperatures, 25-50°C, and the Gibbs-Duhem equation to calculate solute activities. The data have too much scatter and are too sparse at any particular temperature. Furthermore, the maximum concentration of existing water activity data is 29.2 molal and saturation is 42 molal at 50°C.

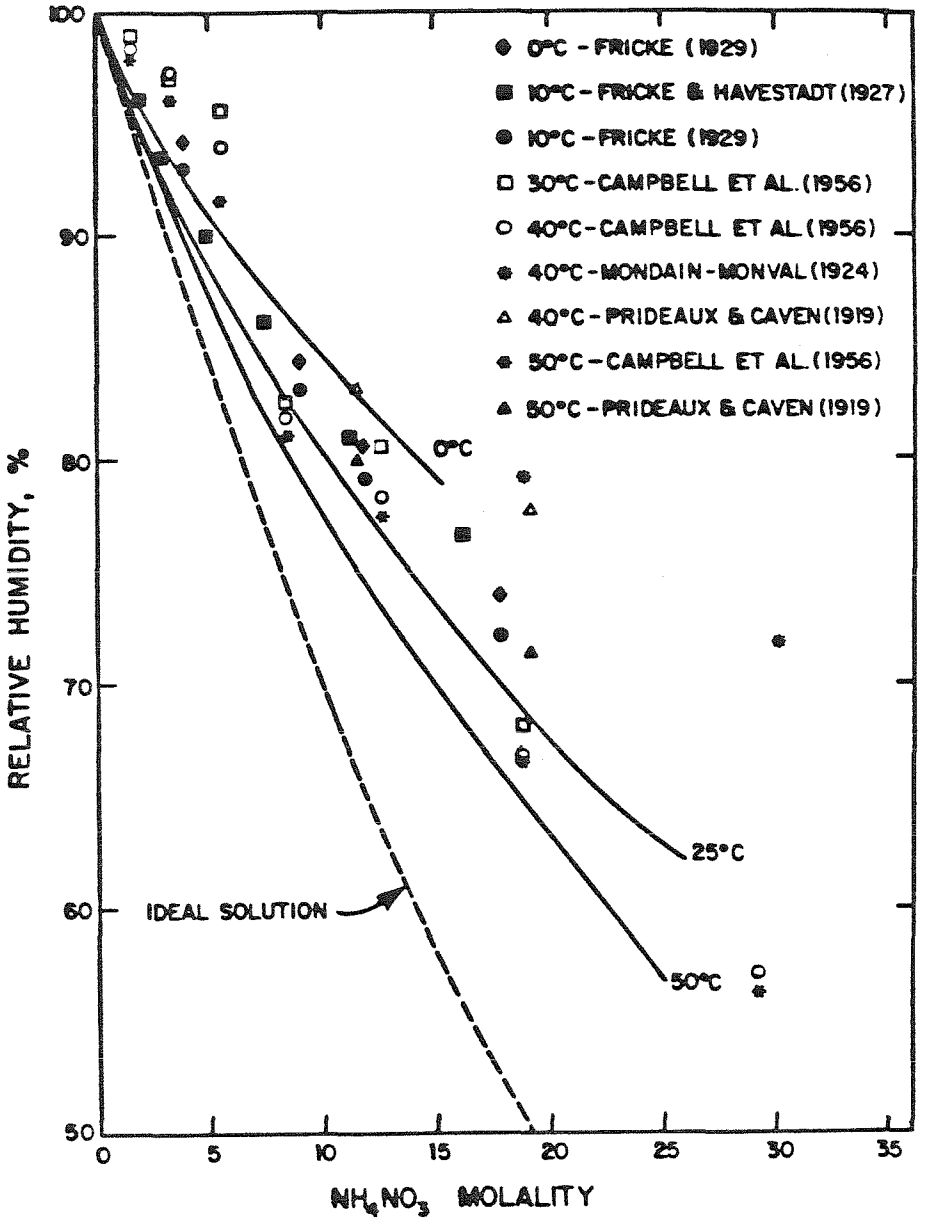


Figure 4. Temperature and concentration dependence of $NH_4NO_3$ solution relative humidity: (- - -) ideal solution prediction; (——) non-ideal solution predictions at 0, 25, and 50°C.

DISCUSSION

Atmospheric measurements of simultaneous ammonia, nitric acid, temperature, relative humidity, aerosol ammonium and aerosol nitrate are very limited. With partial data sets, the merit of the thermodynamic calculations can be demonstrated.

Figure 5 shows diurnal variation of the measured ammonia-nitric acid partial pressure product and the respirable aerosol nitrate at Pittsburg, Ca. (Appel et al., 1979). The trends of the curves are very similar. If the similarity between the diurnal variation of the ammonia-nitric acid partial pressure product and the respirable aerosol nitrate resulted strictly from atmospheric dilution effects, these data when cross plotted, should result in a single curve. The data were analyzed by this method and the test failed. Thus, the similar trend between the observed ammonia-nitric acid partial pressure product and the respirable aerosol nitrate cannot be merely attributed to atmospheric dilution. Also shown are the daily maximum bulk $NH_4NO_3$ dissociation constants calculated from the daily maximum temperature and (4). Ammonia-nitric acid partial pressure products below the daily maximum bulk $NH_4NO_3$ dissociation constant can result from the lack of aerosol ammonium nitrate, the presence of an unreactive solute, the temperature being less than the daily maximum or the relative humidity being greater than the deliquescence point. Ammonia-nitric acid partial pressure products above the daily maximum bulk $NH_4NO_3$ dissociation constant could be explained by kinetic limitations or Kelvin effects. Kinetic limitations are doubtful since the ammonia-nitric acid reaction is very fast (Kaiser and Japar, 1978; Morris and Niki, 1971). Experimental errors could result in positive or negative deviations.

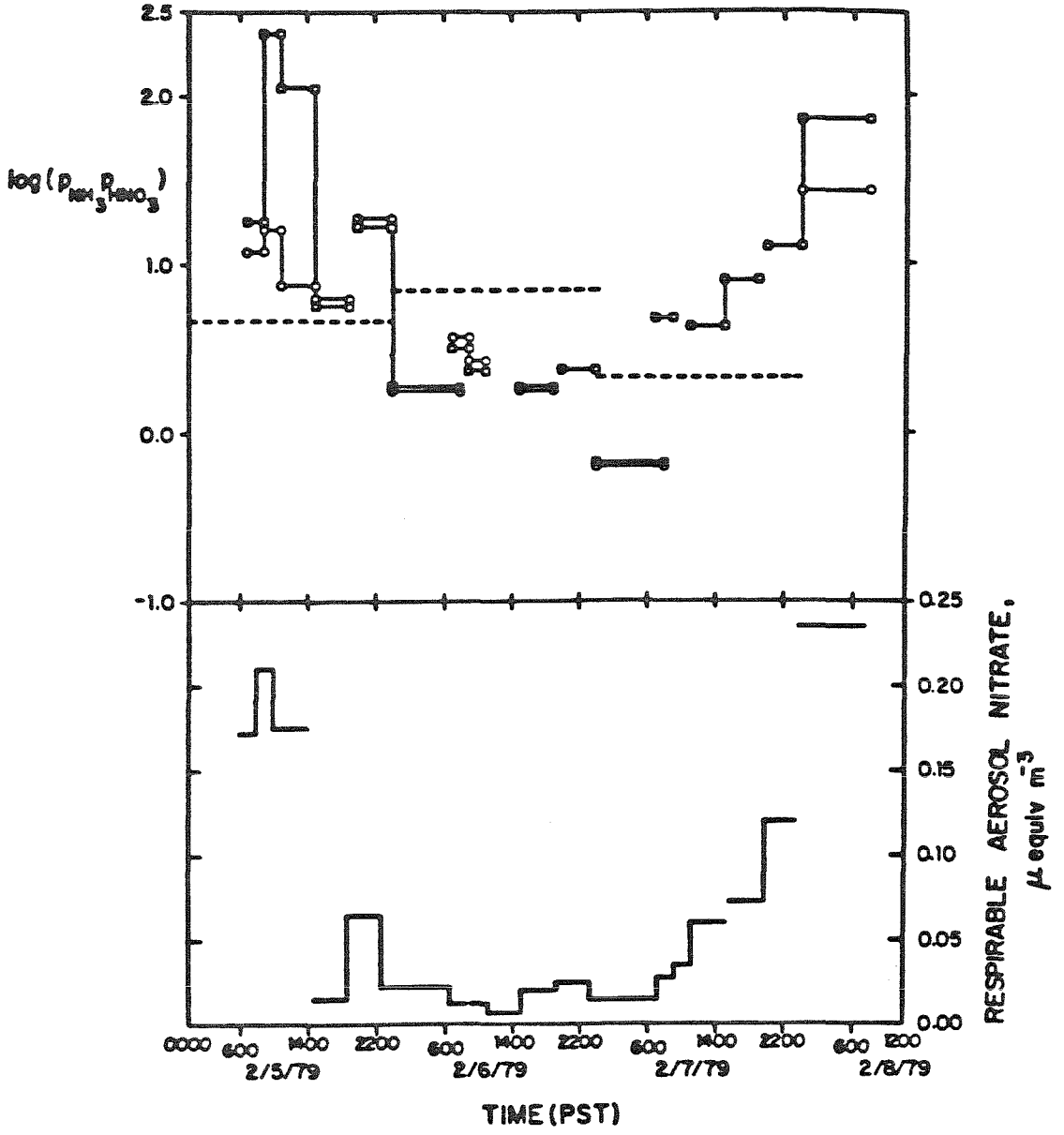


Figure 5. Experimental diurnal $NH_3$-$HNO_3$ product and aerosol nitrate trends at Pittsburg, CA (Appel et al.,1979): (o-o) Product calculated from NaCl impregnated Whatman 41 filter gaseous $HNO_3$ measurements; (□-□) Product calculated from Duralon nylon filter gaseous $HNO_3$ measurements; (- - -) Maximum $NH_4NO_3$ dissociation constant based on the daily maximum temperature and Equation (4); $p_{NH_3} p_{HNO_3}$ in $ppb^2$.

The effect of an unreactive solute in solution with ammonium nitrate on the ammonia-nitric acid partial pressure can be evaluated qualitatively. From the Gibbs-Duhem equation,

$$RH = 100 \exp\left(\frac{-M}{1000}\left[\int_0^m m\, d\ell n\, a_{NH_4NO_3} + \int_0^{m_I} m_I\, d\ell n\, a_I\right]\right) \qquad (23)$$

where $m_I$ = molality of inert solute and $a_I$ = activity of inert solute. Assuming the inert solute is ideal and undissociated,

$$RH = 100 \exp\left(\frac{-M}{1000}\left[\int_0^m m\, d\ell n\, a_{NH_4NO_3} + m_I\right]\right) \qquad (24)$$

Equation (24) shows the addition of an ideal inert solute would decrease the relative humidity above an ammonium nitrate solution for a specific ammonium nitrate molality. Since the additional solute is assumed to be non-interactive with the dissolved ammonium nitrate, the ammonia-nitric acid partial pressure product would be the same as the situation without any inert solute. Thus, the presence of an inert solute results in an ammonia-nitric acid partial pressure product being observed at a lower relative humidity than would be predicted from the pure ammonium nitrate-water system.

The Kelvin effect for solid $NH_4NO_3$ can be evaluated using an expression derived by Banic and Iribarne (1980),

$$d_p = \frac{4\,\sigma\,M}{\rho RT\ \ell n\ S} \qquad (25)$$

where $\sigma$ = $NH_4NO_3$ surface tension, $d_p$ = particle diameter, M = $NH_4NO_3$ molecular weight, $\rho$ = $NH_4NO_3$ density and S = the saturation ratio which equals K for curved surface/K for flat surface. The $NH_4NO_3$ surface tension was approximated

as 108.4 dynes/cm at 25°C by the approach of Rehbinder (1926). The surface tension is approximate because it required extrapolation from 168.5°C across three different $NH_4NO_3$ crystalline structures (Nagatani et al., 1967). With the $NH_4NO_3$ density and molecular weight from Weast (1973), (25) simplifies to

$$d_p = \frac{8.1 \times 10^{-3}}{\ell n\ S} \qquad (26)$$

In Figure 5, saturation ratios greater than 5 are observed. (Compare observed ammonia-nitric acid partial pressure products and the daily maximum bulk $NH_4NO_3$ dissociation constants in Figure 5.) Can these supersaturations be attributed to the Kelvin effect? For a saturation ratio of 5, the calculated particle diameter is 0.005 μm which is too small to be atmospherically realistic since 0.005 μm particles would be readily scavenged by larger particles.

The relative humidity dependence of the ammonia-nitric acid product at Claremont, Ca is displayed in Figure 6 (Appel et al., 1980). Next to each datum is the temperature in centigrade at the time of measurement. Underlined temperatures refer to points positively deviating from the dissociation constant calculated at the temperature and relative humidity of each measurement. Also shown are $NH_4NO_3$ dissociation constant isotherms, 20, 25 and 30°C, calculated using the procedures developed in this work. The data show scatter but are in general agreement with the predictions of this work.

Figure 7 shows the diurnal variation of the ammonia-nitric acid product calculated from measurements at Riverside, Ca (Pitts, 1978, 1979; Tuazon et al., 1980). Also shown are the diurnal variations of the solid $NH_4NO_3$ dissociation constant calculated from (4) and the average temperature profiles for all days and episode days (maximum $O_3$ > 0.2 ppm) between May and October 1976

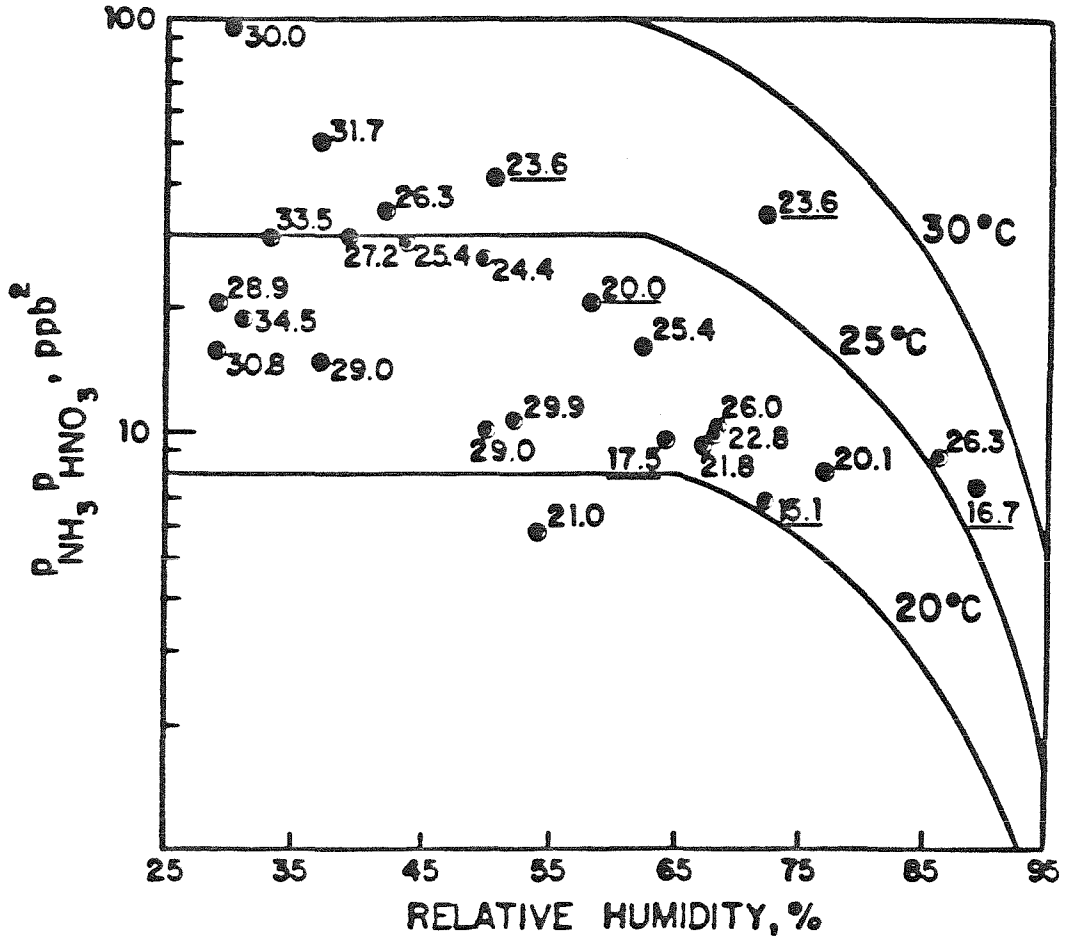


Figure 6. Experimental relative humidity and temperature dependence of the $NH_3$-$HNO_3$ product at Claremont, CA (Adapted from Appel et al., 1980): (——) Predicted $NH_4NO_3$ dissociation constant relative humidity dependence at 20, 25, and 30°C; Values next to data from Appel et al. (1980) are the temperatures in centigrade.

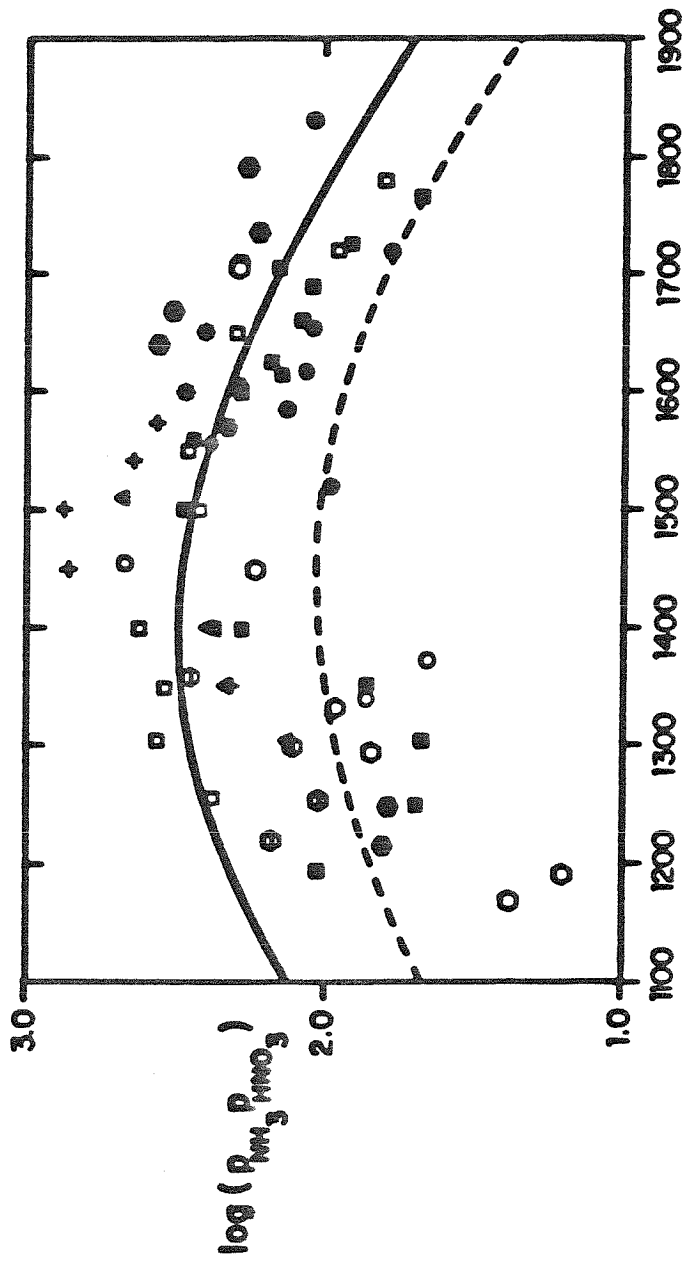


Figure 7. Diurnal $NH_3$-$HNO_3$ product trend calculated from FT-IR measurements at Riverside, CA (Pitts, 1978; Tuazon et al., 1980): (—) solid $NH_4NO_3$ dissociation constant diurnal trend calculated from Equation (4) and the average temperature profile for episode days (maximum $O_3$ > 0.2 ppm), May - October 1976 (Pitts, 1978); (- - -) solid $NH_4NO_3$ dissociation constant diurnal trend calculated from Equation (4) and the average temperature profile for all days, May - October 1976 (Pitts, 1978); Different data symbols refer to different days of measurement; $P_{NH_3} P_{HNO_3}$ in $ppb^2$.

(Pitts, 1978). Note the strong diurnal pattern with the peak occurring between 1400 and 1600 which corresponds to the daily maximum temperature and minimum relative humidity region.

Finally, some comments on how this work should be applied are in order. Figures 6 and 7 show the trends predicted by the thermodynamics generally follow the atmospheric data trends though positive and negative deviations from the pure $NH_4NO_3$ thermodynamics are apparent. Negative deviations can be explained by the presence of additional solutes in solution. Positive deviations cannot be explained with current theoretical development. The polluted atmospheric aerosol can be multicomponent or supersaturated which leads to deviations from the pure $NH_4NO_3$ theoretical predictions. Thus, this work should be used as guidance to identify important parameters in aerosol measurement, give a relative feeling for what the distribution of nitrate is between the gas and aerosol phases and a basis for assembling more detailed multicomponent theories.

Additionally, Figure 3 merits comment. The right ordinate of Figure 3 is $\sqrt{K}$, expressed as nitrate, $\mu g\ m^{-3}$, at $25^{o}C$ and 760 mm Hg. Typical aerosol nitrate values range between 0 and 40 $\mu g\ m^{-3}$ (Stelson et al., 1979). This range is spanned by the ordinate of Figure 3. Thus, the importance of accurately monitoring temperature and relative humidity during aerosol nitrate measurement is apparent.

## CONCLUSIONS

Some important conclusions are evident from this work:

1. A thermodynamic extrapolation method was developed to predict the temperature and relative humidity variation of the $NH_4NO_3$ dissociation constant.
2. The approach of using existing water activity data at temperatures other than $25^{o}C$ to calculate solute activities is shown to be infeasible.

3. The general trends predicted by the thermodynamic model agree with the atmospheric observations of Appel et al. (1979, 1980), Pitts (1978, 1979), and Tuazon et al. (1980).
4. Positive deviations of measured ammonia-nitric acid partial pressure products from the solid $NH_4NO_3$ dissociation constant at the temperatures of measurement cannot be readily explained other than on the basis of experimental error.

ACKNOWLEDGMENT

This work was supported by Environmental Protection Agency grant R806844 and State of California Air Resources Board contract A7-169-30.

REFERENCES

Adams J.R. and Merz A.R. (1929) Hygroscopicity of fertilizer materials and mixtures. Ind. Eng. Chem. 21, 305-307.

Appel B.R., Tokiwa Y., Hoffer E.M., Kothny E. L., Haik M. and Wesolowski J.J. (1980) Evaluation and development of procedures for determination of sulfuric acid, total particle-phase acidity and nitric acid in ambient air - Phase II. Calif. Air Res. Board A8-111-31 Final Report.

Appel B.R., Tokiwa Y., Wall S.M., Haik M., Kothny E.L. and Wesolowski J.J. (1979) Determination of sulfuric acid, total particle-phase acidity and nitric acid in ambient air. Calif. Air Res. Board A6-209-30 Final Report.

Banic C.M. and Iribarne J.V. (1980) Nucleation of ammonium chloride in the gas phase and the influence of ions. J. Geophys. Res. 85, 7459-7464.

Campbell A.N., Fishman J.B., Rutherford G., Schaefer T.P. and Ross L. (1956) Vapor pressures of aqueous solutions of silver nitrate, of ammonium nitrate, and of lithium nitrate. Can. J. Chem. 34, 151-159.

Denbigh K. (1971) The Principles of Chemical Equilibrium, 3rd Edn. Cambridge University Press, London.

Dingemans P. (1941) The vapor pressure of saturated solutions of ammonium nitrate. Rec. Trav. Chim. 60, 317-328.

Doyle G.J., Tuazon E.C., Graham R.A., Mischke T.M., Winer A.M. and Pitts J.N. Jr. (1979) Simultaneous concentrations of ammonia and nitric acid in a polluted atmosphere and their equilibrium relationship to particulate ammonium nitrate. Environ. Sci. Technol. 13, 1416-1419.

Edgar G. and Swan W.O. (1922) The factors determining the hygroscopic properties of soluble substances. I. The vapor pressures of saturated solutions. J. Am. Chem. Soc. 44, 570-577.

Forrest J., Tanner R.L., Spandau D., D'Ottavio T. and Newman L. (1980) Determination of total inorganic nitrate utilizing collection of nitric acid on NaCℓ-impregnated filters. Atmospheric Environment 14, 137-144.

Fricke R. (1929) The thermodynamic behavior of concentrated solutions. Z. Elektrochem. 35, 631-640.

Fricke R. and Havestadt L. (1927) Work of dilution and heat of dilution in the sphere of concentrated solutions. Z. Elektrochem. Angew. Phys. Chem. 33, 441-455.

Gordon R.J. and Bryan R.J. (1973) Ammonium nitrate in airborne particles in Los Angeles. Envrion. Sci. Technol. 7, 645-647.

Gucker F.T. Jr., Ayres F.D. and Rubin T.R. (1936) A differential method employing variable heaters for the determination of the specific heats of solutions, with results for ammonium nitrate at 25°C. J. Am. Chem. Sco. 58, 2118-2126.

Hamer W.J. and Wu Y.C. (1972) Osmotic coefficients and mean activity coefficients of uni-univalent electrolytes in water at 25°C. J. Phys. Chem. Ref. Data 1, 1047-1099.

Harned H.S. and Owen B.B. (1958) The Physical Chemistry of Electrolytic Solutions, ACS Monograph Series No. 137, 3rd Edn. Reinhold Publishing Corporation, New York, Chap. 8

JANAF Thermochemical Tables, 2nd Edn. (1971). NSRDS- NBS 37.

Jänecke E. and Rahlfs E. (1930) The system: $NH_4NO_3$ - $H_2O$. Z. anorg. allg. Chem. 192, 237-244.

Kaiser E.W. and Japar S.M. (1978) Upper limit to the gas phase reaction rates of HONO with $NH_3$ and $O(^3P)$ atoms. J. Phys. Chem. 82, 2753-2754.

Lundgren D.A. (1970) Atmospheric aerosol composition and concentration as a function of particle size and of time. J. Air Pollut. Control Ass. 20, 603-608.

Mondain-Monval P. (1924) Law of the solubility of salts. Compt. rend. 178, 1164-1166.

Mamane Y. and Pueschel R.F. (1980) A method for the detection of individual nitrate particles. Atmospheric Environment 14, 629-639.

Morris E.D. Jr. and Niki H. (1971) Mass spectrometric study of the reactions of nitric acid with O atoms and H atoms. J. Phys. Chem. 75, 3193-3194.

Nagatani M., Seiyama T., Sakiyama M., Suga H. and Seki S. (1967) Heat capacities and thermodynamic properties of ammonium nitrate crystal: Phase transitions between stable and metastable phases. Bull. Chem. Soc. Jpn. 40, 1833-1844.

Parker V.B., Wagman D.D. and Garvin D. (1976) Selected thermochemical data compatible with the CODATA recommendations, NBSIR 75-968.

Pitts J.N. Jr. (1979) Chemical consequences of air quality standards and of control implementation programs: roles of hydrocarbons, oxides of nitrogen, oxides of sulfur and aged smog in the production of photochemical oxidant and aerosol. Calif. Air Res. Board A6-172-30 Final Report.

Pitts J.N. Jr. (1978) Detailed characterization of gaseous and size-resolved particulate pollutants at a South Coast Air Basin smog receptor site: levels and modes of formation of sulfate, nitrate and organic particulates and their implications for control strategies. Calif. Air Res. Board ARB-5-384 and A6-171-30 Final Report.

Prideaux E.B.R. (1920) The deliquescence and drying of ammonium and alkali nitrates and a theory of the absorption of water vapour by mixed salts. J. Soc. Chem. Ind. 39, 182-185T.

Prideaux E.B.R. and Caven R.M. (1919) The evaporation of concentrated and saturated solutions of ammonium nitrate, vapour pressures, heats of solution, and hydrolysis. J. Soc. Chem. Ind. 38, 353-355T.

Rehbinder P. (1926) Surface activity and adsorptive power. II. Water as a surface-active material. Z. Phys. Chem. 121, 103-126.

Roux A., Musbally G.M., Perron G. and Desnoyers J.E. (1978) Apparent molal heat capacities and volumes of aqueous electrolytes at 25°C: $NaClO_3$, $NaClO_4$, $NaNO_3$, $NaBrO_3$, $NaIO_3$, $KClO_3$, $KBrO_3$, $KIO_3$, $NH_4NO_3$, $NH_4Cl$, and $NH_4ClO_4$. Can. J. Chem. 56, 24-28.

Sorina G.A., Kozlovskaya G.M., Tsekhanskaya Y.V., Bezlyudova L.I. and Shmakov N.G. (1977) The specific heats of ammonium nitrate solutions and the partial specific heats of their components. Russ. J. Phys. Chem. 51, 1226-1227.

Spicer C.W. (1974) The fate of nitrogen oxides in the atmosphere. Batelle Columbus Rep. to Coordinating Res. Council and U.S. Environ. Protection Agency Rep. 600/3-76-030.

Stelson A.W., Friedlander S.K. and Seinfeld J.H. (1979) A note on the equilibrium relationship between ammonia and nitric acid and particulate ammonium nitrate. Atmospheric Environment 13, 369-371.

Stelson A.W. and Seinfeld J.H. (1981a) Chemical mass accounting of urban aerosol. Environ. Sci. Technol. 15, 671-679.

Stelson A.W. and Seinfeld J.H. (1981b) Relative humidity and pH dependence of the vapor pressure of ammonium nitrate-nitric acid solutions at 25°C. Accepted for publication in Atmospheric Environment.

Stephen H. and Stephen T. ed. (1963) Solubilities of Inorganic and Organic Compounds. Vol. 1, Part 1, Macmillan, New York, p. 217.

Stephens E.R. and Price M.A. (1972) Comparison of synthetic and smog aerosols. J. Coll. Int. Sci. 39, 272-286.

Tang I.N. (1980) Deliquescence properties and particle size change of hygroscopic aerosols. In Generation of Aerosols, Chap. 7, ed. by K. Willeke, Ann Arbor Science Publisher, Ann Arbor, Michigan.

Tuazon E.C., Winer A.M., Graham R.A. and Pitts J.N. Jr. (1980) Atmospheric measurements of trace pollutants by kilometer pathlength FT-IR spectroscopy. Adv. Environ. Sci. Technol. 10, 259-300.

Vanderzee C.E., Waugh D.H. and Haas N.C. (1980) Enthalpies of dilution and relative apparent molar enthalpies of aqueous ammonium nitrate. The case of a weakly hydrolysed (dissociated) salt. J. Chem. Thermodynamics 12, 21-25.

Wagman D.D., Evans W.H., Parker V.B., Harlöw I., Baily S.M. and Schumm R.H. (1968) Selected values of chemical thermodynamic properties; tables for the first thirty-four elements in the standard order of arrangement, NBS technical note 270-3.

Weast R.C. ed. (1973) Handbook of Chemistry and Physics, 54th Edn. Chemical Rubber Publishing Company, Cleveland, p. D-159.

# CHAPTER 5

## THERMODYNAMIC PREDICTION OF THE WATER ACTIVITY, $NH_4NO_3$ DISSOCIATION CONSTANT, DENSITY AND REFRACTIVE INDEX FOR THE $NH_4NO_3$ - $(NH_4)_2SO_4$ - $H_2O$ SYSTEM AT 25 C

Submitted for publication in Atmospheric Environment.

# THERMODYNAMIC PREDICTION OF THE WATER ACTIVITY, $NH_4NO_3$ DISSOCIATION CONSTANT, DENSITY AND REFRACTIVE INDEX FOR THE $NH_4NO_3$-$(NH_4)_2SO_4$-$H_2O$ SYSTEM AT 25°C

A. W. Stelson and J. H. Seinfeld
Department of Chemical Engineering
California Institute of Technology
Pasadena, California 91125

ABSTRACT

The thermodynamic properties, water activity, density and refractive index, of $NH_4NO_3$-$(NH_4)_2SO_4$-$H_2O$ aerosols are estimated from binary solution data and existing mixing rules. Particle growth is shown to be predictable from the particle composition, the $NH_4NO_3$-$(NH_4)_2SO_4$-$H_2O$ phase diagram and the water activity calculation technique of Kusik and Meissner (1978). Good agreement between the theoretical predictions and the experimental measurements of Tang et al. (1981), Thudium (1978) and Emons and Hahn (1970) is shown. Also, the effect of $(NH_4)_2SO_4$ on the relative humidity dependence of the $NH_4NO_3$ dissociation constant is evaluated.

## INTRODUCTION

Ammonium, nitrate and sulfate comprise a significant portion of the atmospheric aerosol (Appel et al., 1978; Stevens et al., 1978). Two probable chemical forms for the nitrate and sulfate species are ammonium nitrate and ammonium sulfate. Since the ammonium, nitrate and sulfate ions occur in particles of similar size, a thermodynamic study of the interaction between ammonium nitrate and ammonium sulfate would provide a foundation for understanding atmospheric processes involving these species (Cunningham et al., 1974; Patterson and Wagman, 1977; Harrison and Pio, 1981).

The prediction of the size, water activity and $NH_4NO_3$ dissociation constant for aqueous $NH_4NO_3$-$(NH_4)_2SO_4$ aerosols is necessary. Previously, the thermodynamic analysis of this system has been limited by the non-ideal nature of these solutes. This paper will show how the growth, water activity and $NH_4NO_3$ dissociation constant can be calculated from the temperature, relative humidity and $NH_4NO_3/(NH_4)_2SO_4$ ratio. Also techniques for predicting the solution density and refractive index will be discussed. The theory, though specifically applied to the $NH_4NO_3$-$(NH_4)_2SO_4$-$H_2O$ system, can easily be generalized to more complex electrolytic mixtures.

## BACKGROUND

### Growth Studies

The thermodynamic growth properties of atmospheric electrolytic aerosols have been explored extensively (Orr et al., 1958; Winkler and Junge, 1972; Winkler, 1973; Chen, 1974; Tang et al., 1978; Thudium, 1978; Hänel and Zankl, 1979; Saxena and Peterson, 1981; Tang et al., 1981). Tang et al. (1978) demonstrated that mixed salt aerosol particles can undergo stepwise growth

and showed the utility of phase diagrams for understanding these processes. Chen (1974), Thudium (1978), Hänel and Zankl (1979), and Saxena and Peterson (1981) have studied methods for predicting the water activity or osmotic coefficient of a multicomponent aerosol droplet from binary data*. Winkler and Junge (1972) and Winkler (1973) studied the growth of multicomponent atmospheric and synthetic salt aerosols. They observed that the ambient aerosol composite exhibited smooth growth which contrasts with the stagewise growth of the single particle studies of Tang et al. (1978). Orr et al. (1958), Winkler and Junge (1972), and Tang et al. (1981) studied hysteresis effects of drying aerosols, and Orr et al. theoretically and experimentally demonstrated that particles deliquesce at lower relative humidities as their size decreases.

## $NH_4NO_3$ Volatility

The volatility of solid $NH_4NO_3$ in atmospheric aerosols has been studied by Stelson et al. (1979) and Doyle et al. (1979). In particular, Stelson and Seinfeld (1981a, 1981b) have evaluated the temperature, relative humidity and pH dependence of the $NH_4NO_3$ dissociation constant in concentrated solutions of ammonium nitrate and nitric acid. Tang (1981) explored the role of sulfate on the individual ammonia and nitric acid partial pressures above $NH_3$-$HNO_3$-$H_2SO_4$-$H_2O$ solutions.

*Thudium (1978) has shown the mixture rule of Chen (1974) is physically incorrect.

Relation to Ambient Aerosol Sampling

From understanding the role of $(NH_4)_2SO_4$ on the volatility of $NH_4NO_3$, the effect of $(NH_4)_2SO_4$ on the sampling of ammonium nitrate aerosol can be evaluated. Appel and Tokiwa (1981) showed that the reaction of strong acids, $H_2SO_4$ and HCℓ, with $NH_4NO_3$ leads to the loss of aerosol nitrate. A question of importance is - What effect would the internal mixing of a pure $(NH_4)_2SO_4$ aerosol with a pure $NH_4NO_3$ aerosol have on the $NH_4NO_3$ dissociation constant? Ahlberg and Winchester (1978) identified ammonium sulfate as the major sulfate species in Florida aerosol by following the relative humidity dependence of the aerosol sulfur mass median aerodynamic diameter. Another question is - How would the presence of $NH_4NO_3$ affect an aerosol identification technique that utilizes particle growth resulting from water condensation? Finally, Clark et al. (1976) measured the effect of aerosol sulfate formation on aerosol nitrate formation. As the rate of aerosol sulfate formation increased, that of aerosol nitrate formation decreased. A further question is - Is the reduction in the nitrate aerosol formation rate during simultaneous sulfate aerosol formation the result of a change in the distribution of nitric acid between the gas and aerosol phases or is the total amount of nitrate formed reduced?

The thermodynamic theories developed in this paper will give insight into the answers of these questions.

## $NH_4NO_3$-$(NH_4)_2SO_4$-$H_2O$ PHASE DIAGRAM

The $NH_4NO_3$-$(NH_4)_2SO_4$-$H_2O$ phase diagram can be constructed from the data in Silcock (1979) and Emons and Hahn (1970) and is shown in Figure 1. The phase diagram shows several interesting items. By equating chemical potentials at eutonic points, $E_1$ and $E_2$, the $NH_4NO_3$ chemical potential can be shown to be constant along the solubility curve between pure $NH_4NO_3$ in water and $E_3$ and in the regions I, I & II, II, II & III, III and III & IV. If the $NH_4NO_3$ chemical potential is constant throughout these regions, then the $NH_4NO_3$ dissociation constant must be invariant. Similarly, the $(NH_4)_2SO_4$ chemical potential must be constant along the solubility curve between pure $(NH_4)_2SO_4$ in water and $E_1$ and in the regions IV, III & IV, III, II & III, II and I & II. If the chemical form of the aqueous solutes is the same along the solubility curve between $E_1$ and $E_3$ then by equating chemical potentials and by using the Gibbs-Duhem equation, the solution relative humidity should be constant. In Table 1, relative humidity measurements of saturated aqueous $NH_4NO_3$-$(NH_4)_2SO_4$ solutions from Emons and Hahn (1970) are shown. Their data show that the relative humidity varies between $E_1$ and $E_3$, indicating a new dissolved species must be formed. Finally, Figure 1 illustrates a problem when attempting to describe multicomponent aqueous mixtures up to saturation. Since $(NH_4)_2SO_4$ precipitates at a lower ionic strength then $NH_4NO_3$, there is a problem in describing the region of the phase diagram where the ionic strength is greater than the maximum ionic strength of the least soluble species. For the $NH_4NO_3$-$(NH_4)_2SO_4$-$H_2O$ system, this region lies between the solubility curve and the dashed line in Fig. 1. In the next section, this problem will be discussed in more detail.

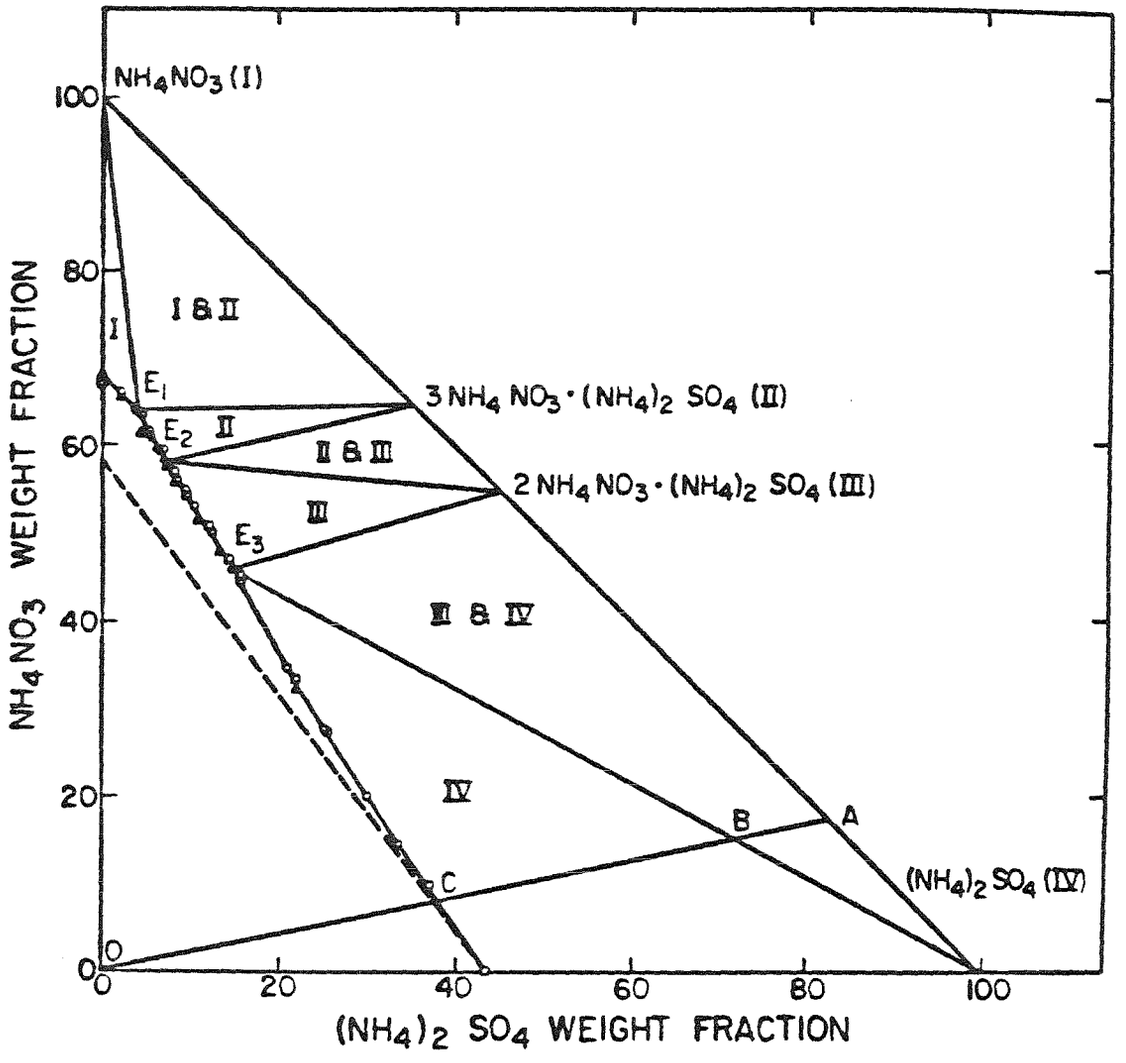


Figure 1. $NH_4NO_3$-$(NH_4)_2SO_4$-$H_2O$ phase diagram at 25°C.
□ - Emons and Hahn (1970); o, +, Δ - Silcock (1979)

ESTIMATION OF THE WATER ACTIVITY AND THE $NH_4NO_3$ DISSOCIATION CONSTANT

Expressions developed by Kusik and Meissner (1978) can be used to estimate the water activity and the solute activity coefficients for the $NH_4NO_3$-$(NH_4)_2SO_4$-$H_2O$ system. The $NH_4NO_3$ activity, $a_{12}$, is given by

$$\ln a_{12} = \frac{2+4Y}{3} \ln \gamma_{12}^{o} + \frac{3-3Y}{4} \ln \gamma_{14}^{o} + \ln \left( \frac{2+Y}{3} \right) YI^2 \quad (1)$$

where $\gamma_{12}^{o}$, $\gamma_{14}^{o}$ = the activity coefficients of $NH_4NO_3$ or $(NH_4)_2SO_4$ alone in water at I, Y = the ionic strength fraction of $NH_4NO_3$,

$$Y = \frac{[NH_4NO_3]}{[NH_4NO_3]+3[(NH_4)_2SO_4]} \quad (2)$$

and I = the total solution ionic strength. The $(NH_4)_2SO_4$ activity, $a_{14}$, is

$$\ln a_{14} = 2Y \ln \gamma_{12}^{o} + \frac{12-3Y}{4} \ln \gamma_{14}^{o} + \ln (2+Y)^2 \left( \frac{1-Y}{27} \right) I^3. \quad (3)$$

From Equations (1) and (3) and the Gibbs-Duhem equation, followed by integration, the water activity can be calculated as

$$\ln a_w = \left( \frac{2+Y}{3} \right) Y \ln a_{w_{12}}^{o} + \left( \frac{2+Y}{2} \right) (1-Y) \ln a_{w_{14}}^{o} - \frac{YM_wI}{6000} (1-Y) \quad (4)$$

where $a_{w_{12}}^{o}$, $a_{w_{14}}^{o}$ = the water activities of $NH_4NO_3$ or $(NH_4)_2SO_4$ aqueous solutions at I, and $M_w$ = the molecular weight of water. The integration was

performed in deriving Equation (4) instead of using the generalized expression in Kusik and Meissner (1978)*

Equations (1), (3) and (4) can be used to evaluate the activities up to an ionic strength of 17.5 molal, the solubility of $(NH_4)_2SO_4$ in water at 25°C. Expressions for the ionic strength dependences of the $NH_4NO_3$ activity coefficient and water activity were obtained from Hamer and Wu (1972). The expressions used for the $(NH_4)_2SO_4$ activity coefficient and water activity ionic strength dependences were based on the isopiestic measurements of Wishaw and Stokes (1954). The solution osmotic coefficients were calculated using the method outlined in Staples and Nuttall (1977) and referenced to the ionic strength dependence of the NaCℓ osmotic coefficient of Hamer and Wu (1972). The more recent NaCℓ expression of Gibbard et al. (1974) was not used since it is in good agreement with the work of Hamer and Wu (1972). The resulting $(NH_4)_2SO_4$ osmotic coefficient data were fit to a polynomial and, with the Gibbs-Duhem equation, the following ionic strength dependence for the $(NH_4)_2SO_4$ activity was obtained,

$$\ln \gamma_{14}^{o} = \frac{-2.3525\sqrt{I}}{1+1.02\sqrt{I}} - 8.369\times10^{-2}I + 7.635\times10^{-3}I^2 - 3.307\times10^{-4}I^3 + 5.783\times10^{-6}I^4 \qquad (5)$$

where the standard deviation of the original regression was $7.55\times10^{-4}$. Still unresolved is how to predict the activity coefficient of $(NH_4)_2SO_4$ in the region of the phase diagram between the dashed line and the solubility curve.

*An error exists in the expression designed to evaluate the extreme right term in Kusik and Meissner's version of Equation (4).

The activity coefficient of $(NH_4)_2SO_4$ at ionic strengths greater than its solubility in water can be approximated four ways from existing data. First, Emons and Hahn (1970) measured the water activity along the solubility curve for the $NH_4NO_3$-$(NH_4)_2SO_4$-$H_2O$ system. From Equation (4), the data of Emons and Hahn (1970) and the $NH_4NO_3$ water activity ionic strength dependence, the hypothetical $(NH_4)_2SO_4$ water activity can be calculated to 26.0 molal, the solubility of $NH_4NO_3$ in water. By using the Gibbs-Duhen equation, the $(NH_4)_2SO_4$ activity coefficient can be obtained. Second, the dissolved ammonium sulfate activity must be constant along the solubility curve between $(NH_4)_2SO_4$ in pure water and $E_1$. Thus, the hypothetical $(NH_4)_2SO_4$ activity coefficient ionic strength dependence can be calculated from the solubility data in Silcock (1979), the $NH_4NO_3$ activity coefficient ionic strength dependence, the activity of a saturated aqueous $(NH_4)_2SO_4$ solution and Equation (3). Third, the $(NH_4)_2SO_4$ activity coefficient data below 17.5 molal can be linearly extrapolated to higher ionic strengths. Fourth, Equation (5) could be used above 17.5 molal.

The results of the four techniques were compared. The second method exhibits a higher ionic strength dependence than the other three. The first method results scattered about the predictions of the third and fourth with neither method showing better agreement. Thus, Equation (5) was used to represent the ionic strength dependence of the $(NH_4)_2SO_4$ activity coefficient above as well as below 17.5 molal.

Using Equation (4), the water activities of $NH_4NO_3$-$(NH_4)_2SO_4$ solutions were predicted and compared to the data of Emons and Hahn (1970) and Thudium (1978). See Tables 1 and 2. The agreement between the predictions and data is good even though the data were taken using distinctly different experimental techniques. The maximum error was 3.7%. Table 1 and Table III of Saxena

Table 1. Comparison of Calculated and Measured Water Activities Along the $NH_4NO_3$-$(NH_4)_2SO_4$ Aqueous Solubility Curve

| I | Y | $a_w$ (Calc.) | $a_w$ (Meas.)† | % Error | Solid Phase* |
|---|---|---|---|---|---|
| 17.46 | 0.000 | 0.800 | 0.801 | - 0.12 | $(NH_4)_2SO_4$ |
| 18.06 | 0.126 | 0.775 | 0.767 | 1.04 | $(NH_4)_2SO_4$ |
| 19.64 | 0.371 | 0.725 | 0.727 | - 0.28 | $(NH_4)_2SO_4$ |
| 20.76 | 0.457 | 0.701 | 0.700 | 0.14 | $(NH_4)_2SO_4$ |
| 23.25 | 0.614 | 0.655 | 0.655 | 0.00 | $(NH_4)_2SO_4$ |
| 23.84 | 0.640 | 0.645 | 0.662 | - 2.57 | $2NH_4NO_3 \cdot (NH_4)_2SO_4$ |
| 24.54 | 0.697 | 0.634 | 0.657 | - 3.50 | $2NH_4NO_3 \cdot (NH_4)_2SO_4$ |
| 25.02 | 0.758 | 0.627 | 0.651 | - 3.69 | $2NH_4NO_3 \cdot (NH_4)_2SO_4$ |
| 25.91 | 0.793 | 0.616 | 0.625 | - 1.44 | $2NH_4NO_3 \cdot (NH_4)_2SO_4$ |
| 25.30 | 1.000 | 0.626 | 0.615 | 1.79 | $NH_4NO_3$ |

†Emons and Hahn (1970)

*Silcock (1979)

Table 2. Comparison of Calculated and Measured Water Activities for Dilute $NH_4NO_3$-$(NH_4)_2SO_4$

| I | Y | $a_w$ (Calc.) | $a_w$* (Meas.) | % Error |
|---|---|---|---|---|
| 1.288 | 0.25 | 0.9791 | 0.9788 | 0.03 |
| 0.882 | 0.25 | 0.9852 | 0.9852 | 0.00 |
| 0.597 | 0.25 | 0.9897 | 0.9896 | 0.01 |
| 0.289 | 0.25 | 0.9947 | 0.9948 | -0.01 |

*Thudium (1978)

and Peterson (1981) are directly comparable. Saxena and Peterson (1981) used Bromley's model with higher order coefficients. Their maximum error was 12.3%. Thus, the approach of Kusik and Meissner (1978) is better suited for $NH_4NO_3$-$(NH_4)_2SO_4$ mixtures.

Finally, the influence of $(NH_4)_2SO_4$ on the $NH_4NO_3$ dissociation constant can be calculated. The appropriate equilibria for the $NH_4NO_3$-$(NH_4)_2SO_4$-$H_2O$ system are listed in Table 3. As stated in the phase diagram discussion, the $NH_4NO_3$ dissociation constant would be invariant along the solubility curve between pure $NH_4NO_3$ in water and $E_3$ and in the regions I, I & II, II, II & III, III and III & IV and is given by the equilibrium constant of Reaction 1 in Table 3 and is independent of relative humidity. Within the aqueous solution region of the phase diagram, the $NH_4NO_3$ dissociation constant varies and is a function of Y and the ionic strength. From Equations (1) and (4) and the equilibrium constant for Reaction 2 in Table 3, the water activity or relative humidity and the Y dependence of the $NH_4NO_3$ dissociation constant can be evaluated and are shown in Fig. 2. The dashed curve is obtained by calculating the relative humidity and the $NH_4NO_3$ dissociation constant along the solubility curve between $E_3$ and pure $(NH_4)_2SO_4$ in water. A striking feature of Fig. 2 is the insensitivity of the $NH_4NO_3$ dissociation constant to the ionic fraction of nitrate. For example, the $NH_4NO_3$ dissociation constant for Y = 0.5 varies from that of pure $NH_4NO_3$ in water by only 40%.

In addition to the $NH_4NO_3$ dissociation constant, the $(NH_4)_2SO_4$ dissociation constant relative humidity dependence can be evaluated from Equations (3) and (4) and Reactions 3 and 4 of Table 3. Evaluation of the $(NH_4)_2SO_4$ dissociation constant is generally not merited because the dissociation

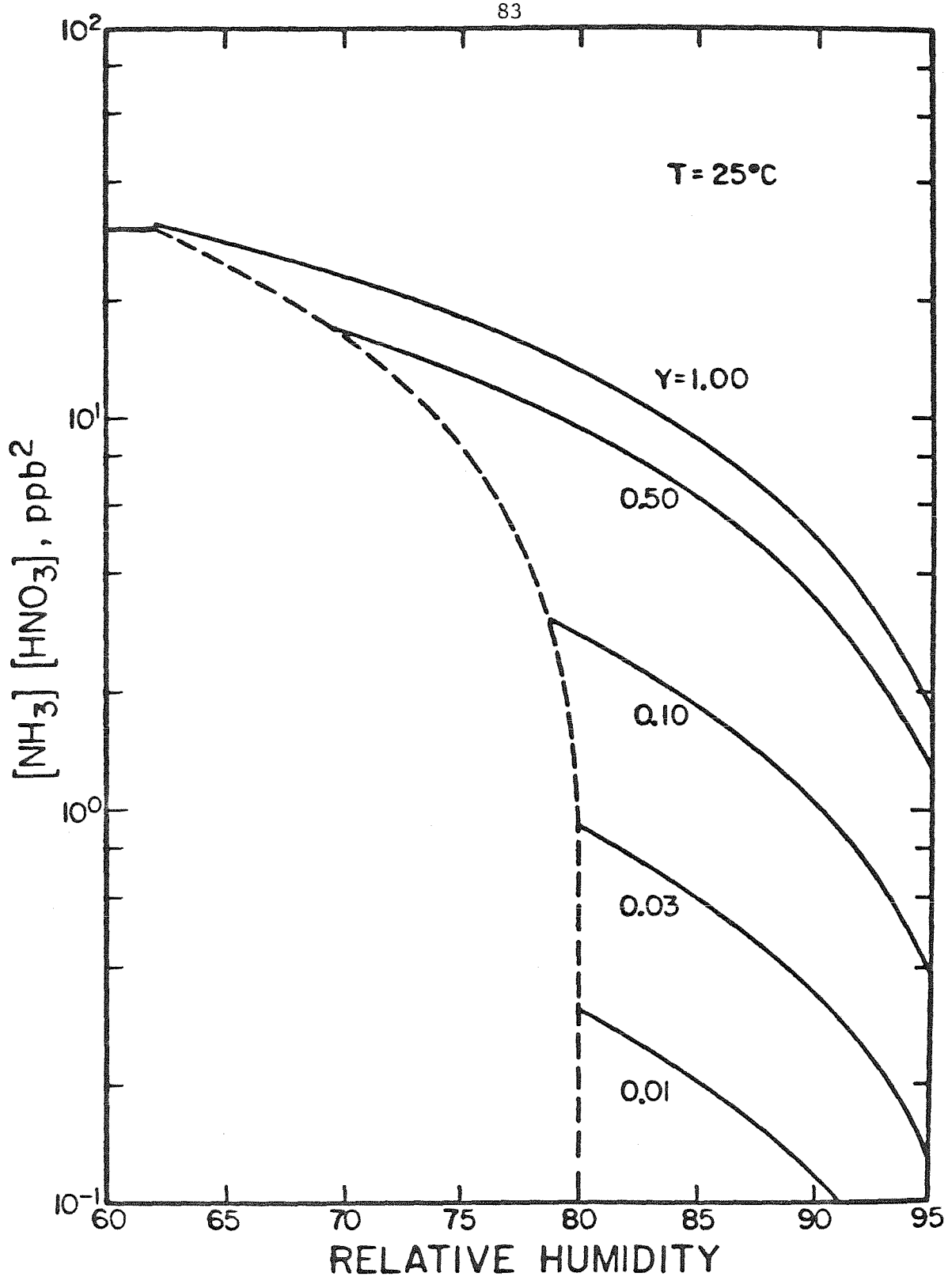


Figure 2. The effect of $(NH_4)_2SO_4$ on the relative humidity dependence of the $NH_4NO_3$ dissociation constant.

Table 3. Equilibrium Constants for the $NH_4NO_3$-$(NH_4)_2SO_4$-$H_2O$ System at 298 K.

| Reaction | Equilibrium Constant* |
|---|---|
| 1. $NH_4NO_3(c,IV) \rightleftarrows NH_3(g) + HNO_3(g)$ | $3.03 \times 10^{-17}$ |
| 2. $NH_4NO_3(aq) \rightleftarrows NH_3(g) + HNO_3(g)$ | $2.71 \times 10^{-18}$ |
| 3. $(NH_4)_2SO_4(c) \rightleftarrows 2NH_3(g) + H_2SO_4(g)$ | $2.33 \times 10^{-38}$ |
| 4. $(NH_4)_2SO_4(aq) \rightleftarrows 2NH_3(g) + H_2SO_4(g)$ | $2.62 \times 10^{-38}$ |

Free Energy Data Sources:

| | |
|---|---|
| $NH_3(g)$, $NH_4NO_3(c,IV)$ | Parker et al. (1976) |
| $HNO_3(g)$, $H_2SO_4(g)$ | JANAF (1971) |
| $NH_4NO_3(aq,m=1)$, $(NH_4)_2SO_4(aq,m=1)$ | Wagman et al. (1968) |

*Thermodynamic equilibrium constants - pressures in atmospheres, aqueous concentration in molality.

constant is small at 25°C. The amount of $(NH_4)_2SO_4$ precursor in the gas phase, the cubic root of the equilibrium constant for Reaction 3 expressed as $(NH_4)_2SO_4$, is about 0.002 μg $m^{-3}$. Thus, the relative humidity dependence of the $(NH_4)_2SO_4$ dissociation constant is not presented in detail.

PARTICLE GROWTH BY PHASE TRANSITION AND WATER CONDENSATION

In addition to the relative humidity and compositional dependence of the $NH_4NO_3$ dissociation constant, it is desirable to predict the growth of a particle by water condensation. The salt weight fraction, $x_s$, of a particle growing in the aqueous solution region of the $NH_4NO_3$-$(NH_4)_2SO_4$-$H_2O$ phase diagram can be calculated from

$$x_s = 1 - \frac{1000}{1000 + \left( YM_1 + \left(\frac{1-Y}{3}\right) M_2 \right) I} \qquad (6)$$

where $M_1$, $M_2$ = the molecular weights of $NH_4NO_3$ and $(NH_4)_2SO_4$, respectively. The water activity over the particle can be predicted from Equation (4). Figs. 3 and 4 compare the theoretical predictions with the experimental data of Tang et al. (1981) for two different $NH_4NO_3/(NH_4)_2SO_4$ molar ratios. Fig. 4 is more complex than Fig. 3 because the aerosol particle goes throught two phase transitions, and part of the particle is solid in some regions. The process in Fig. 4 is shown on the $NH_4NO_3$-$(NH_4)_2SO_4$-$H_2O$ phase diagram, Fig. 1, by the line A-B-C-O (Tang et al., 1981). The aerosol is a solid core surrounded by a saturated solution of composition $E_3$ from A until the particle reaches B. After B the particle grows along the saturation curve from $E_3$ to C. From C to O, the particle growth is governed by Equation (6). Between $E_3$ and C the particle growth can be calculated from

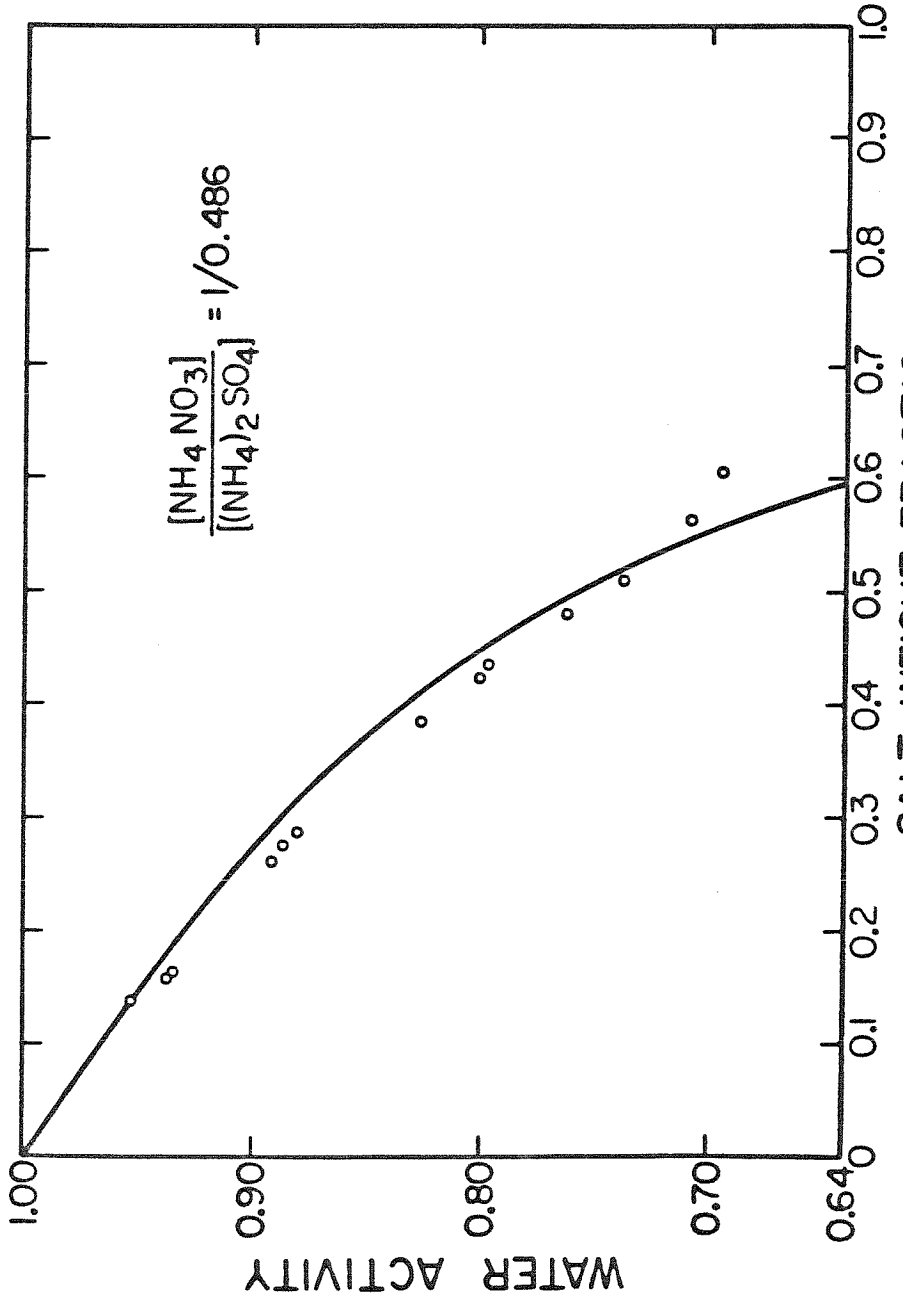


Figure 3. Salt concentration dependence of the water activity for a 44.5-55.5% by wt. $(NH_4)_2SO_4$ - $NH_4NO_3$ mixture.
o - Tang et al. (1981); Solid lines are the theoretical predictions.

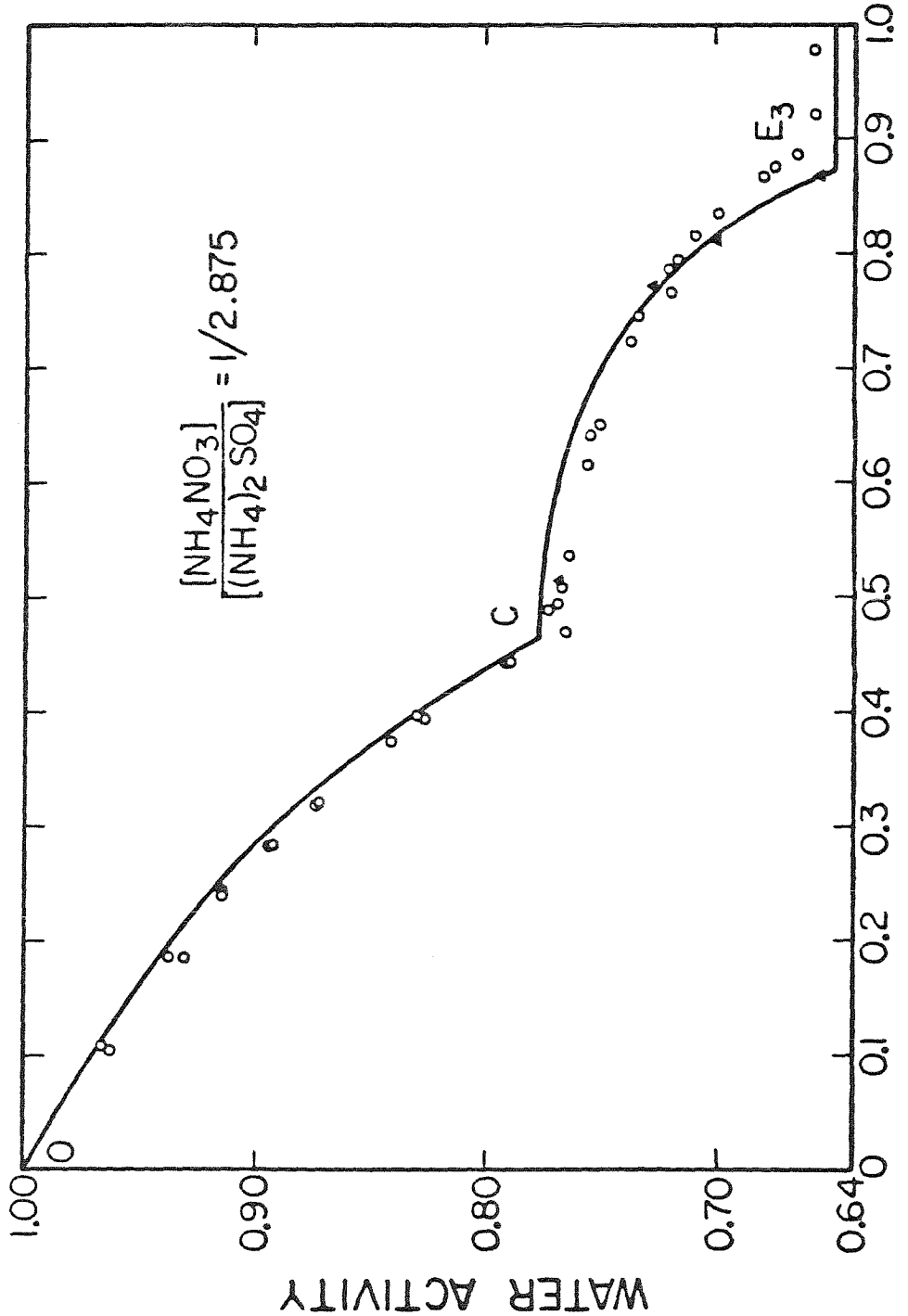


Figure 4. Salt concentration dependence of the water activity for a 82.6-17.4% by wt. $(NH_4)_2SO_4$ - $NH_4NO_3$ mixture.
o - Tang et al. (1981); ▲ - Emons and Hahn (1970); Solid lines are the theoretical predictions.

$$x_s = \frac{(yI)_s}{(yI)_s + \frac{1000}{M_1} z_1^D} \tag{7}$$

where $(yI)_s$ = the $NH_4NO_3$ molality along the saturation curve between $E_3$ and C and $z_1^D$ = the $NH_4NO_3$ mass fraction in the dry particle. Essentially, $NH_4NO_3$ is being used as a tracer between $E_3$ and C since it is completely dissolved in the aqueous phase. From $E_3$ to C on Fig. 4, the growth curve was calculated from Equations (4) and (7) and the solubility data in Silcock (1979) and Emons and Hahn (1970). Also shown in Fig. 4 are growth data calculated from the solubility and water activity data presented in Emons and Hahn (1970). In the region between $E_3$ and $x_s = 1$, the water activity is constant and equals that at $E_3$. The agreement between the theoretical predictions and the experimental data in Figs 3 and 4 is quite encouraging and indicates these techniques may be applicable to more complex multicomponent particles.

PREDICTION OF THE SOLUTION DENSITY

The density, d, of a multicomponent electrolytic solution can be calculated from

$$d = d^0 + \frac{1}{1000} \sum c_i (M_i - d^0 \phi_i) \tag{8}$$

where $d^0$ = the density of water, g $cm^{-3}$, $c_i$ = the molarity of solute i, moles $\ell^{-1}$, $M_i$ = the molecular weight of solute i, g $mole^{-1}$, and $\phi_i$ = the molal volume of solute i, $cm^3$ $mole^{-1}$. Equation (8) is derivable from Young's rule and the definition of the molal volume of a solute (Young and Smith, 1954). The molal volumes in Equation (8) are determined at the total molar ionic strength.

For the aqueous $NH_4NO_3$-$(NH_4)_2SO_4$ system, the $NH_4NO_3$ molal volume ionic strength dependence was calculated using the polynomial fit of Gucker (1934)

which is based on the density data of Adams and Gibson (1932). The polynomial fit of Gucker (1934) was compared to $NH_4NO_3$ molal volumes calculated from density data in Beattie et al. (1928), Campbell et al. (1953) and Geffcken and Price (1934). The agreement was good with the Geffcken and Price data showing some scatter at dilute concentrations. The $(NH_4)_2SO_4$ molal volume ionic strength dependence was obtained by a polynomial regression of molar volume data calculated from the density data in Beattie et al. (1928). The solute molecular weights and the pure water density were taken from Weast (1973). In Fig. 5 the theoretical predictions are compared to experimental measurements for aqueous $NH_4NO_3$-$(NH_4)_2SO_4$ solutions from Tang et al. (1981). The maximum error between the data and predictions is 0.20% indicating the possibility of using Equation (8) for more complex multicomponent electrolytic aerosol solutions.

PREDICTION OF THE REFRACTIVE INDEX

Using the approach developed in Moelwyn-Hughes (1961), the refractive index of an aqueous multicomponent electrolytic solution can be predicted from density and refractive index data for single salts dissolved in water. The refractive index, n, is given by

$$n = \left(\frac{2R+V}{V-R}\right)^{1/2} \tag{9}$$

where R = the mean molar refraction, $cm^3\ mole^{-1}$, and V = the mean molar volume, $cm^3\ mole^{-1}$, and where

$$R = \sum R_i x_i \tag{10}$$

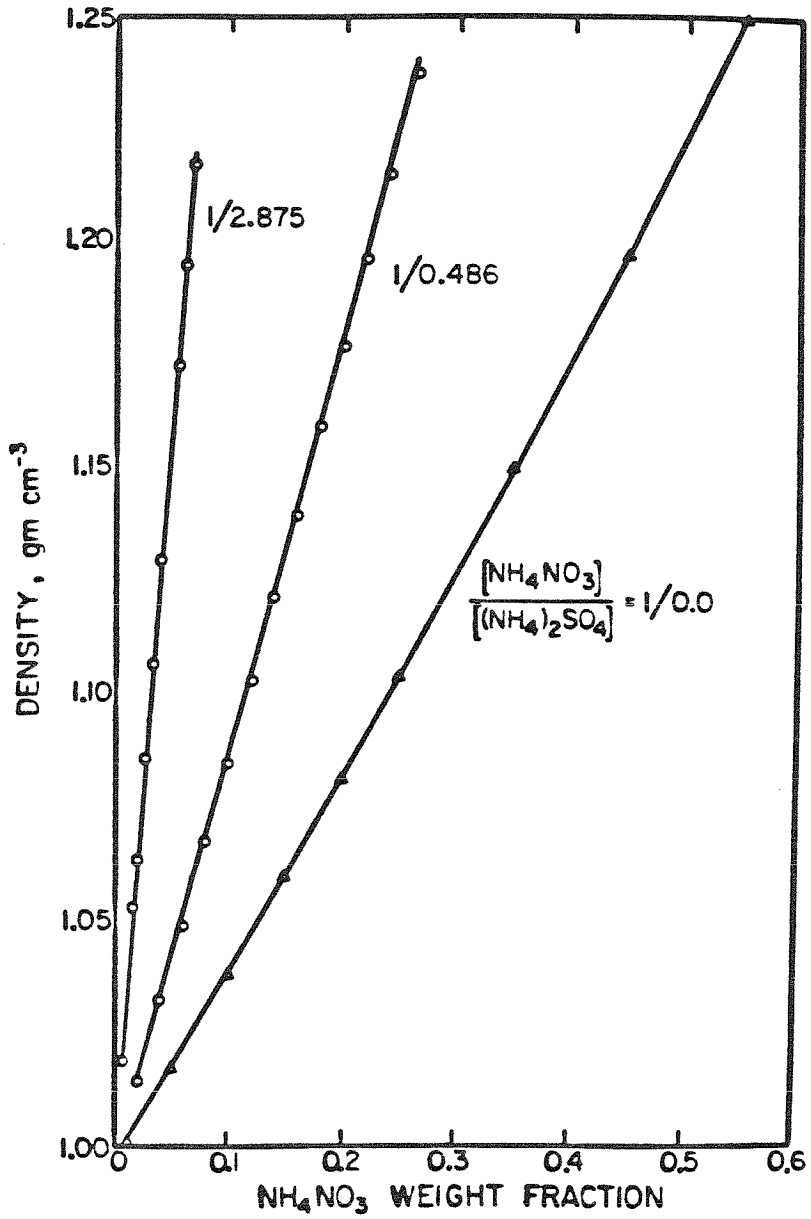


Figure 5. Solution density concentration dependence for various $NH_4NO_3$: $(NH_4)_2SO_4$ molar ratios. o - Tang et al. (1981); Δ - Adams and Gibson (1932); Solid lines are the theoretical predictions.

where $R_i$ = the partial molar refraction of species i, $cm^3$ $mole^{-1}$, and $x_i$ = the mole fraction of species i. The mean molar volume is

$$V = \frac{M}{d} \tag{11}$$

where M = the mean molecular weight, g $mole^{-1}$,

$$M = \sum M_i x_i \ . \tag{12}$$

The solution density prediction technique was described in the preceding section.

The partial molar refraction for water was calculated from the refractive index and density data in Cheneveau (1928) and Stott and Bigg (1928), for $(NH_4)_2SO_4$ from Flöttmann (1928), Pulvermacher (1920) and Rimbach and Wintgen (1910), and for $NH_4NO_3$ from Kruis (1936), Lühdemann (1935) and Geffcken and Price (1934). For all cases the 0.5893 μ wavelength refractive indices were used. The partial molar refractions for $(NH_4)_2SO_4$ and $NH_4NO_3$ were insensitive to ionic strength and varied over the range 23.33-23.98 and 15.20-15.32, $cm^3$ $mole^{-1}$, respectively. In Fig. 6 the theoretical predictions for $R_{NH_4NO_3}$ = 15.20 and $R_{(NH_4)_2SO_4}$ = 23.65 are compared with the experimental measurements of Tang et al. (1981). The agreement between theory and data is quite good indicating the possible applicability of Equations (9-12) to more complex multicomponent aerosol solutions.

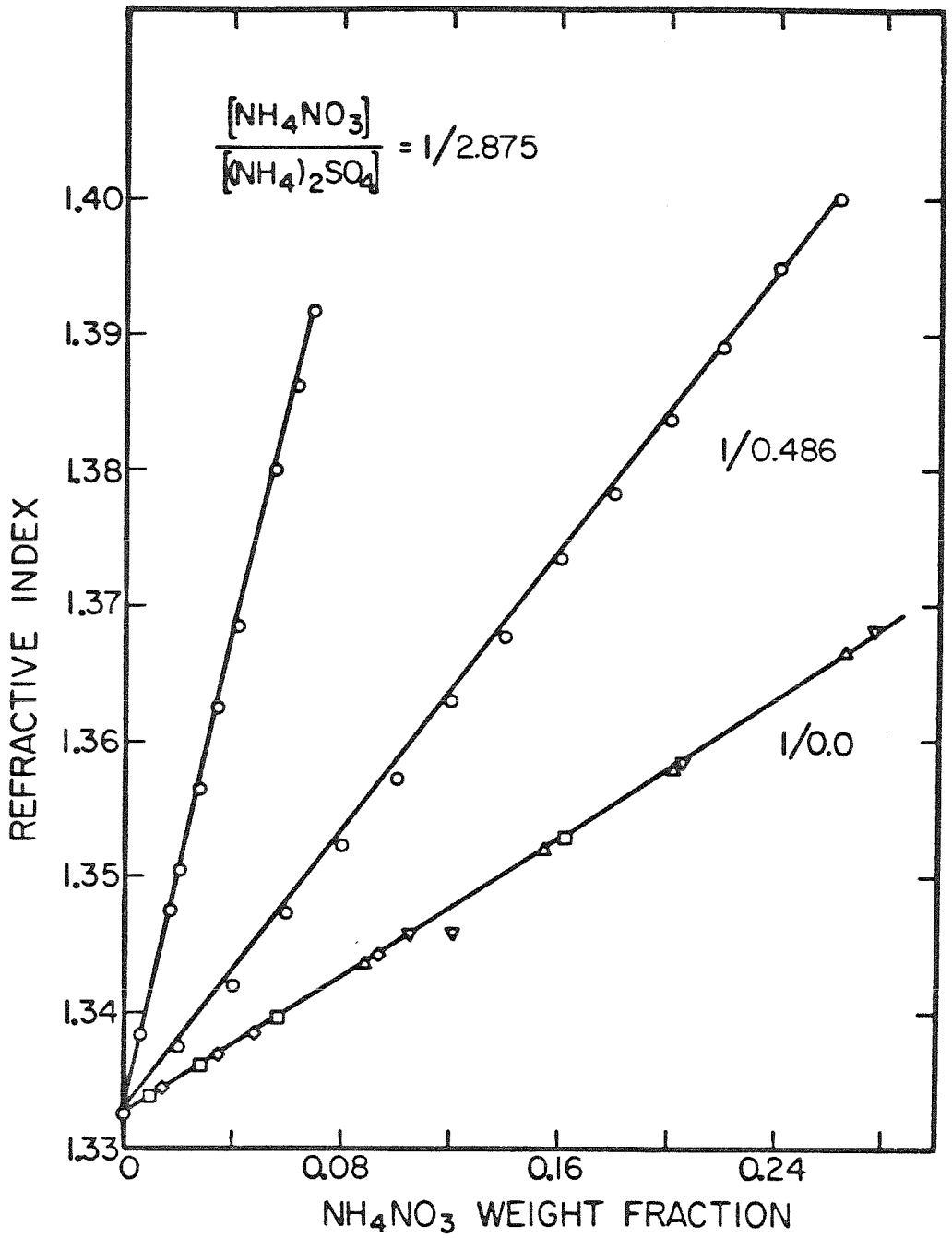


Figure 6. Refractive index concentration dependence for various $NH_4NO_3$: $(NH_4)_2SO_4$ molar ratios. o - Tang et al. (1981); □ - Kruis (1936); ◇ - Geffcken and Price (1934); △ - Lühdemann (1935); ▽ - Pickard et al. (1928); Solid lines are the theoretical predictions.

## DISCUSSION

In the Background section, several questions were highlighted concerning the applicability of the thermodynamic theories presented to aerosol sampling and evaluation methods. From the theories discussed in this paper, answers to these questions can be advanced.

1. What effect would the internal mixing of a pure aqueous $(NH_4)_2SO_4$ aerosol with a pure aqueous $NH_4NO_3$ aerosol have on the $NH_4NO_3$ dissociation constant?

By examining Fig. 2, this question can easily be answered. Since the relative humidity remains constant, the mixing process would follow a relative humidity isopleth. From the mixing process, Y would decrease and likewise $[NH_3][HNO_3]$ would decrease. Thus, the net effect would be to absorb more nitric acid from the gas phase into the aerosol phase provided sufficient ammonia is present.

2. How would the presence of $NH_4NO_3$ effect an aerosol identification technique that utilizes particle growth resulting from water condensation?

The increase in particle radius due to water condensation is given by

$$\frac{r_2}{r_1} = \left(\frac{d_1\ x_{s1}}{d_2\ x_{s2}}\right)^{1/3} \tag{13}$$

where $r_2$, $r_1$ = the final and initial particle radii, $d_2$, $d_1$ = the final and initial particle density and $x_{s2}$, $x_{s1}$ = the final and initial salt weight fraction. From the preceding discussions on predictive techniques for particle growth, water activity and solution density, the effect of $NH_4NO_3$ on the volumetric growth of a $(NH_4)_2SO_4$ aerosol particle can be evaluated for any $NH_4NO_3/(NH_4)_2SO_4$ ratio.

3. Is the reduction in the nitrate aerosol formation rate during simultaneous sulfate aerosol formation the result of a change in the distribution of nitric acid between the gas and aerosol phases or is the total amount of nitrate formed reduced?

This question has already been partially addressed in the answer to question 1. The presence of $(NH_4)_2SO_4$ should decrease the amount of $HNO_3$ in the gas phase. Thus, if the aerosol sulfate was $(NH_4)_2SO_4$, the amount of aerosol nitrate should increase provided enough ammonia is present. The reduced nitrate formation rate observed by Clark et al. (1976) could result from the displacement of $HNO_3$ by $H_2SO_4$ from $NH_4NO_3$ on the filter material as studied by Appel and Tokiwa (1981). Finally, the results of Clark et al. could be explained by the aqueous competitive or inhibited oxidation of nitrite to nitrate. Definitely their results are not due to the presence of $(NH_4)_2SO_4$ alone.

## CONCLUSIONS

The prediction of the thermodynamic properties of $NH_4NO_3$-$(NH_4)_2SO_4$-$H_2O$ aerosols from binary solution data is shown to be feasible. The water activity is obtained using the approach developed by Kusik and Meissner (1978), the solution density from Young's rule and the refractive index from the discussion in Moelwyn-Hughes (1961). The agreement between experimental measurements and theoretical predictions indicates the applicability of these approaches to more complex electrolytic solutions. Particle growth is calculable from the $NH_4NO_3$-$(NH_4)_2SO_4$-$H_2O$ phase diagram, the initial particle composition and the water activity prediction technique. Finally, the effect of $(NH_4)_2SO_4$ on the relative humidity dependence of the $NH_4NO_3$ dissociation constant is shown to be less than 40% for nitrate ionic strength fractions greater than 0.5.

ACKNOWLEDGMENT

This work was supported by U.S. Environmental Protection Agency grant R806844. We would like to thank James J. Morgan for helpful discussions.

REFERENCES

Adams L.H. and Gibson R.E. (1932) Equilibrium in binary systems under pressure. III. The influence of pressure on the solubility of ammonium nitrate in water at 25°C. J. Amer. Chem. Soc. 54, 4520-4537.

Ahlberg M.S. and Winchester J.W. (1978) Dependence of aerosol sulfur particle size on relative humidity. Atmospheric Environment 12, 1631-1632.

Appel B.R., Kothny E.L., Hoffer E.M., Hidy G.M. and Wesolowski J.J. (1978) Sulfate and Nitrate Data from the California Aerosol Characterization Experiment (ACHEX). Envir. Sci. Technol. 12, 418-425.

Appel B.R. and Tokiwa Y. (1981) Atmospheric particulate nitrate sampling errors due to reactions with particulate and gaseous acids. Atmospheric Environment 15, 1087-1089.

Beattie J.A., Brooks, B.T., Gillespie L.J., Scatchard G., Schumb W.C. and Tefft R.F. (1928) Density (specific gravity) and thermal expansion (under atmospheric pressure) of aqueous solutions of inorganic substances and of strong electrolytes. In International Critical Tables of Numerical Data, Physics, Chemistry and Technology, Vol. III, pp. 51-111, McGraw-Hill, New York.

Campbell A.N., Gray A.P. and Kartzmark E.M. (1953) Conductances, densities, and fluidities of solutions of silver nitrate and of ammonium nitrate at 35°. Can. J. Chem. 31, 617-630.

Chen C.S. (1974) Evaluation of the vapor pressure over an aerosol particle. J. Atmos. Sci. 31, 847-849.

Cheńeveau C. (1928) Refractivity of selected solids and liquids. In International Critical Tables of Numerical Data, Physics, Chemistry and Technology, Vol. VII, pp. 12-16. McGraw-Hill, New York.

Clark W.E., Landis D.A. and Harker A.B. (1976) Measurements of the photochemical production of aerosols in ambient air near a freeway for a range of $SO_2$ concentrations. Atmospheric Environment 10, 637-644.

Cunningham P.T., Johnson S.A. and Yang R.T. (1974) Variations in chemistry of airborne particulate material with particle size and time. Envir. Sci. Technol. 8, 131-135.

Doyle G.J., Tuazon E.C., Graham R.A., Mischke T.M., Winer A.M. and Pitts, J.N. Jr. (1979) Simultaneous concentrations of ammonia and nitric acid in a polluted atmosphere and their equilibrium relationship to particulate ammonium nitrate. Envir. Sci. Technol. 13, 1416-1419.

Emons H.H. and Hahn W. (1970) Dampdruckmessungen in system ammonnitrat-ammonsulfat-wasser. Leuna Technischen Hochschule fur Chemie. Wissenschaftliche Zeitschrift 12, 129-132.

Flöttmann Fr. (1928) Über löslichkeitsgleichgewichte. Z. Anal. Chem. 73, 1-39.

Geffcken W. and Price D. (1934) Zur frage der konzentrationsäbhangigkeit des scheinbaren molvolumens und der scheinbaren molrefraktion in verdünnten lösungen. Z. Physik. Chem. B26, 81-99.

Gibbard H.F. Jr., Scatchard G., Rousseau R.A. and Creek J.L. (1974) Liquid-vapor equilibrium of aqueous soldium chloride, from 298 to 373K and from 1 to 6 mol $kg^{-1}$, and related properties. J. Chem. Engng. Data 19, 281-288.

Gucker F.T. (1934) The calculation of partial molal solute quantities as functions of the volume concentration, with special reference to the apparent molal volume. J. Phys. Chem. 38, 307-317.

Hamer W.J. and Wu Y.-C. (1972) Osmotic coefficients and mean activity coefficients of uni-univalent electrolytes in water at 25°C. J. Phys. Chem. Ref. Data 1, 1047-1099.

Hänel G. and Zankl B. (1979) Aerosol size and relative humidity: Water uptake by mixtures of salts. Tellus 31, 478-486.

Harrison R.M. and Pio C.A. (1981) Apparatus for simultaneous size-differentiated sampling of optical and suboptical aerosols: Application to analysis of nitrates and sulfates. J. Air Pollut. Control Assoc. 31, 784-787.

JANAF Thermochemical Tables, 2nd Edn. (1971). NSRDS-NBS 37.

Kruis A. (1936) Die aquivalentdispersion von starken elektrolyten in losung. I. Die messung der konzentrationsabhängigkeit der äquivalentrefraktion im sichtbaren. Z. Physik. Chem. B34, 13-50.

Kusik C.L. and Meissner H.P. (1978) Electrolyte activity coefficients in inorganic processing. A.I.Ch.E. Symp. Ser. 173, 14-20.

Lühdemann R. (1935) Über die konzentrationsabhängigkeit der äquivalentrefraktion einiger salze unde säuren in wässeriger lösung. Z. Physik. Chem. B29, 133-149.

Moelwyn-Hughes E.A. (1961) Physical Chemistry, 2nd Rev. Ed, p. 397. Pergamon Press, New York.

Orr C. Jr., Hurd F.K. and Corbett W.J. (1958) Aerosol size and relative humidity. J. Coll. Sci. 13, 472-482.

Parker V.B., Wagman D.D. and Garvin D. (1976) Selected thermochemical data compatible with the CODATA recommendations. NBSIR 75-968.

Patterson R.K. and Wagman J. (1977) Mass and composition of an urban aerosol as a function of particle size for several visibility levels. J. Aer. Sci. 8, 269-279.

Pickard R.H., Houssa A.H.J. and Hunter H. (1928) Refractivity of mixtures. In International Critical Tables of Numerical Data, Physics, Chemistry and Technology, Vol. VII, pp. 63-108. McGraw-Hill, New York.

Pulvermacher O. (1920) Zur kenntnis wäßriger lösungen. Z. Anorg. Chem. 113, 141-148.

Rimbach E. and Wintgen R. (1910) Über den einfluss der komplexbildung auf raumerfüllung und lichtbrechung gelöster körper. Z. Physik. Chem., Stoich. and Verwand. 74, 233-252.

Saxena P. and Peterson T.W. (1981) Thermodynamics of multicomponent electrolytic aerosols. J. Coll. Int. Sci. 79, 496-510.

Silcock H.L. (1979) Solubilities of Inorganic and Organic Compounds, Vol. 3, Part 2, pp. 157-159. Pergamon Press, New York.

Staples B.R. and Nuttall R.L. (1977) The activity and osmotic coefficients of aqueous calcium chloride at 298.15 K. J. Phys. Chem. Ref. Data 6, 385-407.

Stelson A.W., Friedlander S.K. and Seinfeld J.H. (1979) A note on the equilibrium relationship between ammonia and nitric acid and particulate ammonium nitrate. Atmospheric Environment 13, 369-371.

Stelson A.W. and Seinfeld J.H. (1981a) Relative humidity and temperature dependence of the ammonium nitrate dissociation constant. Atmospheric Environment 15, XXX-XXX.

Stelson, A.W. and Seinfeld J.H. (1981b) Relative humidity and pH dependence of the vapor pressure of ammonium nitrate-nitric acid solutions at 25°C. Atmospheric Environment 15, XXX-XXX.

Stevens R.K., Dzubay T.G., Russwurm G. and Rickel D. (1978) Sampling and analysis of atmospheric sulfates and related species. Atmospheric Environment 12, 55-68.

Stott V. and Bigg P.H. (1928) Density and specific volume of water. In International Critical Tables of Numerical Data, Physics, Chemistry and Technology, Vol. III, pp. 24-26. McGraw-Hill, New York.

Tang I.N., Wong W.T. and Munkelwitz H.R. (1981) The relative importance of atmospheric sulfates and nitrates in visibility reduction. Atmospheric Environment 15, XXX-XXX.

Tang I.N. (1980) On the equilibrium partial pressures of nitric acid and ammonia in the atmosphere. Atmospheric Environment 14, 819-828.

Tang I.N., Munkelwitz H.R. and Davis J.G. (1978) Aerosol growth studies - IV. Phase transformation of mixed salt aerosols in a moist atmosphere. J. Aer. Sci. 9, 505-511.

Thudium J. (1978) Water uptake and equilibrium sizes of aerosol particles at high relative humidities: Their dependence on the composition of the water-soluble material. Pageoph 116, 130-148.

Wagman D.D., Evans W.H., Parker V.B., Harlöw I., Baily S.M. and Schumm R.H. (1968) Selected values of chemical thermodynamic properties; tables for the first thirty-four elements in the standard order of arrangement, NBS technical note 270-3.

Weast R.C. ed. (1973) Handbook of Chemistry and Physics, 54th Edn. CRC Press, Cleveland.

Winkler P. (1973) The growth of atmospheric aerosol particles as a function of the relative humidity - II. An improved concept of mixed nuclei. Aerosol Science 4, 373-387.

Winkler P. and Junge C. (1972) The growth of atmospheric aerosol particles as a function of the relative humidity. Part I: Method and measurements at different locations. J. Rech. Atmos. (Mémorial Henri Dessens) 1972, 617-638.

Wishaw B.F. and Stokes R.H. (1954) Activities of aqueous ammonium sulphate solutions at 25°C. Trans. Faraday Soc. 50, 952-954.

Young T.F. and Smith M.B. (1954) Thermodynamic properties of mixtures of electrolytes in aqueous solutions. J. Phys. Chem. 58, 716-724.

# CHAPTER 6

# FUTURE RESEARCH

In many ways the approaches developed in this thesis can be expanded and and applied to urban aerosol problems. Some examples of these areas are outlined in the following sections.

I. Displacement Reactions

The heterogeneous reactions of gaseous acids, HBr, HCl, $H_2SO_4$ and $HNO_3$, with pre-existing solid or aqueous aerosols is an area needing experimental and theoretical work. A typical reaction studied by Robbins et al.(1959) is

$$NaCl(s \text{ or } aq) + HNO_3(g) \Leftrightarrow NaNO_3(s \text{ or } aq) + HCl(g). \quad (1)$$

The role of the displacement reaction,

$$NH_4NO_3(s) + HCl(g) \Leftrightarrow NH_4Cl(s) + HNO_3(g), \quad (2)$$

on filter deposited aerosol material has been explored by Apoel and Tokiwa (1981). Thus, an understanding of these reactions is important for ambient aerosol chemistry as well as sampling.

II. Heterogeneous Neutralization Reactions

This area is similar to Topic I but involves the reaction of a gaseous acid with an aerosol base or vice versa. Robbins and Cadle(1958) studied the reaction of gaseous ammonia with sulfuric acid droplets. A typical example of the alternate reaction scheme, gaseous acid reacting with an aerosol base, is

$$HNO_3(g) + NaOH(aq) \Leftrightarrow NaCl(aq \text{ or } s) + H_2O(g). \quad (3)$$

These reactions have an important role in gaseous or aerosol acidic deposition processes.

III. Photo - Oxidation of Nitrite to Nitrate

The oxidation of nitrite to nitrate in sunlight has been shown by Dahr et al.(1934,1936). They demonstrated this oxidation is greatly accelerated by the presence of titanium, zinc and iron oxides ($TiO_2$, ZnO and $Fe_2O_3$). Since soil dust is a source of large ambient aerosol particles and soil contains $TiO_2$ and $Fe_2O_3$, this mechanism may be an important source for large particle nitrate formation (Stelson and Seinfeld, 1981).

IV. Refractive Indices and Densities of Multicomponent Ambient Aerosol Solutions

In Chapter 5 equations were derived that enabled the calculation of the refractive index and the density of aqueous multicomponent ionic solutions. These equations were tested on data for the $NH_4NO_3$ - $(NH_4)_2SO_4$ - $H_2O$ system and excellent agreement was obtained. The ambient aqueous aerosol solutions cannot be merely described by $NH_4NO_3$ and $(NH_4)_2SO_4$ and are complex multicomponent mixtures (Stelson and Seinfeld, 1981). Therefore, these equations should be more rigorously tested before being applied to visibility modelling and improved sampling techniques.

V. Atmospheric Aerosol Density Monitoring

From aerosol mass and volume distribution data, the size dependence of the aerosol density can be calculated. In addition, size composition data are desirable. The mass distribution can be measured with a cascade impactor and the volume distribution with an optical particle counter and an electrical aerosol analyzer. Chemical composition data are obtainable by some combined size classification and filter measurement technique. The typical ambient aerosol density can vary from 1.00 g $cm^{-3}$ for water to 9.5 g $cm^{-3}$ for lead oxide (Lange, 1944). Thus, a reasonable range for density measurements exists.

These measurements can be used to answer several important questions.

1) Does the correction from aerodynamic diameter to true particle diameter significantly alter the aerosol mass distribution?

2) Can the density data, composition size distribution and total chemical composition data be used to improve observed aerosol to source signature balances?

3) Thermodynamic analysis indicates the aerosol density should decrease as the relative humidity increases. Does this occur and at what rate?

4) If the aerosol is predominantly an aqueous electrolytic solution, how do the density predictions from Equation (8) in Chapter 5 compare with ambient measurements?

REFERENCES

Appel B.R. and Tokiwa Y. (1981) Atmospheric particulate nitrate sampling errors due to reactions with particulate and gaseous strong acids. Atmospheric Environment 15, 1087-1089.

Dhar N.R. and Tandon S.P. (1936) Oxidation of nitrites to nitrates in sunlight. J. Indian Chem. Soc. 13, 180-184.

Dhar N.R., Tandon S.P., Biswas N.N. and Bhateacharya A.K. (1934) Photo-oxidation of nitrite to nitrate. Nature 133, 213-214.

Lange N.A. (1944) Handbook of Chemistry, 5th Ed, pp. 154-265. Handbook Publishers, Sandusky, Ohio.

Robbins R.C. and Cadle R.D. (1958) Kinetics of the reaction between gaseous ammonia and sulfuric acid droplets in an aerosol. J. Phys. Chem. 62, 469-471.

Robbins R.C., Cadle R.D. and Eckhardt D.L. (1959) The conversion of sodium chloride to hydrogen chloride in the atmosphere. J. Meteorology 16, 53-56.

Stelson A.W. and Seinfeld J.H. (1981) Chemical mass accounting of urban aerosol. Environ. Sci. Technol. 15, 671-679.

# APPENDIX A

## ON THE DENSITIES OF AQUEOUS SULFATE SOLUTIONS

Accepted for publication in Atmospheric Environment.

ON THE DENSITIES OF AQUEOUS SULFATE SOLUTIONS

We have noted a disagreement among density data from different sources for $NH_4HSO_4$ solutions. The most recent source of data on $NH_4HSO_4$ solution densities is Tang (1980). Figure 1 is a reproduction of Figure 1 of that work. Note the relative positions of the curves for $(NH_4)_2SO_4$, $(NH_4)_3H(SO_4)_2$, $NH_4HSO_4$, and $H_2SO_4$. His cited source for $(NH_4)_2SO_4$ and $H_2SO_4$ density data is International Critical Tables (1928). Tang (1980) states that the $NH_4HSO_4$ and $(NH_4)_3H(SO_4)_2$ density data were obtained experimentally and refers to Tang and Munkelwitz (1977, 1978). From study of the latter reference, it appears that the $NH_4HSO_4$ density curve is, in fact, based on a single data point from the International Critical Tables (1928) together with the interpolation formula (Moelwyn-Hughes, 1961)

$$\rho = \frac{\rho_1}{1 - \alpha w_2} \qquad (1)$$

where $\rho$ = the solution density in gm $ml^{-1}$, $\rho_1$ = water density in gm $ml^{-1}$, $w_2$ = weight fraction of solute, and $\alpha$ is a constant determined from a given value of $\rho$ at a known $w_2$. Based on the International Critical Tables' $NH_4HSO_4$ solution density at $25^{\circ}$ and the solubility of $NH_4HSO_4$ interpolated from data in Seidell and Linke (1965), $\alpha$ can be evaluated.

The $NH_4HSO_4$ solution density values calculated from (1) are found to agree closely with those in Table 1 of Tang and Munkelwitz (1977). The densities from Table 1 of that reference, together with those of $(NH_4)_2SO_4$ and $H_2SO_4$ from International Critical Tables (1928) are shown in Figure 2. The $(NH_4)_2SO_4$ and $H_2SO_4$ solution densities in Figures 1 and 2 are in excellent agreement as expected. Note the relative positions of the $H_2SO_4$, $(NH_4)_2SO_4$ and $NH_4HSO_4$ curves in Figure 2, as compared with those in Figure 1. Tang (1980) does not state why

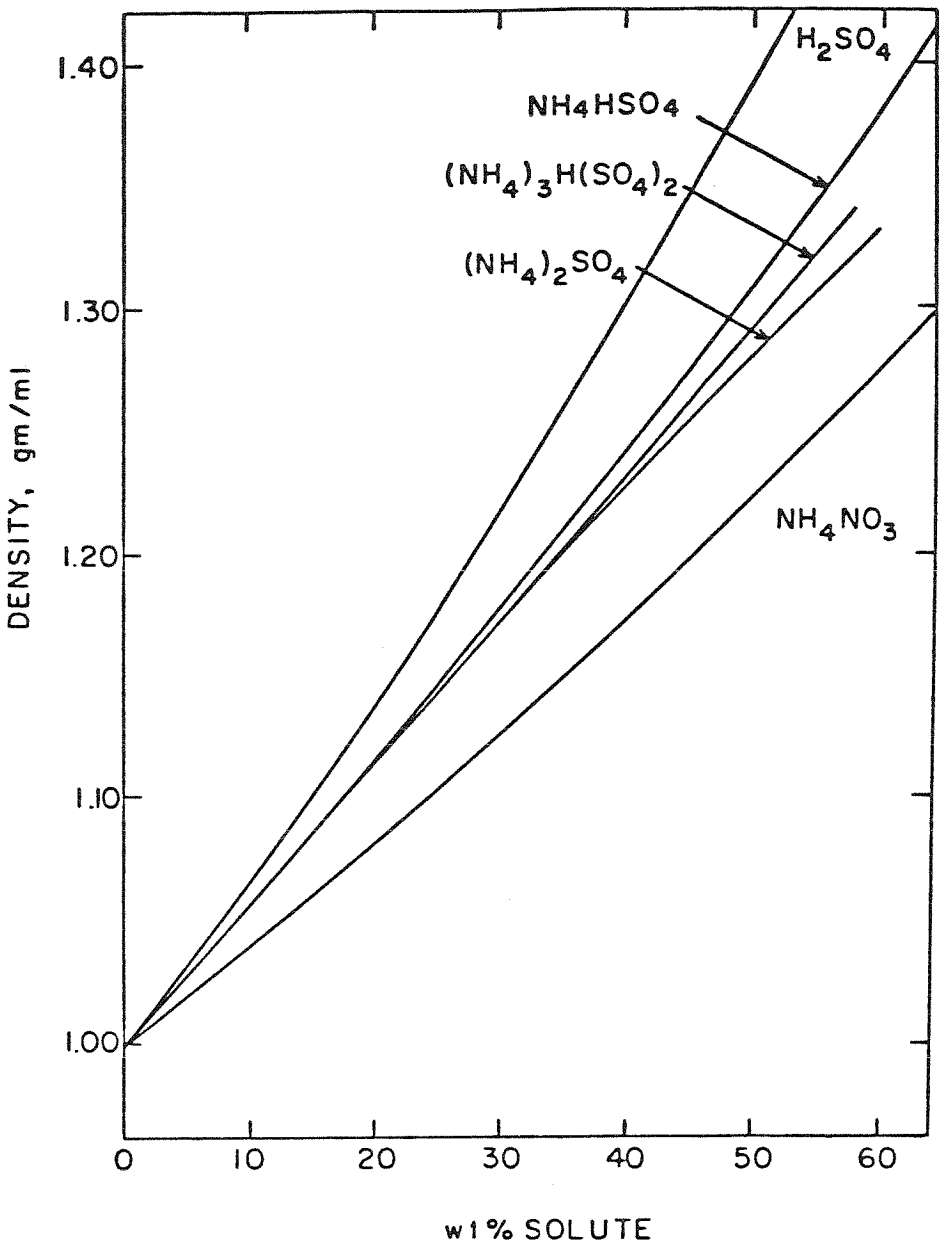


Figure 1. Densities of aqueous sulfate and nitrate solutions at 25°C [Figure 1 of Tang (1980)].

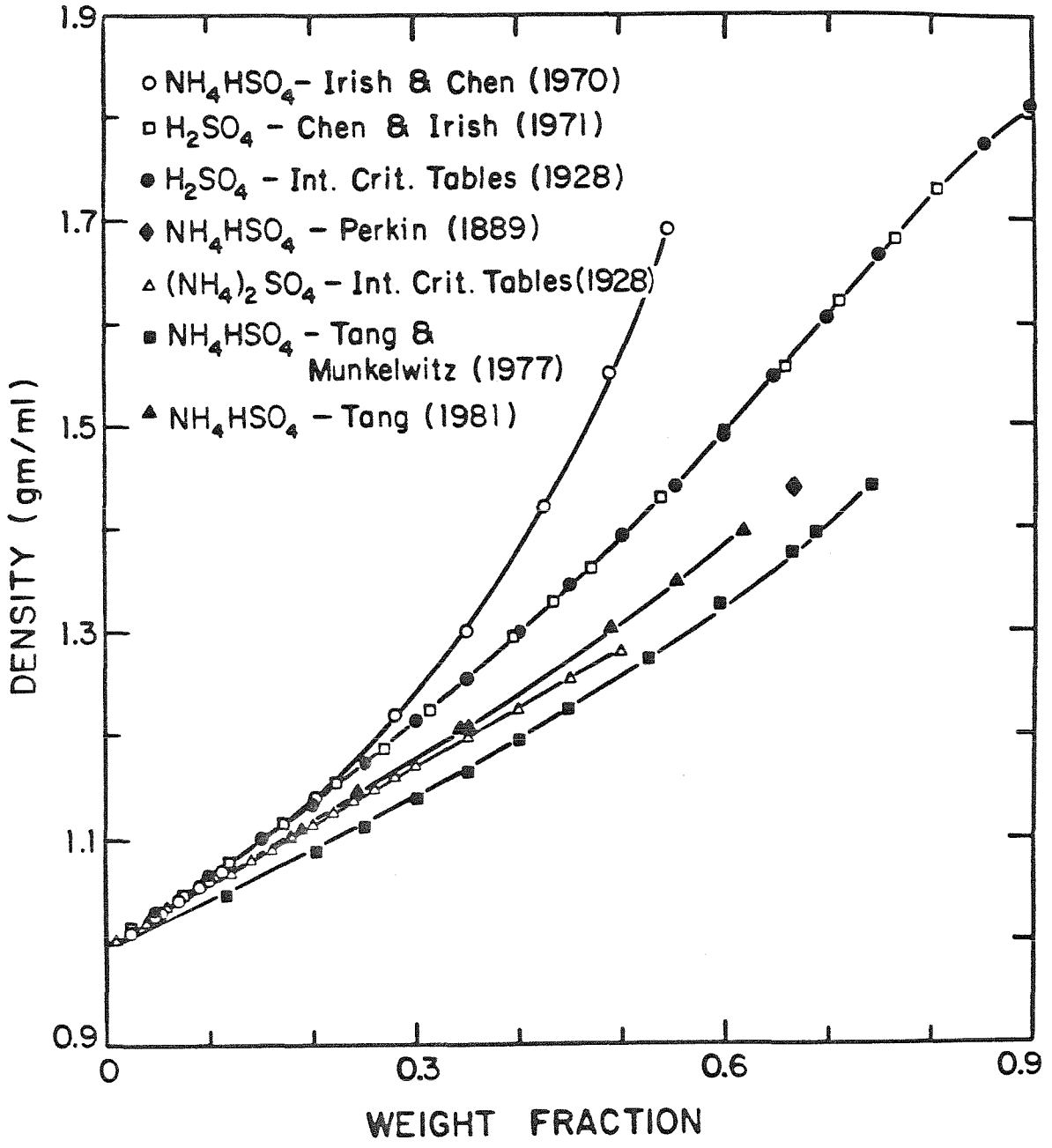


Figure 2. Calculated and measured sulfate solution densities at 25°C.

he has shifted the relative positions of the $(NH_4)_2SO_4$ and $NH_4HSO_4$ density curves from those in his earlier paper.

Also shown in Figure 2 is the point reported in the International Critical Tables (1928) for the density of 66.67 percent $NH_4HSO_4$ solution. It appears that Tang and Munkelwitz (1977) mistook the $NH_4HSO_4$ value from the International Critical Tables (1928) to be that for a saturated solution at 25°C. The original reference, Perkin (1889), reports the specific gravity for a 66.67 percent $NH_4HSO_4$ solution. Thus, apparently the International Critical Tables (1928) misquoted Perkin (1889) and Tang and Munkelwitz (1977) further misconstrued the International Critical Tables (1928). The specific gravity has been converted to the density using the density of water from Weast (1973). The correction is small, about 0.3 percent.

An additional calculation of $H_2SO_4$ and $NH_4HSO_4$ solution densities can be carried out. Irish and Chen (1970) and Chen and Irish (1971) report molar concentrations for $H_2O$ and $H_2SO_4$ or $NH_4HSO_4$ from which solution densities can be calculated from

$$\rho = \frac{M_s[S] + 18[H_2O]}{1000} \qquad (2)$$

where $M_s$ is the molecular weight of the sulfate salt and [S] and $[H_2O]$ are the molar concentrations of the sulfate salt and water. Densities calculated on this basis are shown in Figure 2. The sulfuric acid densities are in excellent agreement with those of the International Critical Tables (1928), whereas the densities of $NH_4HSO_4$ solutions differ with those reported by Tang and Munkelwitz (1977). It appears clear that an error exists in the $NH_4HSO_4$ data of Irish and Chen (1970).

Although Mellor (1964) cites Postnikov et al. (1936) as a reference for $NH_4HSO_4$ solution density data, Postnikov et al. (1936) in fact studied $NH_4HSO_3$.

As noted above, Tang (1980) disagrees with his own previous work (Tang and Munkelwitz, 1977) and with International Critical Tables (1928), and Irish and Chen (1970) disagree with all the other sources. The importance of knowing the correct density can be demonstrated by converting molality to molarity for a $NH_4HSO_4$ solution. The appropriate formula for conversion is

$$[S] = \frac{\rho}{\frac{1}{m_s} + \frac{M_s}{1000}} \qquad (3)$$

where $m_s$ = molality of sulfate salt. For a 50 weight percent $NH_4HSO_4$ solution (8.687 molal), (3) becomes $[S] = 4.344\rho$. Using Figures 1 and 2, different values for the solution density are obtained, as indicated in Table 1. Table 1 shows the discrepancy between the data sources is significant. This disagreement is unfortunate since this molality corresponds to a water acitivity of 0.69 and $NH_4HSO_4$ deliquesces at 0.397 (Tang and Munkelwitz, 1977).

Personal communication from Tang (1981) included $NH_4HSO_4$ solution density measurements which are shown in Figure 2. These data smoothly extrapolate to the point of Perkin (1889). At 50 weight percent $NH_4HSO_4$, the calculated molarity based on this data is 5.675, which agrees well with Tang (1980) and Perkin (1889) in Table 1. Thus, the correct $NH_4HSO_4$ density concentration dependence is the $NH_4HSO_4$ curve in Figure 1 or the $NH_4HSO_4$ curve labelled Tang (1981) in Figure 2.

A. W. Stelson
J. H. Seinfeld
Department of Chemical Engineering
California Institute of Technology
Pasadena, California 91125

Table 1. Densities and Molarities of a 50% $NH_4HSO_4$ Solution

| Data Source | $\rho$, g $ml^{-1}$ | [S], moles $\ell^{-1}$ |
|---|---|---|
| Tang (1980) | 1.308 | 5.682 |
| Tang and Munkelwitz (1977) | 1.259 | 5.469 |
| Irish and Chen (1970) | 1.583 | 6.876 |
| Perkin (1889)* | 1.293 | 5.615 |

*Calculated using Perkin's $NH_4HSO_4$ specific gravity datum and (1).

References

Chen H. and Irish D. E. (1971) A Raman spectral study of bisulfate-sulfate systems. II. Constitution, equilibria, and ultrafast proton transfer in sulfuric acid. J. Phys. Chem. 75 (17), 2672-2681.

International Critical Tables (1928). Volume III, p. 56-60. McGraw-Hill, New York.

Irish D.E. and Chen H.(1970) Equilibria and proton transfer in the bisulfate-sulfate system. J. Phys. Chem. 74 (21), 3796-3801.

Mellor J.W. (1964) Mellor's Comprehensive Treatise on Inorganic and Theoretical Chemistry, Volume VIII, Supplement I, N(Part I), p. 503, John Wiley & Sons, New York.

Moelwyn-Hughes E.A. (1961) Physical Chemistry, 2nd ed., p. 808, Pergamon Press, Oxford.

Perkin W.H. (1889) LXVIII. - The magnetic rotatory power of nitrogen compounds, also of hydrochloric, hydrobromic, and hydriodic acids, and of some of the salts of ammonia and the compound ammonias. J. Chem. Soc. 55, 680-749.

Postnikov V.F., Kirillov I.P., Nabiev M. and Khaidarov V (1936) The viscosity of single salt aqueous solutions. J. Appl. Chem. (USSR) 9, 1926-1928.

Seidell A. and Linke W. F. (1965) Solubilities of Inorganic and Metal Organic Compounds, 4th ed., American Chemical Society, Washington.

Tang I.N. (1981) Personal Communication.

Tang I.N. (1980) On the equilibrium partial pressures of nitric acid and ammonia in the atmosphere. Atmos. Environ. 14, 819 - 828.

Tang I.N. and Munkelwitz H. R.(1978) The optical and thermodynamic properties of $(NH_4)_3H(SO_4)_2$ (Letovicite) aerosols, Presented at the May 1978 Industrial Hygiene Conference, Los Angeles.

Tang I.N. and Munkelwitz H. R.(1977) Aerosol growth studies - III. Ammonium bisulfate aerosols in a moist atmosphere. J. Aer. Sci. 8, 321-330.

Weast R.C. (1973) Handbook of Chemistry and Physics, 54th. Edn. CRC Press, Cleveland.

# APPENDIX B

## PREDICTION OF THE DENSITY OF AMMONIUM BISULFATE SOLUTIONS

Accepted for publication in the Journal of Physical Chemistry.

# PREDICTION OF THE DENSITY OF AMMONIUM BISULFATE SOLUTIONS

A. W. Stelson and J. H. Seinfeld
Department of Chemical Engineering
California Institute of Technology
Pasadena, California 91125

## ABSTRACT

The densities of ammonium bisulfate solutions are predicted from molal volume and bisulfate dissociation data. Good agreement is shown between measured ammonium bisulfate solution densities and the predictions. A discrepancy between densities predicted using tabulated data from Irish and Chen and measured ammonium bisulfate solution densities is resolved (1,2).

The concentration dependence of the density of ammonium bisulfate solutions has recently been studied (1). It was found that the $NH_4HSO_4$ solution densities calculated from the data for the molarities of $NH_4HSO_4$, $[NH_4HSO_4]$, and water, $[H_2O]$, in Table I of Irish and Chen (2) differed substantially from available data. The objective of this communication is twofold: (a) to determine the source of this discrepancy, and (b) to ascertain whether the extent of bisulfate dissociation in $NH_4HSO_4$ solutions is accurately represented by the data in Irish and Chen (2). The validity of the $NH_4HSO_4$ molarity and extent of bisulfate dissociation data in that table will be determined by comparing predicted and measured $NH_4HSO_4$ solution densities.

Although we focus on resolving the $NH_4HSO_4$ solution density discrepancy, we also illustrate a general technique by which the densities of aqueous ammonium sulfate-sulfuric acid solutions can be calculated from dissociation data.

The molal volume of an electrolyte, $\phi_i$, can be calculated by

$$\phi_i = - \frac{1000}{[E_i]} \left( \frac{d}{d^o} - 1 \right) + \frac{M_{E_i}}{d^o} \qquad (1)$$

where $d^o$ = density of water, $[E_i]$ = the electrolyte molarity, d = the solution density, and $M_{E_i}$ = electrolyte molecular weight (3). For a mixture of electrolytes the mean molal volume, $\Phi$, can be predicted by Young's rule,

$$\Phi = \frac{\Sigma[E_i]\phi_i}{\Sigma[E_i]} \qquad (2)$$

where $\phi_i$ for each electrolyte is taken at the same molar ionic strength (4).

From Equation (2), a generalized expression can be derived for predicting the molal volume of an ammoniated sulfate salt, $\Phi\left((NH_4)_x(H)_y(SO_4)_{\frac{x+y}{2}}\right)$,

$$\Phi\left((NH_4)_x(H)_y(SO_4)_{\frac{x+y}{2}}\right) = \frac{2\beta x}{x+y}\,\phi(NH_4^+) + \frac{2y(1-\gamma)}{x+y}\,\phi(HSO_4^-)$$

$$+\left(\frac{2\beta x+2\gamma y}{x+y} - 1\right)\phi(SO_4^{-2}) + \frac{2\gamma y}{x+y}\,\phi(H^+) + \frac{2x(1-\beta)}{x+y}\,\phi(NH_4SO_4^-) \qquad (3)$$

where x, y = the ammonium and hydrogen stoichiometric coefficients of the sulfate salt, $\beta = [NH_4^+]/([NH_4^+] + [NH_4SO_4^-])$, and $\gamma = [H^+]/([HSO_4^-] + [H^+])$. The total sulfate salt concentration conveniently cancels out of the numerator and denominator in Equation (3). The ionic strength, $I_v$, of the sulfate solution is given by

$$I_v = \left(\frac{4\beta x+4\gamma y}{x+y} - 1\right)\left[(NH_4)_x(H)_y(SO_4)_{\frac{x+y}{2}}\right]. \qquad (4)$$

Typically, ionic molal volume data are not available except for very dilute solutions so the molal volumes of electrolytic salts must be used. Equation (3) can be rewritten as

$$\phi\left((NH_4)_x(H)_y(SO_4)_{\frac{x+y}{2}}\right) = a_1\phi(NH_4^+,NH_4^+,SO_4^=) + \left(\frac{2\beta x+2\gamma y}{x+y} - 1 - a_1\right)\phi(H^+,H^+,SO_4^=)$$

$$+\left(\frac{2y-2\gamma y-2\beta x}{x+y} + 2a_1 + a_2\right)\phi(H^+,HSO_4^-) + \left(\frac{2\beta x}{x+y} - 2a_1 - a_2\right)\phi(NH_4^+,HSO_4^-)$$

$$+ a_2\phi(NH_4^+,NH_4SO_4^-) + \left(\frac{2x-2\beta x}{x+y} - a_2\right)\phi(H^+,NH_4SO_4^-) \qquad (5)$$

where $a_1$ and $a_2$ are constants. Equation (5) was written including terms for $NH_4SO_4^-$ ion-pairs. The thermodynamic literature disagrees over the presence

of $NH_4SO_4^-$ ion-pairing. The Raman spectroscopy work of Irish and Chen (2), Chen and Irish (5) and Young et al. (6) indicates the amount of $NH_4SO_4^-$ ion-pairs is small via their internal consistency checks. Indirectly, Reardon (7) infers a significant amount of $NH_4SO_4^-$ ion-pairing exists. In agreement with the Raman data, we will assume the amount of $NH_4SO_4^-$ ion-pairs is small. Thus, $\beta = 1$ and $a_2 = 0$. Equation (5) simplifies to

$$\Phi\left((NH_4)_x(H)_y(SO_4)_{\frac{x+y}{2}}\right) = a_1\phi(NH_4^+,NH_4^+,SO_4^=)$$

$$+\left(\frac{2x+2\gamma y}{x+y} - 1 - a_1\right)\phi(H^+,H^+,SO_4^=) + \left(\frac{2y-2\gamma y-2x}{x+y} + 2a_1\right)\phi(H^+,HSO_4^-)$$

$$+\left(\frac{2x}{x+y} - 2a_1\right)\phi(NH_4^+,HSO_4^-) \qquad (6)$$

With sulfuric acid solution densities, sulfuric acid dissociation data and an expression for the hydrogen-sulfate molal volume, $\phi(H^+,H^+,SO_4^=)$, the hydrogen-bisulfate molal volume, $\phi(H^+,HSO_4^-)$, can be calculated by

$$\phi(H^+,HSO_4^-) = \frac{\Phi(H_2SO_4)+(2\gamma-1)\phi(H^+,H^+,SO_4^=)}{2-2\gamma} \qquad (7)$$

where $\Phi(H_2SO_4)$ = the sulfuric acid molal volume. Equation (7) is derivable from Equation (6) with $a_1 = 0$, $x = 0$ and $y = 2$.

The hydrogen-sulfate molal volume can be determined by an approach analogous to that of Lindstrom and Wirth (8),

$$\phi(H^+,H^+,SO_4^=) = \phi(X^+,X^+,SO_4^=) - 2\phi(X^+,C\ell^-) + 2\phi(H^+,C\ell^-) \qquad (8)$$

where the molal volumes, $\phi(\ )$, are determined at constant ionic strength, $\phi(X^+,X^+,SO_4^=)$, $\phi(X^+,C\ell^-)$, $\phi(H^+,C\ell^-)$ = the molal volumes of $X_2SO_4$, $XC\ell$ and $HC\ell$, respectively and $X^+$ = the $Na^+$, $NH_4^+$ or $K^+$ cation. (It is assumed that $NH_4C\ell$, $NaC\ell$, $KC\ell$, $HC\ell$, $(NH_4)_2SO_4$, $Na_2SO_4$ and $K_2SO_4$ totally dissociate within the concentration range of interest.) The $(NH_4)_2SO_4$ and $H_2SO_4$ molal volumes can be calculated with density data from Beattie et al. (9), the $K_2SO_4$ molal volume from Dunn (10) and Wirth (11) and the $Na_2SO_4$ molal volume from Dunn (10), Geffcken and Price (12), Beattie et al. (9), and Gibson (13). The $NH_4C\ell$ molal volume can be calculated with density data from Beattie et al. (9), Pearce and Pumplin (14) and Stokes (15), the $NaC\ell$ molal volume from Millero (16), Wirth (17), Dunn (18), Kruis (19) and Beattie et al. (9), the $KC\ell$ molal volume from Wirth (11), Geffcken and Price (12), Dunn (18), Kruis (19) and Beattie et al. (9) and the $HC\ell$ molal volume from Beattie et al. (9), Wirth (17), Millero et al. (20) and Dunn (10). The ionic strength dependences of the molal volumes can be obtained by fitting polynomials to the data. The ionic strength dependences of $\phi(H^+,H^+,SO_4^=)$ calculated from the $NH_4^+$, $K^+$ and $Na^+$ cation data are shown in Figure 1 in addition to the tabulated values taken from Lindstrom and Wirth (8) and Klotz and Eckert (21). The $K^+$ and $Na^+$ data agree quite well whereas the $NH_4^+$ data disagree with the others at low ionic strengths. The three different $\phi(H^+,H^+,SO_4^=)$ expressions will be used to calculate the sensitivity of $\phi(H^+,HSO_4^-)$ to $\phi(H^+,H^+,SO_4^=)$.

With the sulfuric acid dissociation data of Chen and Irish (5) and Young et al. (6), $\phi(H^+,HSO_4^-)$ can be calculated from Equation (7). The $\phi(H^+,HSO_4^-)$ ionic strength dependences from Lindstrom and Wirth (8) and Klotz and Eckert (21) are shown in Figure 2 in addition to the $\phi(H^+,HSO_4^-)$ ionic strength

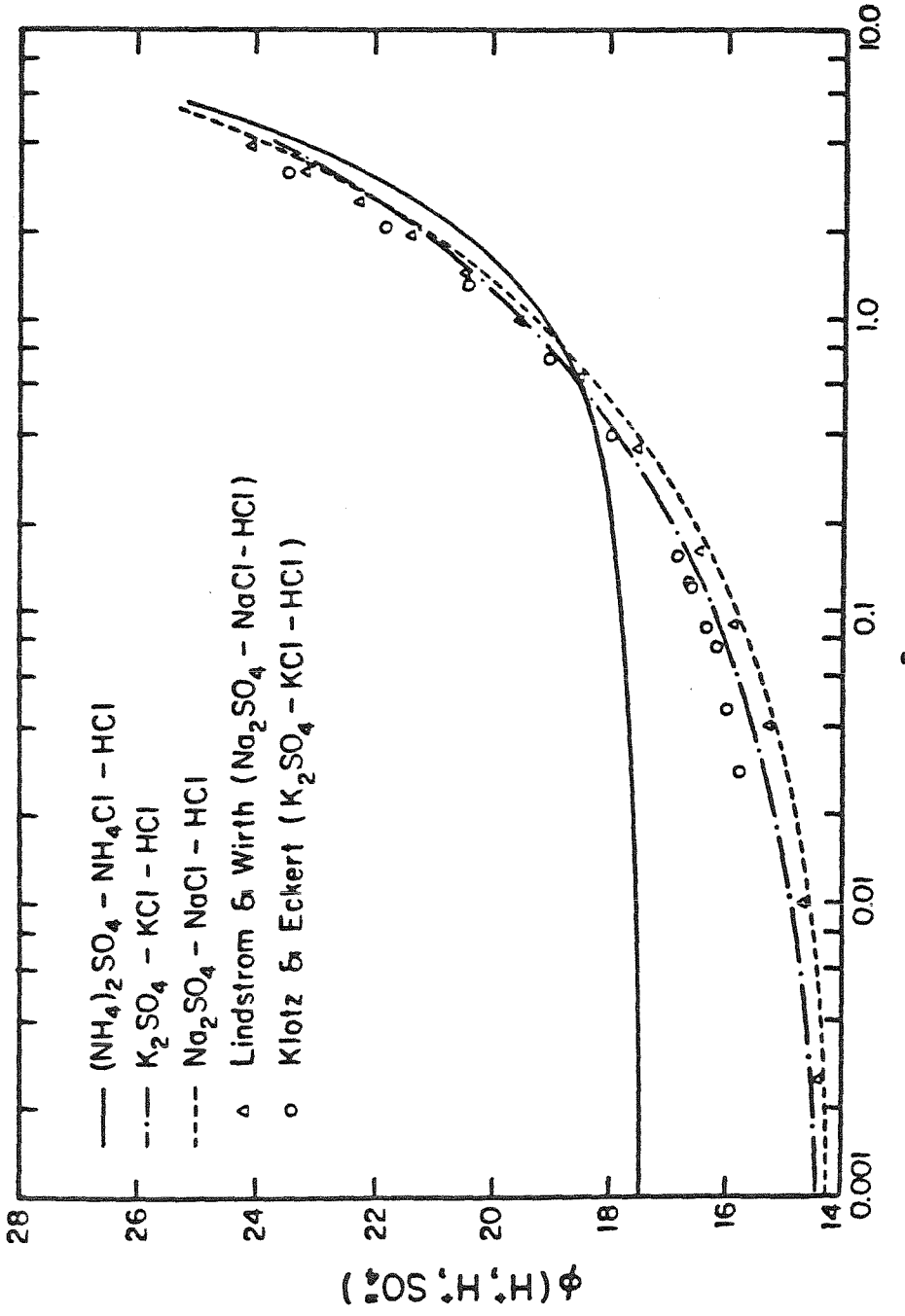


Figure 1. $\phi(H^+, H^+, SO_4^=)$ ionic strength dependence.

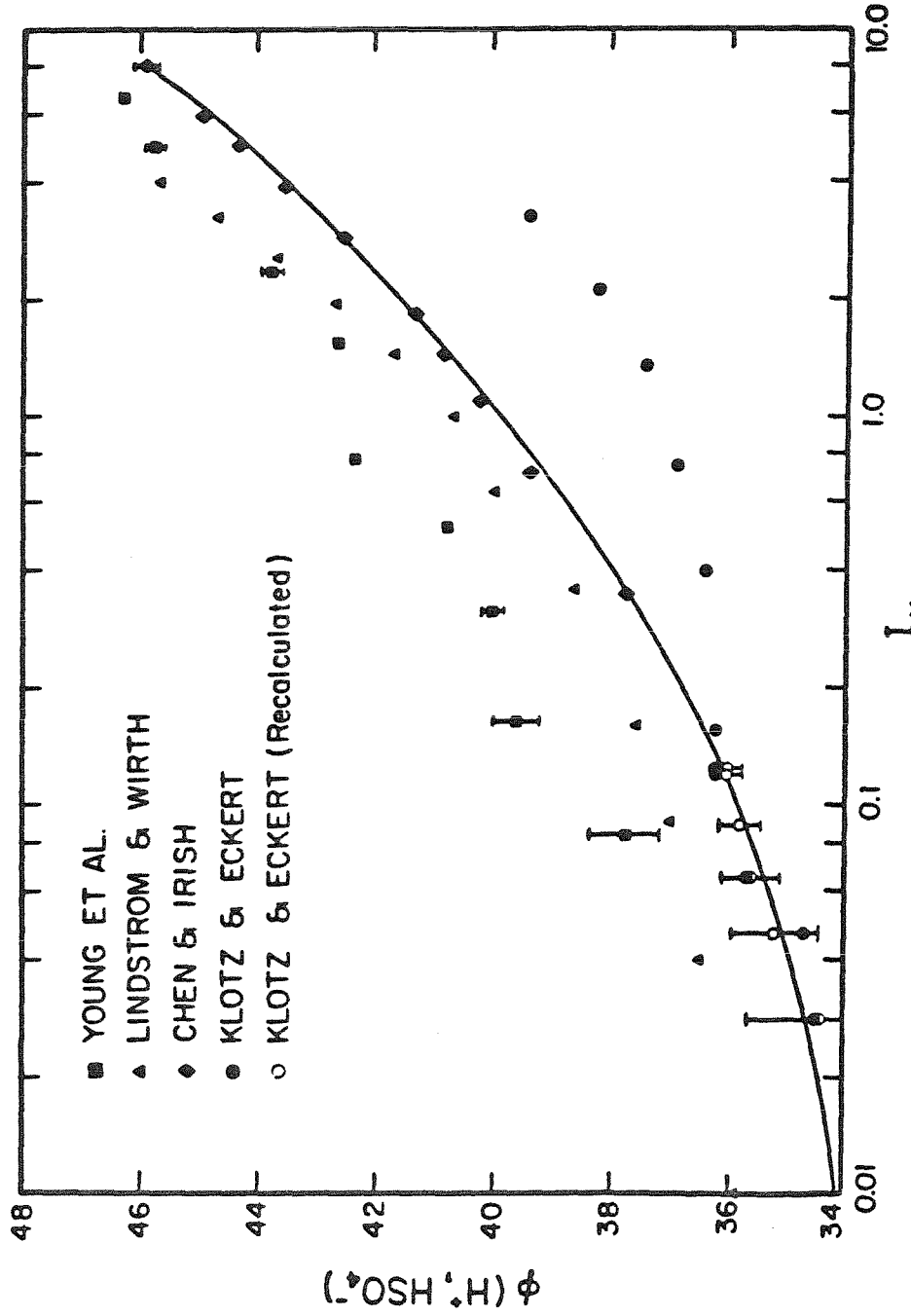


Figure 2. $\phi(H^+, HSO_4^-)$ ionic strength dependence. The solid line is the least square fit to the data of Klotz and Eckert (20), $I_v \leq 0.14$, and Chen and Irish (2).

dependences calculated from the data of Chen and Irish (5) and Young et al. (6). The individual data sources shown distinctively different $\phi(H^+,HSO_4^-)$ ionic strength trends. The error bars in Figure 2 represent the standard deviation of $\phi(H^+,HSO_4^-)$ evaluated from the $K^+$, $Na^+$ and $NH_4^+$ data and the points are the mean values. Below an ionic strength of 0.14, the results of Klotz and Eckert (21) were recalculated using the expressions for $\phi(H^+,H^+,SO_4^=)$ in this paper.

The data in Figure 2 were evaluated in order to ascertain the best representation for $\phi(H^+,HSO_4^-)$. The data of Chen and Irish (5), Young et al. (6) and Klotz and Eckert (21), $I_v \leq 0.14$, are thought to be the best quality. Above an ionic strength of 0.14, the Klotz and Eckert (21) data are poorer since they assumed the classical ionization constant to be invariant. Lindstrom and Wirth (8) assumed $\phi(H^+,HSO_4^-) = \phi(H^+,H_2PO_4^-)$ + an adjustment factor and thus, $\phi(H^+,HSO_4^-)$ shown in Figure 2 is actually $\phi(H^+,H_2PO_4^-)$ modified. The best representation for $\phi(H^+,HSO_4^-)$ is obtained from the data of Chen and Irish (5) and Klotz and Eckert (21), $I_v \leq 0.14$, since these data smoothly extrapolate to each other, whereas, the data of Young et al. (6) and Klotz and Eckert (21), $I_v \leq 0.14$, are discontinuous. The data of Chen and Irish (5) and the recalculated results of Klotz and Eckert (21) were fit via a least squares technique to a polynomial,

$$\phi(H^+,HSO_4^-) = 33.25 + 9.03\ I_v^{1/2} - 2.773\ I_v + 0.4134\ I_v^{3/2} \qquad (9)$$

where the standard deviation is $\pm$ 0.12. The solid curve in Figure 2 is Equation (8) and will be used to represent the ionic strength dependence of $\phi(H^+,HSO_4^-)$.

To calculate the $NH_4HSO_4$ molal volume, the ammonium-bisulfate molal volume, $\phi(NH_4^+,HSO_4^-)$, must be known. The ammonium-bisulfate molal volume can be calculated from

$$\phi(NH_4^+,HSO_4^-) = \phi(H^+,HSO_4^-) + \phi(NH_4^+,C\ell^-) - \phi(H^+,C\ell^-) \qquad (10)$$

The ionic strength dependence of $\phi(NH_4^+,HSO_4^-)$ can be determined with the $\phi(H^+,HSO_4^-)$ ionic strength dependence calculated from the sulfuric acid dissociation data of Chen and Irish (5) and Klotz and Eckert (21).

Analogous to the approach of Lindstrom and Wirth (8), $\phi(NH_4^+,NH_4^+,SO_4^=)$ and $\phi(H^+,H^+,SO_4^=)$ can be replaced by

$$\phi(NH_4^+,H^+,SO_4^=) = \frac{1}{2}\left(\phi(NH_4^+,NH_4^+,SO_4^=) + \phi(H^+,H^+,SO_4^=)\right) \quad , \qquad (11)$$

By substitution of Equation (11) into Equation (6) and solving for $a_1$, one obtains

$$\phi\left((NH_4)_x(H)_y(SO_4)_{\frac{x+y}{2}}\right) = \left(\frac{2x+2\gamma y}{x+y} - 1\right)\phi(NH_4^+,H^+,SO_4^=)$$

$$+\left(\frac{2y}{x+y} - 1\right)\phi(H^+,HSO_4^-) + \left(1 - \frac{2\gamma y}{x+y}\right)\phi(NH_4^+,HSO_4^-) \; . \qquad (12)$$

From the ionic strength dependences of $\phi(NH_4^+,H^+,SO_4^=)$, $\phi(H^+,HSO_4^-)$ and $\phi(NH_4^+,HSO_4^-)$ and bisulfate dissociation data for $NH_4HSO_4$ solutions, the molar volume of $NH_4HSO_4$, $\Phi(NH_4HSO_4)$, and the density of $NH_4HSO_4$ solutions can be calculated. From Equation (12),

$$\phi(NH_4HSO_4) = \gamma\phi(NH_4^+,H^+,SO_4^=) + (1-\gamma)\phi(NH_4^+,HSO_4^-) \; . \qquad (13)$$

With the dissociation data of bilsulfate in ammonium bisulfate solutions of Young et al. (6) and Irish and Chen (2), the molal volume of ammonium bisulfate can be calculated using Equation (13) (22). After the ammonium bisulfate molal volume has been calculated, the density can be determined from

$$d = \frac{\left[(NH_4)_x(H)_y(SO_4)_{\frac{x+y}{2}}\right]}{1000}\left(M_{(NH_4)_x(H)_y(SO_4)_{\frac{x+y}{2}}} - d^o\phi\left[(NH_4)_x(H)_y(SO_4)_{\frac{x+y}{2}}\right]\right) + d^o \qquad (14)$$

where $M_{(NH_4)_x(H)_y(SO_4)_{\frac{x+y}{2}}}$ = the molecular weight of $(NH_4)_x(H)_y(SO_4)_{\frac{x+y}{2}}$.

The density has been calculated for 0.206 to 6.571 molar or 0.39 to 9.76 ionic strength ammonium bisulfate solutions. The solubility of ammonium chloride is 5.70 molar, and thus, the molal volume data of ammonium chloride had to be smoothly extrapolated to 9.76 molar (14). The calculated solution densities are compared to the densities calculated from the $[NH_4HSO_4]$ and $[H_2O]$ data in Table I of Irish and Chen (2) and the measurements of Tang (23) and Beattie et al. (9) in Figure 3. The agreement between the predicted $NH_4HSO_4$ solution densities from molal volume and dissociation data and the data of Tang (23) and Beattie et al. (9) is good, whereas the solution densities calculated from the $[NH_4HSO_4]$ and $[H_2O]$ data in Table I of Irish and Chen (2) disagree with the theoretical predictions and the experimental measurements. Thus, the water molalities in the paper of Irish and Chen (2) must be in error, since the solution densities calculated from the ammonium bisulfate molarities, $[NH_4HSO_4]$, agree well with the theoretical predictions from the data of Young et al. (6) and the data of Tang (23) and Beattie et al. (9).

Recent communication from D. E. Irish (24) included a polynomial fit to the $NH_4HSO_4$ density data used in Irish and Chen (2),

$$d = 0.99671 + 0.604706\times10^{-1}[NH_4HSO_4] - 0.108981\times10^{-2}[NH_4HSO_4]^2 + 0.106394\times10^{-4}[NH_4HSO_4]^3 \quad (15)$$

Equation (15) agrees with the data of Tang (23) and Beattie et al. (9), in support with our observation that the water molarities in Table I of Irish and Chen (2) must have been calculated incorrectly. The $NH_4HSO_4$ solution

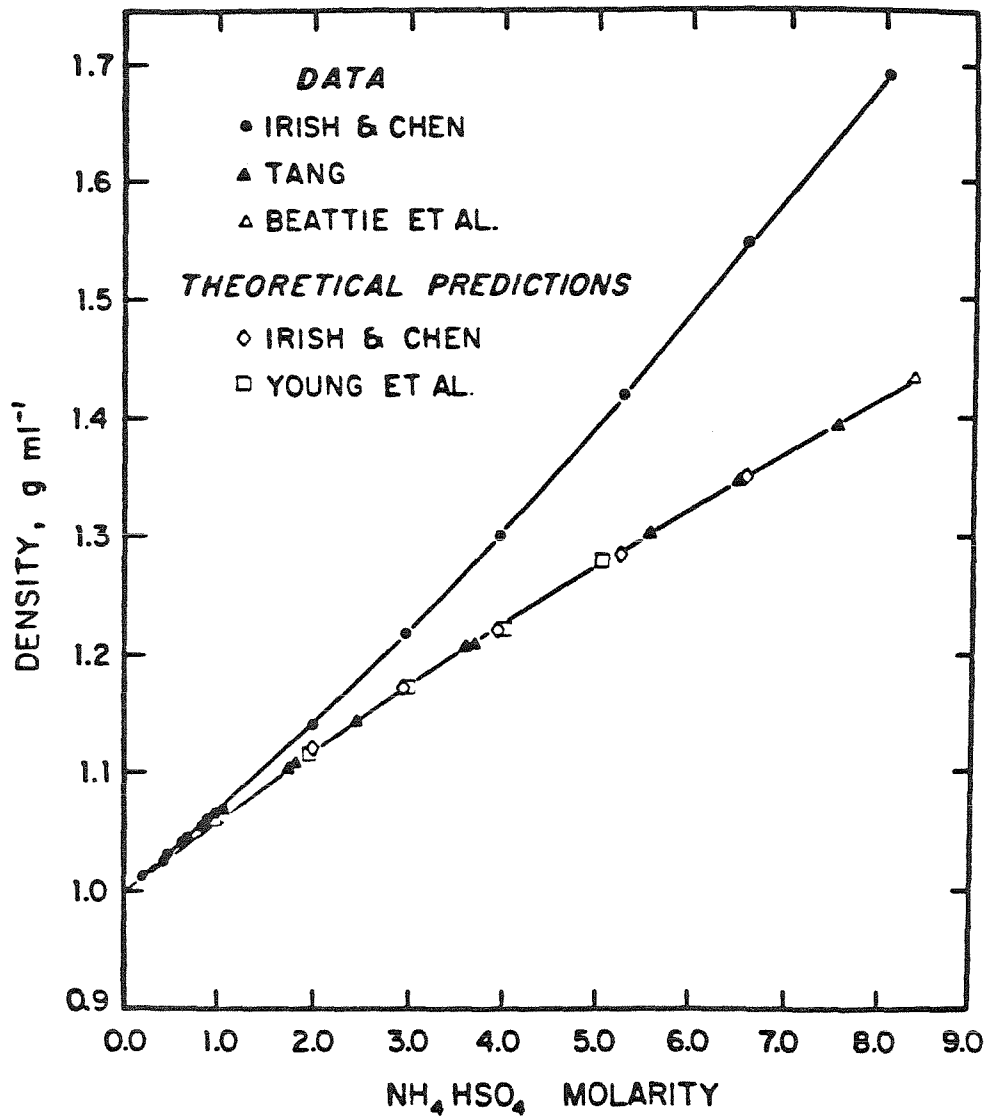


Figure 3. Density of $NH_4HSO_4$ solutions. The lines are the authors' representation of the data of Tang (22) and Beattie et al. (8) and Irish and Chen (2).

densities predicted from Equation (15) agree with the theoretical predictions based on dissociation and molar volume data within 0.40% for Irish and Chen (2) and 0.65% for Young et al. (6).

In addition to isolating the error source in the paper of Irish and Chen (2), we have illustrated a technique by which the densities of ammoniated sulfate solutions can be calculated from dissociation data or vice versa. Specifically, this work discussed ammonium bisulfate solutions but Equation (12) can be applied to any aqueous ammonium sulfate-sulfuric acid solution.

Literature Cited


1. Stelson, A.W.; Seinfeld, J.H. Atmos. Environ., 1981, 15, XXX.
2. Irish, D.E.; Chen, H. J. Phys. Chem. 1970, 74, 3796.
3. Millero, F.J. Chem. Rev., 1971, 71, 147.
4. Young, T.F.; Smith, M.B. J. Phys. Chem. 1954, 58, 716.
5. Chen, H.; Irish, D.E. J. Phys. Chem. 1971, 75, 2671.
6. Young, T.F.; Maranville, L.F.; Smith, H.M. In "The Structure of Electrolytic Solutions," Hamer, W.J., Ed.; Wiley: New York, 1959; Chapter 4.
7. Reardon, E.J. J. Phys. Chem. 1975, 79, 422.
8. Lindstrom, R.E.; Wirth, H.E. J. Phys. Chem. 1969, 73, 218.
9. Beattie, J.S.; Brooks, B.T.; Gillespie, L.J.; Scatchard, G; Schumb, W.C.; Tefft, R.F. In "International Critical Tables of Numerical Data, Physics, Chemistry and Technology," Washburn, E.W., Ed; McGraw-Hill: New York, 1933; Vol. III, p. 51.
10. Dunn, L.A. Trans. Faraday Soc. 1966, 62, 2348.
11. Wirth, H.E. J. Am. Chem. Soc. 1937, 59, 2549.
12. Geffcken, W.; Price, D. Z. Phys. Chem. 1934, B26, 81.
13. Gibson, R.E. J. Phys. Chem. 1927, 31, 496.
14. Pearce, J.N.; Pumplin, G.G. J. Am. Chem. Soc. 1937, 59, 1221.
15. Stokes, R.H. Aust. J. Chem. 1975, 28, 2109.
16. Millero, F.J. J. Phys. Chem. 1970, 74, 356.
17. Wirth, H.E. J. Am. Chem. Soc., 1940, 62, 1128.
18. Dunn, L.A. Trans. Faraday Soc. 1968, 64, 1898.
19. Kruis, A. Z. Phys. Chem. 1936, B34, 1.
20. Millero, F.J.; Hoff, E.V.; Kahn, L. J. Solution Chem. 1972, 1, 309.
21. Klotz, I.M.; Eckert, C.F. J. Am. Chem. Soc. 1942, 64, 1878.

22. For Irish and Chen (2), the dissociation data of bisulfate in ammonium bisulfate solutions were taken directly from Table I. The polynomial presented in Chen and Irish (5) was not used since it inaccurately represents the data of Irish and Chen (2) at high $NH_4HSO_4$ molarities.

23. Tang, I.N., Brookhaven National Laboratory, personal communication, 1981.

24. Irish, D.E., University of Waterloo, personal communication, 1981.